STRATEGIES FOR THE MANAGEMENT AND PREVENTION OF COMPLICATIONS IN REFRACTIVE LASER SURGERY

STRATEGIEËN VOOR BEHANDELING EN HET VOORKOMEN VAN COMPLICATIES VAN REFRACTIECHIRURGIE MET DE LASER

FARHAD HAFEZI

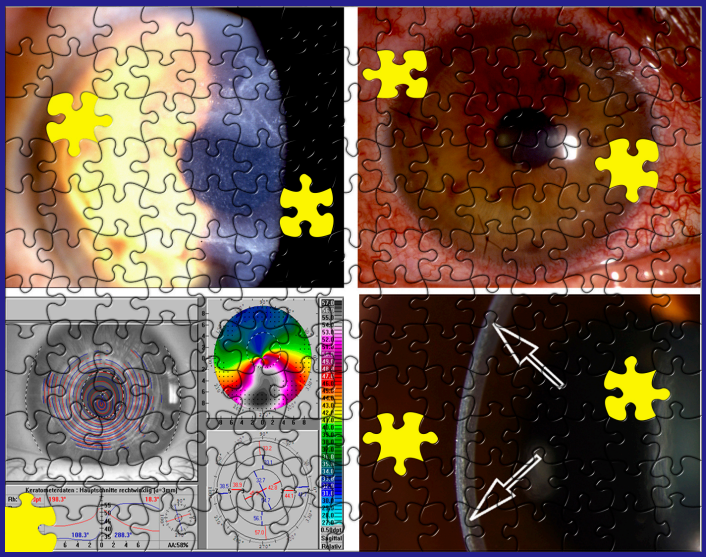

Strategies for the management and prevention of complications in refractive laser surgery

Strategieën voor behandeling en het voorkomen van complicaties van refractiechirurgie met de laser

Farhad Hafezi

Strategies for the management and prevention of complications in refractive laser surgery

Strategieën voor behandeling en het voorkomen van complicaties van refractiechirurgie met de laser

PhD thesis, Erasmus University Rotterdam, The Netherlands, 2007

Farhad Hafezi

Cover:

Design and layout by Farhad Hafezi

Printed by ADAG Copy, Zurich, Switzerland

Strategies for the Management and Prevention of Complications in Refractive Laser Surgery

Strategieën voor behandeling en het voorkomen van complicaties van refractiechirurgie met de laser

Thesis

to obtain the degree of Doctor from the
Erasmus University Rotterdam
by command of the
Rector Magnificus

Prof. Dr. S.JW.J. Lamberts

and according to the decision of the Doctorate board
The public defence shall be held on

January 23, 2008 at 13.45 hrs

by
Farhad Hafezi
born in Remscheid, Germany
and citizen of Fribourg, Switzerland

Promotie commissie

Promotoren:	Prof. dr. G. van Rij
Overige leden:	Prof. dr. L. Feenstra
	Prof. dr. G.P.M. Luyten
	Prof. dr. J.C. van Meurs
	Prof. dr. H.W. Tilanus
	Prof. dr. C.E. Remé
	Dr. T.J.T.P van den Berg
	Prof. dr. A.F. Deutman

For my mother Alina, my father Abolfazl, Zarrin, Micha, Farah, Fariba
and
my Nikkilove

Contents

Publications and manuscripts based on studies included in this thesis

1. Seiler T, Hafezi F, Iseli HP, Koller T, Alkara N. Reoperations after LASIK. Klin Monatsbl Augenheilkd 2006; 223(6):509-512
2. Hafezi F, Jankov M, Mrochen M, Wullner C, Seiler T. Customized ablation algorithm for the treatment of steep central islands after refractive laser surgery. J Cataract Refract Surg 2006; 32(5):717-721
3. Hafezi F, Mrochen M, Fankhauser F, 2nd, Seiler T. Anterior lamellar keratoplasty with a microkeratome: a method for managing complications after refractive surgery. J Refract Surg 2003; 19(1):52-57
4. Hafezi F, Mrochen M, Seiler T. Two-step procedure to enlarge small optical zones after photorefractive keratectomy for high myopia. J Cataract Refract Surg 2005; 31(12):2254-2256
5. Seiler T, Hafezi F. Corneal cross-linking-induced stromal demarcation line. Cornea 2006; 25(9):1057-1059
6. Hafezi F, Kanellopoulos J, Wiltfang R, Seiler T. Corneal collagen crosslinking with riboflavin and ultraviolet A to treat induced keratectasia after laser in situ keratomileusis. J Cat Refr Surg 2007; 33(12):2035-2040
7. Mrochen M, Hafezi F, Jankov M, Seiler T. Ablation profiles in corneal laser surgery. Current and future concepts. Ophthalmologe 2006; 103(3):175-183
8. Mrochen M, Bueeler M, Iseli HP, Hafezi F, Seiler T. Transferring wavefront measurements into corneal ablations: an overview of related topics. J Refract Surg 2004; 20(5):S550-554
9. Koller T, Iseli HP, Hafezi F, Mrochen M, Seiler T. Q-factor customized ablation profile for the correction of myopic astigmatism. J Cataract Refract Surg 2006; 32(4):584-589
10. Iseli HP, Mrochen M, Hafezi F, Seller T. Clinical photoablation with a 500-Hz scanning spot excimer laser. J Refract Surg 2004; 20(6):831-834

Abbreviations

BSCVA	Best spectacle-corrected visual acuity
BSS	Balanced salt solution
C	Celsius
D	Diopters
FDA	(National) Food and drug administration
FFKC	Forme fruste keratoconus
FML	Fluorometholone
FWMH	Full Width at Half Maximum
Hz	Hertz
IOP	Intraocular pressure
IROC	Institute for Refractive and Ophthalmic Surgery
J	Joule
KC	Keratoconus
LASIK	Laser in situ keratomileusis
LKP	Lamellar keratoplasty
mJ	Millijoule
mm	Millimeter
mW	Milliwatt
nm	Nanometer
µm	Micrometer
OSA	Optical Society of America
PKP	Penetrating keratoplasty
PMCD	Pellucidal marginal cormeal degeneration
PRK	Photorefractive keratectomy
PTK	Photorefractive keratotomy
Q factor	Determinand of corneal asphericity
rms	Root-mean-square
rmsh	Root-mean-square of higher order
RST	Residual stromal thickness
SCI	Steep central island
SD	Standard deviation
UCVA	Uncorrected visual acuity
UVA	Ultraviolet A
VA	Visual acuity
W	Watt
X-linking	Corneal collagen crosslinking with riboflavin/UVA

Part 1

Introduction

1.1

Complications in refractive laser surgery

Since the introcduction of the excimer laser in ophthalmology in 1986, refractive surgery has seen an enormous increase in the number of procedures. In 2002, the total number of refractive laser procedures worldwide has passed the total number of phacoemulsification surgery, thus making these procedures the most frequently performed in ophthalmic surgery.

A variety of medical indications exist for this type of surgery such as correction of high anisometropia or irregular astigmatism following penetrating keratoplasty, corneal scarring or complicated cataract surgery. However, the most frequent indication is the patient's wish to be independent of spectacles. The term "lifestyle surgery" may be applicable to this kind of surgery and due to its cosmetic nature and the financial interest linked to it, many high volume laser centers perform 20'000 or more operations per year. Often, these centers do not use state-of the-art equipment and postoperative care in some cases ("LASIK tourism") is only rudimentary.

Therefore, the number of complications has also increased markedly. These complications may be:

"preoperative" complications due to surgeons inadvertence such as induction of keratectasia

intraoperative complications that might either be microceratome-related such as cutting errors or laser-related such as decentered ablation, creation of small or irregular optical zones and formation of steep central islands

early postoperative complications including diffuse lamellar keratitis, epithelial ingrowth, sterile infiltrates, corneal melting, fungal keratitis and wrinkling syndroma

late postoperative complications including iatrogenic keratectasia, glare and halos due to small optical zones and monocular diplopia in decentered ablation or irregular astigmatism

1.2 Objective and outline

Our work deals with the management and prevention of complications in refractive laser surgery.

Our main contributions to the field are:

- The development of a new ablation profile for the treatment of steep central islands
- The development of a new surgical technique in automated lamellar keratoplasty
- To demonstrate that corneal collagen cross-linking with riboflavin-UVA can be used to arrest LASIK-induced iatrogenic keratectasia

The main aim of our ongoing work is the application of the UVA cross-linking method in patients suffering from corneal irregularities such as progressive keratokonus and pellucid corneal marginal degeneration in order to make these corneas accessible to refractive laser surgery. The aim is not a cosmetic outcome but rather a homogenization of the irregular surface so that contact lenses or glasses may be fitted with more ease.

Part 2

Management of Complications in Refractive Laser Surgery

2.1

Reoperations after LASIK surgery

Abstract

Objective. *Reoperations after refractive surgery have increased in frequency during the past 10 years. The spectrum of the indications for repeat LASIK may have changed.*

Methods. *All cases of reoperations after refractive surgery performed between May 1, 2004 and April 30, 2005 at the Institute of Refractive and Ophthalmic Surgery (IROC) were retrospectively investigated regarding indication for repeat surgery and visual and refractive results. The 1-month results were used to estimate the refractive and visual success rate.*

Results. *Of the 76 reoperations, 69 were performed as re-lifts, 3 eyes had new lamellae cut, and 3 cases needed keratoplasty. The reoperations took place 7.5±13 months after the primary operation (range 0.5 to 60 months). The most frequent indication was residual astigmatism of 0.5 D and more. Visual loss of more than 1 decimal line did not occur and unaided visual acuity increased from 0.64 to 1.05. No complications were reported, however, 3 eyes needed additional enhancement.*

Conclusions. *Reoperations after LASIK performed as re-lifts appear to be effective and reasonably safe when using the technique described and respecting a residual stromal thickness of 280 microns.*

Seiler T, Hafezi F, Iseli HP, Koller T, Alkara N.

Klin Monatsbl Augenheilkd 2006; 223:509-512

Introduction

Besides a faster visual rehabilitation and a minor healing answer, the early and uncomplicated reoperation represents one of the main advantages of the laser in situ keratomileusis (LASIK) operation when compared to surface ablation. After initial controversy on whether a surface-parallel cut (re-cut) or blunt preparation of the primary cut (re-lift) should be preferred, [1] today the majority of reoperations after LASIK is performed using the re-lift variant. [2]

The simplicity of the reoperation as well as new individualized ablation algorithms, e.g. wavefront- or topography-guided, has changed both the spectrum and the frequency of reoperations in the past years. [2-9] In this work we present reoperations that were performed during one year at our Institute with special emphasis on indication and early postoperative results.

Patients and Methods

Patients

68 patients that have undergone one or more reoperations between may 2004 and may 2005 in the Institute for Refractive and Ophthalmic Surgery (IROC) in Zurich, Switzerland, were enrolled in this study. This group consisted of patients that had primary surgery at our Institute (n = 51) and of external patients that were either referred to us (n = 8) or contacted us spontaneously (n = 9). Preoperative investigation included slit lamp examination of the anterior and posterior segment, autorefractometry (Humphrey model 599, Carl Zeiss, Jena, Germany) including glare and low-contrast visual acuity, manual refraction, uncorrected and best-corrected visual acuity with and without pinhole, corneal topography (Keratograph C, Oculus, Wetzlar, Germany equipped with Topolyzer software, Wavelight, Erlangen, Germany), aberrometry (Wavefront Analyzer, Wavelight, Erlangen, Germany), applanation tonometry and ultrasound pachymetry of the central cornea (SP-2000, Tomey, Nagoya, Japan).

In selected cases, the posterior cornea was analyzed using a Scheimpflug camera (Pentacam, model 70700, Oculus, Wetzlar, Germany). The patient signed a consent form after the potential advantages and the risks of the reoperation were explained and discussed. In particular, the potential necessity of a second reoperation for fine-tuning of the result was emphasized.

The operative technique

In the majority of cases, blunt dissection of the primary lamella was per-

formed (n = 69). In 3 cases after PRK, however, a new lamella was cut. Following asymmetrical marking of the cornea, the blunt preparation of the lamella was performed under the operating microscope of the laser using a special spatula (model Vryghem, Moria, France). In a next step, the entire lamella was liberated using a conventional iris spatula and everted (Calzone technique). Is in all cases where the rmsh value for the 7mm-pupil was 0.6 µm and more (OSA notation) and four reliable and consistent measurements with a range of less than ±0,1 µm were obtained.

On the first postoperative day, the bandage contact lens was removed and slit lamp examination and uncorrected visual acuity were performed. Further controls took place at 1 month, 3 months and 1 year after the reoperation. Investigations at these times included the same examinations as performed preoperatively. As a postoperative medication a combination of antibiotic and steroid eye drops was prescribed (Maxitrol eye drops, Alcon, Hunenberg, Switzerland) twice to four times daily for two weeks, depending on the level of postoperative inflammation.

Table 1 Indications for Re-LASIK

Group	*Number*
Residual astigmatism	31
Overcorrection (myopia)	13
Undercorrection (myopia)	7
Overcorrection (hyperopia)	7
Undercorrection (hyperopia)	6
Optical inhomogenities (decentration, small optical zone)	10
Following penetrating keratoplasty	3

Results

76 reoperations were performed in 68 patients during the observational period. Deep stroma melting required a deep lamellar keratoplasty in one case and in two cases, automated lamellar keratoplasty [12] was performed due to a primary cut error with consecutive scarring and recurrent epithelial ingrowth. Since these cases required longer observation and reoperations, they were taken out of the study group. In one case with an intraoperative residual stromal thickness of less than 280 µm, the reoperation was aborted after re-lifting of the flap. Hence, the study group contained 64 patients in which 72 reoperations were performed. Three eyes were operated twice (4.2%) and in 5 patients, both eyes were operated. Three post-PRK eyes needed cutting of a flap with a microceratome in order to perform the reoperation as a LASIK pro-

cedure. The other 69 reoperations were performed as re-lift procedures with blunt preparation of the initial lamella.

The various indications for the re-LASIK procedures are listed in table 1. The by far largest group were eyes in which a postoperative astigmatism of 0.5 D or more was present, followed by under- or overcorrection after former myopic or hyperopic correction. The subgroup with optical inhomogeneities included decentered and flattened optical zones and irregular optical zones of unknown origin. LASIK following penetrating keratoplasty represented another small subgroup (n=3). In these cases, a multistep procedure is the procedure of choice, anyway.

Reoperations took place at 7,5±13 months after primary surgery with a range from 2 weeks to 60 months. 21 reablations were performed as wavefront-guided and 7 reablations as topography-guided operations. The remaining 44 reablations were accomplished as Q factor-optimized procedures. All eyes from optical inhomogeneities subgroup were wavefront-guided procedures and three eyes from the keratoplasty subgroup were performed as topogra-phy-guided treatments.

The early postoperative phase was inconspicuous in 70 cases. In 2 cases, diffuse lamellar keratitis grade 2 required intensified topical steroid therapy for two weeks. At 1 month after surgery, 32 corneas (44%) showed an epithelial ingrowth that was clinically judged as monolayered since the epithelium remained optically clear and no signs of keratinisation (milky aspect) were detectable. These cases showed no further progression at 3 months after surgery and thus required no treatment. In the subgroup with residual astigmatism, refractive astigmatism was reduced from 0.99±0.76 D (range 0,5 to 3,0 D) to 0.32±0.35 D at 1 month after surgery. In the subgroup consisting of spherical under- and overcorrection, all eyes were ±0.5 D target refraction at one month after surgery.

Table 2 Change in BSCVA as an indicator of Re-LASIK safety

Changes in lines (decimal scale)	+2	+1	0	-1	-2
Number	2	20	39	8	0

Uncorrected visual acuity (UCVA), seen as a determinant of visual success

of the reoperation, increased from 0.64±0.24 to 1.05±0.27 in the total patient population (without intended monovision, n = 8). The performance in best spectacle-corrected visual acuity (BSCVA) is seen as a determinant of the safeness of a refractive laser procedure and is presented in table 2. For the three eyes that underwent two reoperations, the last result was included. In the subgroup suffering from optical inhomogeneities, one patient reported persistent monocular double vision under mesopic conditions even after the second reoperation.

Discussion

Hersh and co-workers initially determined the 10%-incidence of reoperations after LASIK surgery. [2] Our study confirms this percentage with 8.5% of reoperations following primary surgery.

This relatively high percentage may have several causes. First, the expectations of the patients have increased markedly, not least triggered by aggressive marketing campaigns (lifestyle operations). Second, reoperations performed as LASIK are safer and less complicated than surface retreatments. Third, the modern individualized ablation profiles drastically increased the success rates of reoperations. Here, not only residual aberrations but also the aberrations induced by the primary treatment [13, 14] can be corrected.

Over- and undercorrection of astigmatism still seems to be one of the major causes of reoperations after refractive laser surgery [2, 9, 15-17] with multifactor causes: on one hand, preoperative cylinder and axis can be determined with less accuracy than the sphere. Furthermore, little is known on the axial dependency of corneal asphericity. [18] On the other hand, the axis in the reclined patient might turn due to cyclotorsion. [19] We have addressed the latter in our patients through preoperative marking of the axis in the upright position. Nevertheless, accuracy of astigmatism correction still remains insufficient. Therefore, the increased probability of a reoperation should be addressed in all patients with correction of astigmatism prior to primary surgery.

Refractive corrections following penetrating or lamellar keratoplasty represent a special subgroup. Since the LASIK cut may alter corneal biomechanics and corneal shape, a reoperation is highly probable and can be anticipated. Others have therefore suggested performing just the cut in a first procedure. [20] This would enable to correct for the induced aberrations in the second procedure. In the three cases presented here, the

topography-guided treatment for the homogenization of the optical surface was performed along with the LASIK cut in a one-step procedure. If necessary, a second reoperation must be performed within the first two months after the initial reoperation due to rapid adherence of the lamella to the transplant interface.

The visual changes presented in table 2 show that re-LASIK is a safe and efficient procedure. Visual loss of more than one decimal line is seen as a complication in refractive laser surgery. [21] In our study, no eyes lost more than one decimal line. However, only one-month postoperative data were included in this study and some late complications might alter the results presented here. On the other hand, minimal healing response and early refractive stability represent hallmarks of a LASIK procedure and can be determined with accuracy at one month after surgery already.

2.2

Customized Ablation Algorithm for the Treatment of Steep Central Islands after Refractive Laser Surgery

Abstract

Objective. *Steep central island (SCI) formation after photorefractive keratectomy (PRK) and laser in situ keratomileusis (LASIK) represents a major drawback in the visual rehabilitation of patients after refractive laser surgery. Due to the small size of SCI, current ablation algorithms are unable to properly calculate an ablation pattern for customized re-treatment. Here we present the use of a new ablation algorithm for the treatment of SCI that occurred after PRK or LASIK surgery.*

Methods. *Basically, this algorithm uses a smaller zone of approximation and takes into account the spherical shift induced by removal of the SCI.*

Results. *In all 3 eyes treated, best spectacle-corrected visual acuity increased to 20/16 and remained stable at the 1 and 3 month follow-up with disappearance of the SCI in corneal topography.*

Conclusions. *This new treatment algorithm may be of benefit to patients suffering from visual side effects due to SCI formation after previous PRK or LASIK surgery.*

Hafezi F, Jankov M, Mrochen M, Wullner C, Seiler T.

J Cat Refr Surg 2006; 32:717-721

Introduction

Nowadays refractive laser surgery of the cornea has become a safe and effective procedure. However, some technical advances have only been achieved in the past few years and many patients treated previously suffer from optical complications such as small optical zones, decentred ablation and the formation of steep central islands (SCI). [22-27] Whereas a number of strategies and customized treatment techniques have been developed to overcome the first two issues, [5, 24, 28-31] the latter often remains unresolved with current treatment algorithms.

Recently, attempts were taken to treat SCI by topography-guided customized treatments. However, current ablation algorithms have difficulties to properly approximate difference height maps due to the small size of the SCI. Here we present a new ablation strategy to correct for SCI after previous photorefractive keratectomy (PRK) and laser in situ keratomileusis (LASIK).

Technique

Definition of steep central islands

Definition of diameter and steepening of SCI shows variation between authors. [23, 32-34] We used the definition established by Krueger et al. where SCI were defined as areas of steepening of at least 3D and 1.5 mm in diameter. [23]

The ablation algorithm

The principle of the new algorithm is based on the fact that the surface representation of irregular corneas by means of an aspheric surface is associated with a certain amount of fitting error, especially in case of spatially localized irregularities. Thus, fitting an asphere to a corneal shape with a SCI and subtracting this aspheric fit from the original height data, one will be left with a difference height map of the SCI that can be used for an ablation profile.

In our study, the data used for deriving a customized profile for central island treatments were based on corneal topography height maps provided by the Wavelight Topolyzer System using the central 3.5 mm only. The height data are fitted to an aspherical shape function and in a second step subtracted from the original data set. The residual height information that also includes

the measured height information of the SCI was exported to the Wavelight "eye-Q" laser system. The required approximation by means of single laser spots (spot diameter 1 mm) was performed using a special and adapted version of the Wavelight T-CAT program (topography-guided customized ablation treatment). The proposed ablation pattern was modified adding myopic correction within the SCI area until a homogenous ablation pattern with zero ablation depth at the edges and the height of the SCI as calculated by the Munnerlyn's formula was met (usually -0,5 to -1.0 D). Test ablations were performed on special test targets (Wavelight Laser Technology) before each treatment and visually compared to the planned ablation profile. Treatment was performed using a scanning-spot laser with a 0.8-mm spot size, a Gaussian-like spot profile, and a 400-Hz repetition rate (Wavelight Allegretto). The eye tracking system had a response time of fewer than 6 milliseconds.

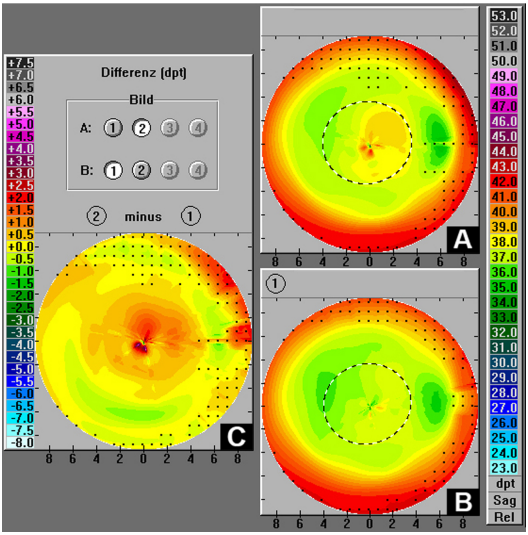

Figure 1. Pre- and postoperative corneal topographies (axial representation) and its difference map. The preoperative topography shows the CSI (A) whereas at one day after surgery, the CSI has disappeared (B). The difference power map of pre- versus postoperative status shows the ablation occurred (C).

Preoperative examinations, treatment and postoperative care

Preoperative examination included uncorrected (UCVA) and best spectacle-corrected visual acuity (BSCVA), slit lamp examination of the anterior segment, fundus examination, corneal topography (Topolyzer, Wavelight Laser Technologie, Erlangen, Germany) and optical

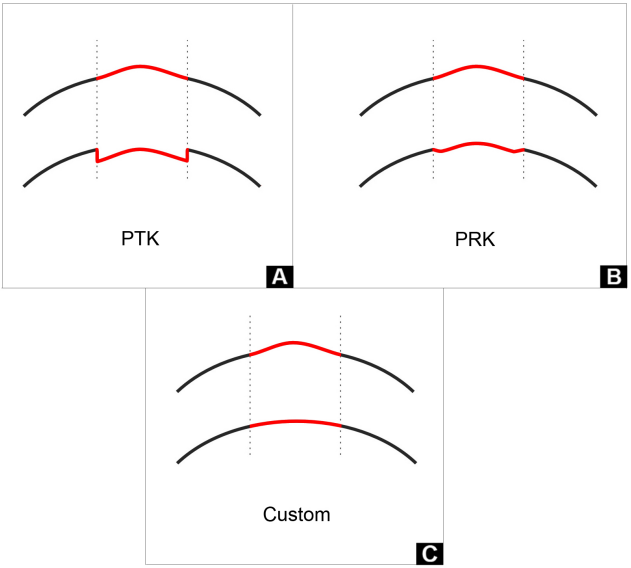

Figure 2. Comparison of different ablation patterns. When using a 7mm approximation zone (A), the CSI is significantly undertreated. When using a 3.5mm approximation zone without spherical correction (B), again, the CSI is not addressed. When adjusting the spherical correction to -0.5D within the 3.5mm approximation zone (C), the CSI is fully treated.

pachymetry (Pentacam). Treatment was performed using the Wavelight Concerto laser system (Wavelight Laser Technologie, Erlangen, Germany) and was performed as LASIK or PRK. In the case of Re-LASIK treatment (representative case reported here), the original flap was lifted prior to ablation. At the end of treatment, a bandage contact lens was applied to the eye, either soaked with antibiotic eye drops (LASIK) or antibiotic ointment was put on the cornea before the bandage contact lens was applied (PRK). LASIK: the bandage contact lens was removed the next day and the cornea was examined for signs of inflammation. Dexamethasone eye drops were then applied twice daily for 1 week, followed by a single application daily for another week. Postoperative follow-ups were performed at 1 day, 1 month and 3 months after treatment. PRK: patients were examined daily for closure of corneal epithelium and the bandage contact lens was removed at day 3 after surgery. After complete closure of the epithelium, dexamethasone eye drops were applied twice daily for 6

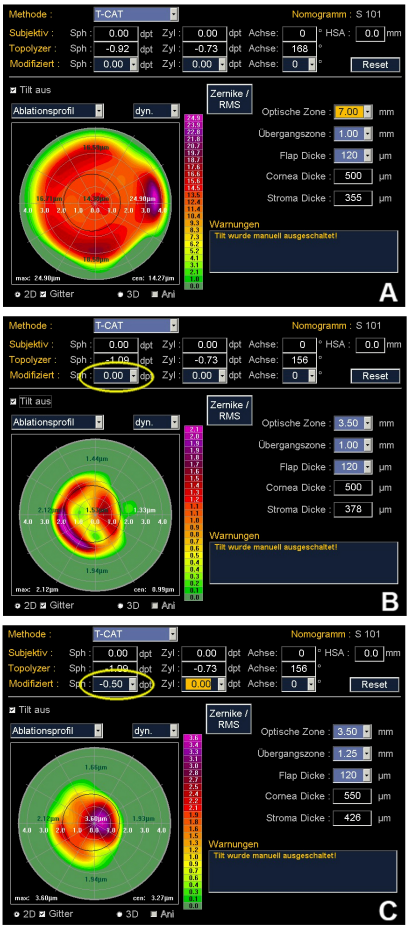

Figure 3. Standard and customized treatment strategies for the correction of CSI. In previous studies, either PTK (A) or PRK (B) ablation modes were used in combination of assessment of CSI's height by the Munnerlyn formula. Due to the nature of the ablation algorithms, neither a PTK (top-hat) nor a PRK (parabolic) algorithm fully correct for the CSI whereas the new customized algorithm (C) presented here provides full CSI correction.

weeks. Additional postoperative follow-ups were performed at 1 month and 3 months after treatment.

Results

In the past year, we have used this technique in a total of three cases. We will present the new technique with one representative case. The other two patients were treated accordingly and in both cases, UCVA and increased from 20/60 to 20/16 early and late postoperatively.

Representative case

A 47-year-old man was examined in November 2004. He had a history of previous LASIK in 2003 for Sph: -5.0 Cyl-0.75 @ 5º on his right eye. Before the procedure, best spectacle-corrected visual acuity (BSCVA) was 20/16 for the right eye. At the time of our first examination his postoperative UCVA and BSCVA was 20/40 with improvement with pinhole to 20/20. Corneal topography showed a SCI (Fig. 1A) and central corneal thicknesses of 500 µm. He re-

ported glare and halos at night and inconvenience of vision.

After relifting of the flap, treatment was performed as a topography-guided LASIK procedure. At the first postoperative day, UCVA was 20/20 and increased to 20/16 at 1 month after treatment. At the 1 month and 3 month follow-up, corneal topography revealed disappearance of the SCI (Fig. 1B). Accordingly, glare and halos under mesopic conditions were diminished.

Discussion

A steep central island represents an area of localized steepening in the central cornea leading to multifocality. [22, 27] Steep central islands may occur both after PRK and LASIK. 1,6 Symptoms include ghost imaging, halos, glare, night driving disability, reduced BSCVA, reduced contrast sensitivity and monocular diplopia leading to slow visual rehabilitation. [23, 35] Under experimental conditions, SCI formation has been almost exclusively observed after treatment with broad beam lasers and rarely with scanning slit and flying spot systems. [34]

In PRK, steep central islands occur in up to 70% of cases at one week after treatment. [23] However, they tend to resolve with time to an incidence of 2% at 6 months after surgery. [24, 25] Apparently, in PRK, the strong epithelial and stromal healing response levels out irregularities leading to gradual disappearance of SCI. In LASIK, in contrast, SCI formation occurs in only 5 to 12% of cases at 1 week after treatment. [25, 32] However, at 6 months after surgery, typically, three out of four steep central islands were still present. [25] This might be due to the nature of the LASIK procedure leading to a limited epithelial and stromal wound healing reaction.

Although the incidence of SCI formation is nowadays significantly reduced by the use of flying spot laser systems, it nevertheless should be regarded as important in clinical routine since a large number of patients who have been treated with first- and second-generation laser systems still require retreatments for correction.

The nature of SCI formation still remains unclear. In the past, two different mechanisms were hypothesized responsible: First, ablation shock waves may induce intrastromal shifts of water leading to different levels of corneal hydration in the centre and the periphery [36, 37] and second, the laser beam might be blocked centrally by the ejected vortex plume of gaseous and particulate debris generated during surgery. [23, 32, 38] In support of the second hypothesis, Cua

and Pepose reported an increased incidence of SCI after LASIK in a laser system where the plume evacuator was accidentally installed improperly. [39]

To prevent SCI formation, various laser systems incorporated anti-steep central island programs where a specific overcorrection within the central 25% of the ablation zone should compensate for the undercorrection. However, results were not always satisfactory. [24, 34, 40-42] Moreover, other attempts were undertaken to correct steep central islands by topography-guided re-treatments using topography only as a descriptor of the power of the SCI rather than the actual height data, still solely relying on Munnerlyn's formula and a standard PTK or PRK formula (Fig. 2). [43] However, current algorithms are unable to properly approximate the difference height map due to the small size of steep central islands.

We present a new ablation algorithm based on the following principle: a precise corneal topography allows the generation of a correct height map. The difference to the best-fit conoid may then be calculated and approximated by Zernike polynomials. The

key point of the technique presented here lies in the precision of approximation, which is dependent on the ablation area. Fig. 3A and 3b demonstrate the Zernike fit error for different areas of approximation. When using the standard approximation area with a diameter of 7 mm the Zernike fit error is in the order of microns, which is close to the height of the island itself. In consequence, most of the island would be missed using this algorithm (Fig. 3A). However, when decreasing the area of approximation to 3.5 mm the Zernike fit error is in the submicron range (at least in the area of interest) (Fig. 3B). Furthermore, the spherical correction must be adjusted because removal of the SCI includes a spherical shift, which is not related to the refraction of the eye treated. We adjusted the sphere in a way that no tissue is removed at the edges of the ablation area (Fig. 3C) and the height of the SCI as determined by Munnerlyn's formula is removed. In the case presented the refractive height of the SCI was 2 diopters and the diameter was 2mm. According to Munnerlyn's formula the height was

$$1/3 \times 22 \times 3\ \mu m = 4\ \mu m$$

The peak amount of tissue removed equals 3.6 µm, which is close to the height calculated. In 1998, Manche et al. presented cases of SCI removal using a PTK ablation mode and proposed to use a PRK mode to improve results. [43] However, both approaches do not address

the true shape of the SCI but match only the central amount of tissue removed by the height of the SCI (Fig. 3A,B). Usually, SCI are not symmetric having a higher refractive power in the centre with variable slopes in different meridians. Therefore, they rather need a customized ablation algorithm as the one presented here.

The strategy whether to lift the flap or perform a surface ablation clearly depends on the depth of ablation. Scarring of the cornea should occur only if Bowman's membrane is penetrated during ablation. In cases where the ablation depth is larger than 7 to 8 microns we suggest to either perform a relift with subsequent ablation in the stromal bed or to alternatively perform a PRK on the flap followed by the application of mitomycin C (2 sponges soaked with mitomycin C 0.02%, 1 minute of action each).

Our approach was to decrease the area of approximation in order to more accurately treat the SCI. An alternative approach would be the use of higher orders of approximation higher than the sixth order. Since higher order approximations using Zernike polynomials are inconvenient and slowly converting, the mathematical alternative would be Fourier or Taylor analysis. Although this approach has already been used clinically, we have not found any scientific and peer-reviewed report on this topic.

In summary, this new ablation algorithm represents a promising step towards the visual rehabilitation of patients suffering from visual impairment due to steep central island formation after refractive surgery.

2.3

Anterior Lamellar Keratoplasty with a Microkeratome: a Method for Managing Complications after Refractive Surgery

Abstract

Objective. *To demonstrate a technique of anterior lamellar keratoplasty (LKP) with a standardized and automated preparation of surface-parallel cuts appropriate for addressing several problems after LASIK and PRK.*

Methods. *Noncomparative case series of 10 eyes with complications after LASIK and PRK. Lamellar cuts were performed in donor and recipient eyes by means of an automated microceratome (Schwind, Kleinostheim, Germany). Lamellar grafts were fixed by only 4 single sutures. In two cases, a re-lift LASIK was performed after 6 months.*

Results. *Surgery was uneventful and visual acuity (VA) was improved in all cases. Residual irregular astigmatism and refractive error was corrected in two cases by means of computer-assist ablation resulting in a further improvement of BCVA and unaided VA.*

Conclusions. *Anterior lamellar keratoplasty with a microceratome is an easy-to-perform procedure and can be used for the management of certain complications of PRK and LASIK.*

Hafezi F, Mrochen M, Fankhauser F 2nd, Seiler T.

J Refract Surg 2003; 19(1):52-57

Introduction

To date, keratoplasty following refractive surgery is a rare procedure when compared to the number of corneas transplanted after cataract surgery because of postoperative corneal decompensation. However, in the past few years the frequency of refractive surgery has increased dramatically and i.e. exceeded that of cataract surgery in the USA by a factor of 2 in 1999. Thus, refractive surgery will inevitably encounter a significant increase of postoperative complications in the near future. These are located in the anterior cornea and include severe scarring after photorefractive keratectomy (PRK), cutting errors and recurrent epithelial ingrowth after laser in situ keratomileusis (LASIK). [44, 45]

Recently, a new technique for the management of such complications was presented: therapeutic lamellar keratoplasty (LKP) with an automated microceratome which combines the known technique of superficial lamellar keratoplasty with the automated preparation of the donor lamella and the recipient wound bed using microkeratomes originally developed for LASIK. [46] Here, we present the results of automated anterior lamellar keratoplasty in a series of 10 eyes that had superficial complications after refractive laser surgery of the cornea.

Patients and Methods

Patients

Ten eyes of 10 consecutive patients, referred to our department because of complications after refractive surgery, underwent anterior lamellar keratoplasty with a microceratome from January 1999 to July 2000. Four eyes had an irregular corneal surface due to cutting errors and epithelial ingrowth after LASIK for correction of myopic astigmatism (Fig. 1), 4 eyes showed apical scars after hyperopic PRK, and 2 eyes displayed severe scarring (haze 4) more than 1 year after myopic PRK. Patient's age ranged from 28 to 51 years with an average of 34 ± 12 years.

Due to the multifocality and the turbidity of the corneas only a gross refraction was possible (Table). To illustrate preoperative multifocality a corneal topography is shown in Figure 2. Informed consent was obtained after a thorough explanation of the benefits and risks of the operation. Institutional review board approval was not required for this study.

Examinations

Preoperatively and at months 1, 3, and 6 after surgery patients received a standard ophthalmic examination including unaided and best spectacle-corrected visual acuity (BCVA), slit lamp inspection, indirect fundus examination (with subsequent direct ophthalmoscopy using the Goldmann contact lens in the presence of apparent retinal lesions), applanation tonometry, and corneal topography (C-scan, Technomed, Baesweiler, Germany). Corneal central and peripheral pachymetry (SP-2000, Tomey, Nagoya, Japan) was performed prior to surgery.

Surgical Management

The basic idea of anterior lamellar keratoplasty with a microceratome is to create a free cup in the donor and recipient eye using the identical automated microceratome. The graft is then placed on the host wound bed and fixed with four temporary and one permanent superficial suture in a way that allows a re-lift LASIK to be performed to correct residual refractive error and irregular astigmatism, if needed.

Preparation of the grafts

The graft was prepared out of the whole eye with controlled intraocular pressure (IOP). The eye was pressurized using a canule inserted through the optic nerve connecting the vitreous cavity with a water reservoir to achieve an IOP of 60 mmHg. Recipient and donor corneas were marked with an asymmetric 5 ray-radial marker. Only eyes with intact epithelium were used for transplantation.

Particular care was taken to the following points to guarantee constant donor corneal disc diameter: in 8 of the cases the lamella was prepared by means of the Schwind mikrokeratome II (Schwind, Kleinostheim, Germany) equipped with a special cutting head that provides lamellae of a thickness of 180 ± 26 µm as determined by optical pachymetry in pig eyes. Briefly, the cornea was applanated by means of a quartz plate, followed by the cut, which was performed using a surface-parallel sapphire blade. A second suction ring fixed the lamella during the cut and cut length was adjusted electronically to create a free cup. The lamellae had a constant diameter of 8.5 mm due to the geometry of the applanation area of the microkeratome. To achieve constant corneal thickness, only corneas from donors who died less than 12 hours prior to transplantation were used. To avoid swelling of the transplant after harvesting it was stored in Licorol DX R-solution (Chauvin, Labege, France) until

the recipient wound bed was prepared appropriately.

In the two cases showing cutting errors after LASIK the identical technique was used. Here, however, a microceratome of the Cariazzo-Barraquer type (Supratome, Schwind, Kleinostheim, Germany) was used and the cut was completed manually with a blade.

Preparation of the recipient

The recipient cornea was prepared by creation of a free surface-parallel lamella using the identical marker and automated microceratome as in the donor eye. In the two cases with cutting errors, again, the existing cut was completed manually. In one case (after hyperopic PRK) a lateral canthotomy was performed to obtain sufficient suction. The wound bed was cleaned carefully by means of a wet sponge and a blunt hockey knife and the epithelium was stripped back at the cut edges. The whole procedure was performed under retrobulbar anaesthesia.

Transplantation

The graft was placed onto the wound bed with the graft's marks aligned to those of the recipient. After two transient sutures, 4 single superficial sutures were placed at 3, 6, 9, and 12 o'clock so that tension lines would form a regular rhombus. Sutures were placed superficially in the anterior stroma crossing the wound bed only close to the edge. The interface was then carefully floated with balanced salt solution (BSS) to prevent epithelial ingrowth. An additional superficial suture was placed nasally superior and remained at least 6 months or until a decision could be made whether a re-lift of the transplant was necessary. At the end of the procedure, a bandage lens soaked with ofloxacine 0,5% was used to decrease postoperative foreign body sensation.

Postoperative Management

The bandage lens was removed at post-op day one and the corneal epithelium was examined by fluorescein staining. As soon as the epithelium was fluorescein-negative the 4 radial sutures were removed. Until removal of the sutures topical medication included antibiotic drops (ofloxacine 0.5%) every two hours. After removal of the sutures patients were instructed to use rimexolol drops (Vexol, Alcon, Ft. Worth, Texas) 4 times a day for two months and tapered during post-op months three and four.

The correction of a residual refractive error and the correction of irregular astigmatism was undertaken in two cases at 6 months after transplantation using topography guided LASIK (ORK-software, Multiscan, Schwind, Kleinos-

theim, Germany) and a re-lift of the flap. At 6 months after automated lamellar keratoplasty the manifest refraction as well as corneal topography had stabilized.

Results

Surgery went uneventful in all 10 eyes. In two eyes, the graft epithelium was loose and oedematous and was removed during the operation. At day 1 after surgery, the graft was swollen with prominent edges in all cases. The 4 sutures were removed after healing of the epithelium and clarification of the lamella, which occurred within 6 days in all eyes. In no case additional sutures were necessary. Eight cases displayed residual donor epithelium healing lines at months 1 and 3, which were interpreted as epithelial rejection lines. In 7 of the 10 eyes a central steepening was apparent at months 1 and 3 that decreased within 6 months after surgery. In one case at three months after surgery a sterile infiltrate occurred in the interface that healed under topical corticoid therapy within a week.

Visual results are listed in Table 1. Visual acuity recovered within the first

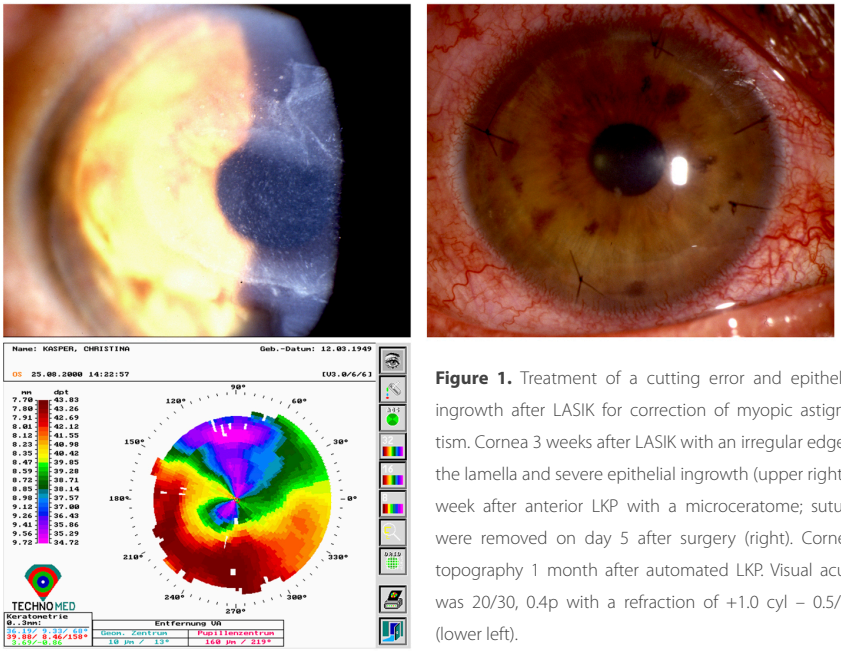

Figure 1. Treatment of a cutting error and epithelial ingrowth after LASIK for correction of myopic astigmatism. Cornea 3 weeks after LASIK with an irregular edge of the lamella and severe epithelial ingrowth (upper right). 1 week after anterior LKP with a microceratome; sutures were removed on day 5 after surgery (right). Corneal topography 1 month after automated LKP. Visual acuity was 20/30, 0.4p with a refraction of +1.0 cyl – 0.5/60° (lower left).

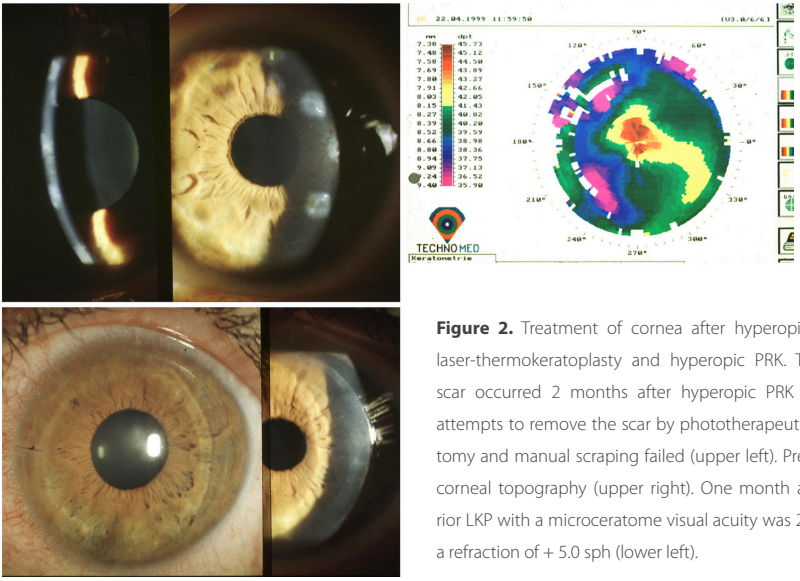

Figure 2. Treatment of cornea after hyperopic HO:YAG laser-thermokeratoplasty and hyperopic PRK. The apical scar occurred 2 months after hyperopic PRK and two attempts to remove the scar by phototherapeutic keratectomy and manual scraping failed (upper left). Preoperative corneal topography (upper right). One month after anterior LKP with a microceratome visual acuity was 20/50 with a refraction of + 5.0 sph (lower left).

month after surgery but BCVA was limited by the multifocal cornea. Visual rehabilitation to a BCVA of 20/40 or better was achieved in 7 of the 10 eyes. On average, BCVA improved from 20/200 ± 20/200 to 20/40 ± 20/100 ($p < 0.05$).

A typical example is described in the following case report:

A 42-year-old female patient received bilateral simultaneous LASIK for myopic astigmatism in a local laser centre. Preoperative BCVA was 20/20 OU. According to the operation report a cutting error occurred in the left eye. The flap had an irregular form and was incomplete. After manual flap completion a 3.5 D laser treatment for correction of myopia was performed. Postoperative BCVA was never better than 20/100 and when the patient was referred to our department on post-op day 21 visual acuity was counting fingers. The flap was oedematous and epithelial ingrowth had led to melting of the flap (Fig. 1). We removed the primary flap by completing the original cut, cleaned the wound bed carefully by means of a hockey knife, and performed an anterior lamellar keratoplasty with a microceratome.

After removal of the 4 sutures BCVA was 20/100 and improved to 20/60 at 1 month and 20/30 at month 3 after keratoplasty. BCVA did not improve further and a topography-guided laser treatment was performed at month 6 includ-

Table 1 Visual acuity after automated lamellar keratoplasty

Case	*Reason for grafting*	*Preoperative*	*Postoperative at 6 months*
1	Complicated LASIK	20/200	20/40
2	Complicated LASIK	CF*	20/30
3	Complicated LASIK	20/100	20/40
4	Complicated LASIK	20/400	20/50
5	Severe scar after PRK	20/200	20/60
6	Severe scar after PRK	20/200	20/30
7	Apical scar after HORK**	20/100	20/50
8	Apical scar after HORK	20/400	20/40
9	Apical scar after HORK	20/100	20/30
10	Apical scar after HORK	20/200	20/25

* Counting fingers **hyperopic PRK

ing an uncomplicated re-lift of the flap. One month after this re-operation unaided VA was 20/25 (+1).

A second case demonstrates the effect of automated LKP in a cornea after hyperopic HO:YAG laserthermokeratoplasty and hyperopic PRK where all previous attempts to remove the apical scar failed (Fig. 2). Here, BCVA increased from 20/100 preoperatively to 20/50 one month postoperatively.

Discussion

The key findings of this study are that in cases with visually significant complications after lamellar refractive surgery automated LKP led, within a reasonable rehabilitation time, to a visual acuity of 20/40 in 70% of the cases. Further improvement might be obtained by re-operations using computer-assist ablation (topography- or wavefront-guided).

By the midst of the last century anterior LKP was a popular and frequently used method in corneal surgery. However, in the 1960s anterior LKP was subsequently replaced by PKP. This tendency was accelerated by the growing knowledge of the molecular events leading to graft rejection and the development of improved surgical instrumentation and techniques. [47]

LASIK and PRK, however, are lamellar techniques and therefore the majority of problems after refractive surgery occur at the anterior surface of the cornea:

scarring after PRK, cutting errors during LASIK and recurrent epithelial ingrowth after LASIK with melting of the flap. [44, 45] In some cases, those conditions cannot be managed other than by keratoplasty.

We suggest that in these cases LKP rather than PKP should be envisaged for the following reasons: [48] First, the corneal endothelium is not transplanted resulting in fewer rejections and less rigid selection criteria for donor material. Second, anterior LKP is less invasive than PKP thus reducing complications.

In the case of iatrogenic keratectasia however, where the biomechanical stability of the residual stroma is insufficient for anterior LKP, penetrating keratoplasty until recently represented the technique of choice. A new alternative way to manage iatrogenic keratectasia may be deep lamellar keratoplasty where a significant part of the corneal stroma is replaced by donor stroma while the recipient's endothelium and Descemet's membrane are still preserved. [49]

Until recently, lamellar keratoplasty was technically difficult to perform and optical rehabilitation, one of the main goals, was not always achieved. Furthermore, the manual preparation of the lamellae (donor and recipient) often caused irregularities of the interface with subsequent consequences on postoperative healing and vision. The approach presented here, inaugurated recently and independently from us, may help to overcome these problems since the manual preparation of the surface-parallel cuts is markedly improved by a standardized technique and reproducible thickness of donor and recipient lamellae is achieved. This standardization significantly shortens postoperative rehabilitation by allowing suture removal already after a few days.

Another advantage of automated LKP in the management of complications after refractive surgery is the possibility of a re-treatment by lifting the flap to correct for any residual refractive error or irregular astigmatism reducing the patient's visual acuity. Here the remaining superficial suture serves as an artificial hinch allowing a re-lift of the flap similar to the re-lift performed in re-LASIK.

Although the superficial suture might induce some degree of corneal astigmatism we believe that its function as a hinch is more important for the procedure than its astigma-tism-inducing effect. The additional laser ablation may be performed as topo-graphy-guided ablation in gross irregularities or as wavefront-guided ablation for fine-tuning of corneal optics. [31] The two re-lifts performed at 6 months after surgery

were uneventful and resulted in an improvement in best spectacle-corrected visual acuity to 20/30 in both cases.

In summary, we suggest that anterior LKP with a microceratome may be used for surface problems of the cornea and particularly problems after LASIK and PRK: the procedure is easy to perform using the same cutting technique as for LASIK. Furthermore, sutures can be removed after a few days and later refractive reoperations open further alleys for visual rehabilitation. In this small series we have not encountered problematic rejections of transplanted lamellae. However, such rejections have been reported elsewhere to be rare. Therefore, longer follow-up and a larger number of cases are required to estimate the effective clinical value of this procedure.

2.4

Two-step Procedure to Enlarge Small Optical Zones after Photorefractive Keratectomy for High Myopia

Abstract

Objective. *Here we describe a method for the visual rehabilitation of patients suffering from small optical zones and related complaints after photorefractive keratectomy (PRK) and laser in situ keratomileusis (LASIK) for high myopia. In many of these cases that occurred in the early 1990s, low central corneal thickness in combination with residual myopia does not allow for enlargement of the small optical zone by a topography-guided treatment in the first instance.*

Methods. *In a first step, a clear lens exchange is performed aiming at hyperopia. This enables us to perform in a second step a topography-guided customized PRK with marked enlargement of the optical zone.*

Results. *At 3 months after surgery, the optical zone is usually enlarged by 2 to 3 mm with massive reduction of preoperative visual symptoms under mesopic conditions.*

Conclusions. *Such two-step procedures may be of distinct benefit to patients suffering from small optical zones and low central corneal thickness.*

Hafezi F, Mrochen M, Seiler T.

J Cataract Refract Surg 2005; 31:2254-2256

Introduction

In the early and mid 1990s photorefractive keratectomy (PRK) for myopia of more than -7.0 D sphere was a frequently performed procedure. [50] By that time, relatively little was known about corneal wound healing and the procedures often led to corneal scarring, decentered ablations, regression and, in the case of excessive surface ablation, even to iatrogenic central keratectasia. [51, 52] Even if none of the above mentioned complications occurred, the treatment was associated with small optical zones with resulting halos and glare under mesopic conditions and even monocular diplopia. [53, 54] Many of these former refractive patients seek help in recently developed techniques such as customized ablations. [29] However, many of these cases show residual myopia combined with critically low central corneal thickness. Here, a primary topography-guided treat-ment to enlarge the optical zone is obsolete because of distinct keratectasia risk (Fig. 1). [51, 52]

We have therefore developed a 2-step procedure for the treatment of such cases: in a first step, a clear lens exchange shifts the patient to hyperopia. Calculation of a topography-based ablation profile now shows that ablation in the centre of the cornea is minimal (Fig. 2), thus enabling the customized topography-guided treatment (Fig. 3).

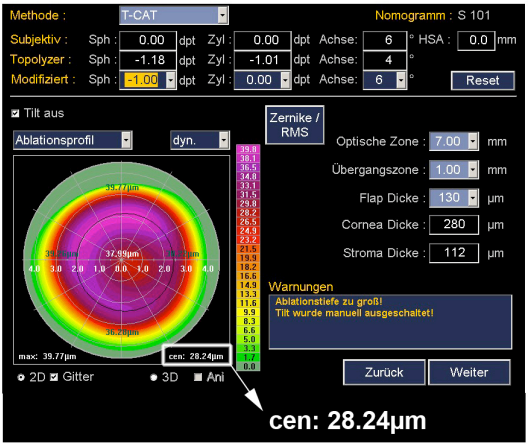

Figure 1. Ablation profile approximated by Zernike polynomials based on topographies taken before any procedure was undertaken. Enlargement of the optical zone cannot be performed because residual central corneal thickness would be dangerously low.

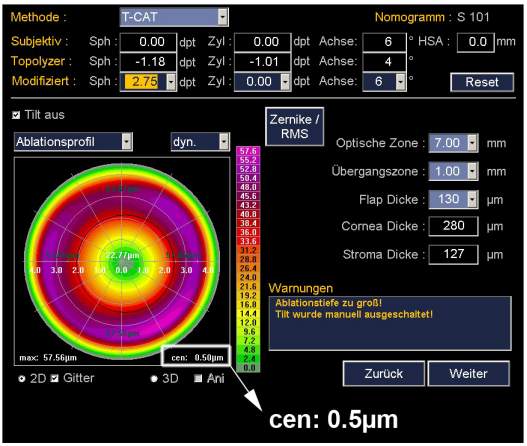

Figure 2. Ablation profile approximated by Zernike polynomials based on topographies taken after a clear lens exchange (same patient as figure1). Now, the ablation profile focuses on the peripheral cornea whereas central corneal thickness remains unchanged.

Technique

In the past two years, we have used this technique in a total of 5 patients. Here, the proceeding is demonstrated in the case of a 41-year-old man who was examined in October 2003. He had a history of previous PRK in 1996 for -9.0 D sphere on both eyes. Uncorrected visual acuity (UCVA) was 0.5 for the right eye and 0.7 for the left eye. Best spectacle corrected visual acuity (BSCVA) was 0.8 for both eyes with -1.0 D sphere. Corneal topographies (axial representation) showed bilateral small optical zones of approximately 2mm (right eye, Fig. 3A) and central corneal thicknesses of 280 (right eye) and 270 (left eye) µm, respectively. He reported massive glare and halos under mesopic conditions (pupil size ≥5mm), especially on the right eye.

Symptoms were more pronounced on the right eye and we decided to first treat the right eye until the patient's symptoms would improve markedly. Central corneal pachymetry was 280 µm and prohibited further central ablation. Enlarging the optical zone even refractively neutral would require a central (PTK) ablation thus further thinning the cornea centrally (Fig. 1).

Based on corneal topography we calculated the ablation pattern (T-Cat software, Wavelight Technologies, Erlangen, Germany) for expanding the optical zone to a diameter of 5 to 6 mm. We then optimized the spherical part of the ablation so that the central keratectomy depth was zero, which happened at a spherical correction of +2.0D. Therefore, we performed a clear lens exchange in this pre-presbyopic patient with in-

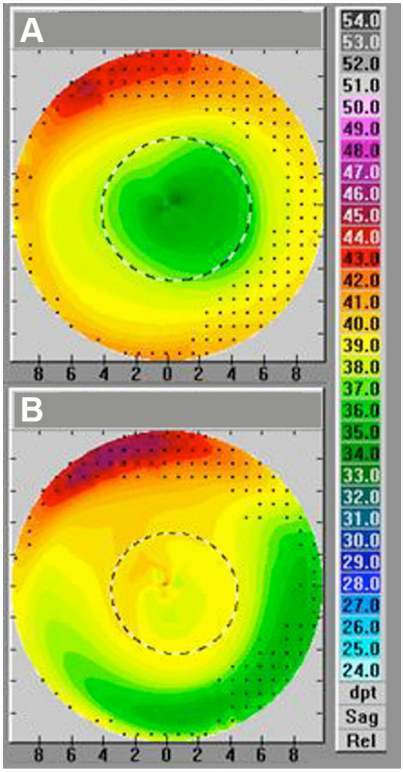

Figure 3. Topographies (axial representation) taken before (A) and at 3 months after (B) the 2 step-procedure. A significant enlargement of the optical zone from 2 mm to 5 to 6 mm was achieved despite low central corneal thickness.

tended hyperopia of +2.0D. Inclusion criteria for the clear lens exchange in this patient were his age (pre-presbyopic) and the absence of stromal scars as a complication of the former surface ablation. We used Haigis formula for calculation of the refractive power of the IOL7 and implanted an ACRYSOF© Lens (Alcon, Ft. Worth/TX, USA).

At 2 months after the first procedure, UCVA was 0.4 and BSCVA was 0.8 with +2.75 D sphere. Again, ablation profiles were calculated now leaving the central cornea unaltered (Fig. 2). 6 months later, we performed a PRK for correction of hyperopia and enlargement of the optical zone. 3 months later, UCVA was 0.8. Zernike analysis of the pre- and postoperative corneal topographies revealed virtually identical coma-like aberrations, however an improvement in spherical aberrations by a factor of 2.7 and accordingly, halos and glare were massively reduced. The optical zone was distinctly enlarged from 2 mm before

the 2-step procedure to 5 to 6 mm (Fig. 3A,B).

Discussion

Topography-guided customized PRK has been repeatedly used for the enlargement of small optical zones after initial PRK for high myopia. [29] However, small optical zones with low residual corneal thicknesses are a frequently encountered entity after PRK for high myopia in the early and mid 1990s. [50] Here, the risk of induction of postoperative keratectasia [52, 55] often prohibits any further central ablation or does not allow for full spherical correction.

This dilemma may be solved by first performing a clear lens exchange thus shifting the patient to hyperopia. The second step in visual rehabilitation is a customized topography-guided PRK treatment for hyperopia ablating the peripheral cornea where sufficient corneal thickness is still present.

In such way, enlargement of the optical zone up to 7 mm of diameter is possible. Such 2-step-proce-dures may be of general benefit in the visual rehabilitation of presbyopic patients suffering from small optical zones in the absence of corneal scars after PRK for high myopia.

2.5

Corneal Crosslinking-induced

Stromal Demarcation Line

Abstract

Objective. *Corneal collagen cross-linking by UVA/riboflavin (X-linking) represents a new method for the treatment of progressive keratoconus and currently is under clinical investigation. In order to avoid UVA irradiation damage to the corneal endothelium, the parameters for X-linking are set in a way that effective treatment only occurs in the first 300 µm of the corneal stroma. Here, X-linking not only strengthens the biomechanical properties of the cornea but also induces keratocyte apoptosis. To date, the effectiveness of treatment could only be monitored indirectly by postoperative follow-up corneal topographies or using corneal confocal microscopy. Here we describe a corneal stromal demarcation line indicating the transition zone between crosslinked anterior corneal stroma and untreated posterior corneal stroma. The demarcation line is biomicroscopically detectable in slit lamp examination as early as 2 weeks after treatment.*

Methods. *X-linking was performed in sixteen cases of progressive keratoconus and corneas were examined biomicroscopically and by means of corneal topography and pachymetry before and after treatment.*

Results. *In 14 of 16 cases a thin stromal demarcation line was visible at a depth of approximately 300µm over the whole cornea following X-linking treatment.*

Conclusions. *This newly observed demarcation line may result from differences in the refractive index and/or reflection properties of untreated versus X-linked corneal stroma and represents an effective tool to biomicroscopically easily monitor the depth of effective X-linking-treatment in keratoconus.*

Seiler T, Hafezi F.

Cornea 2006;25:1057-1059

Introduction

Keratoconus represents a disorder of the corneal stroma that is associated with decreased biomechanical strength of the tissue, probably due to diminished intra- and interfibrillar crosslinks of the collagen fibers. [56] Recently, a new method has been developed for the treatment of progressive keratoconus, which currently is under clinical investigation: corneal collagen cross-linking with riboflavin/UVA (X-linking). [57, 58] Here, additional crosslinks are formed using UVA and riboflavin as a chromophore. The method has been studied extensively in various animal models for years [57, 59-61] and was successfully applied in a phase 1 clinical trial for progressive keratoconus in humans. [62] Basically, X-linking treatment markedly stiffens the cornea and increases the biomechanical strength by a factor 1.4 in vivo in rabbit corneas and by a factor 4.5 ex vivo in human corneas. [57, 63] To avoid potential irradiation damage to the corneal endothelium by UVA light, the technical parameters are set in a way that only the anterior 300 µm of corneal stroma are treated.

To date, the transition zone between X-linked and untreated corneal stroma could only be visualized using corneal confocal microscopy. [64]

Here we report biomicroscopical identification of a corneal stromal demarcation line that corresponds to this transition zone.

Materials and Methods

Inclusion criteria

16 patients suffering from progressive keratoconus (age range 18 to 39 years, mean age 26.4 years) with maximal corneal K readings of 60 D and central corneal thickness of at least 400 µm were treated by corneal collagen X-linking with riboflavin/UVA. Inclusion criteria were the identification of progressive keratectasia in corneal topographies using both the Schwiegerling Z3 coefficient [65] and an increase of maximal K-readings in several consecutive recordings over a period of up to 6 months, along with anamnestically reported deterioration of vision. Preoperative as well as postoperative examination included slit lamp examination, best spectacle-corrected visual acuity (BSCVA), corneal topography as well as a pachymetry map (Pentacam, Oculus Instruments, Wetzlar, Germany) and applanation tonometry.

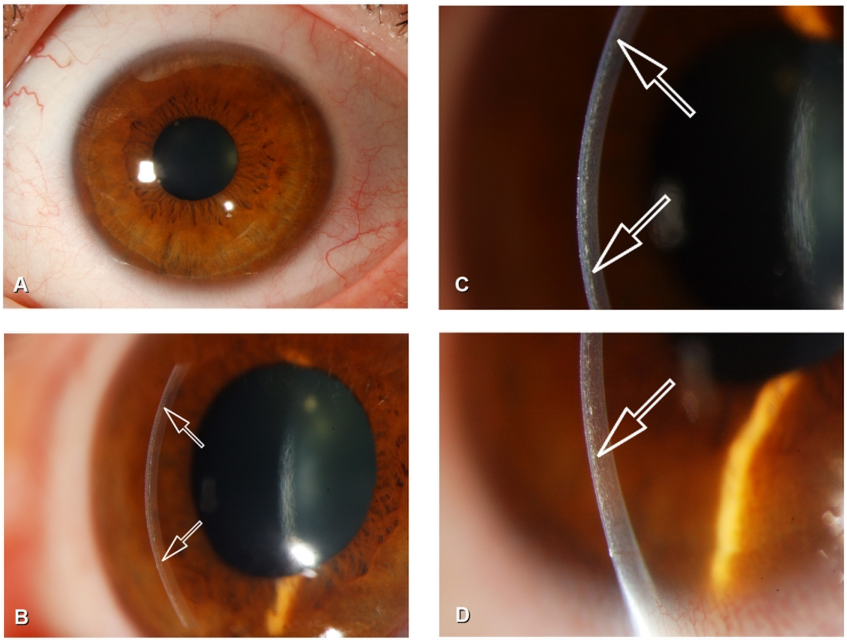

FIGURE 1. Corneal demarcation line after X-linking. A, Regular aspect of the cornea at 2 weeks after X-linking (top left). B, The demarcation line (arrows) lies in a depth of approximately 300µm. The conical shape of the line is explained by the increasing thickness of the cornea in the periphery. C, In the central cornea, the line (arrows) can be identified at approximately 60% corneal depth. D, In the (thicker) periphery the line (arrow) lies at approximately 30-40%.

Preparation of 0.1% riboflavin solution

Dilute Vitamin B2-riboflavin-5-phosphate 0.5% (G. Streuli & Co. AG, Uznach, Switzerland) with dextran T500 (Roth AG, Karlsruhe, Germany) to achieve a 0.1% Riboflavin solution. The solution was protected from light and used within 24 hours.

Corneal collagen riboflavin/UVA-cross-linking (X-linking)

The procedure was performed as described previously. [62] Briefly, topical anaesthesia was applied prior to the procedure using tetracaine 1% and oxybuprocaine 0.4% eye drops (Novartis Pharma, Bern, Switzerland). The corneal epithelium was mechanically removed with a diameter of 6 mm using a blunt knife and riboflavin 0.1% solution was

instilled repeatedly for approximately 20 minutes. Penetration of the cornea and presence of riboflavin in the anterior chamber (riboflavin shielding) was monitored with slit lamp examination. UVA irradiation was performed using an optical system (Köhler illumination) with a light source consisting of an array of 7 UV diodes (365 nm; Nichia, Nuernberg, Germany) with a potentiometer in series to allow for regulation of voltage. Prior to treatment, intended irradiance of 3 mW/cm^2 surface irradiance (5.4 J/cm^2 surface dose) was calibrated using a UVA meter (LaserMate-Q; LASER 2000, Wessling, Germany) at a working distance of 1 cm. Irradiance was performed for 30 minutes using 3 mW/cm^2, corresponding to a dose of 5.4 J/cm^2.

During treatment, riboflavin solution was applied every 5 minutes to saturate the cornea with riboflavin and drops of physiological salt solution were applied every 2 minutes to moisten the cornea. After the treatment, a bandage contact lens soaked with preservative free antibiotic (Ofloxacin) was applied until complete closure of the corneal epithelium, followed by application of fluorometholon eye drops twice daily for 6 weeks.

Results

Postoperative healing was uneventful in all cases. In accordance to previously published data, [62] we detected no side effects of the anterior or posterior segment: in particular, corneal endothelium showed no signs of cytotoxic damage and lens transparency and intraocular pressure remained unchanged.

However, in 14 out of 16 patients, we identified a demarcation line in the deep corneal stroma detectable by slit lamp examination (Fig. 1). In the central corneal stroma, the line can be identified at approximately 60% corneal depth (Fig. 1B,C). The line is best identified with a thin slit and high illumination levels using a slit lamp that provides high levels of white light. In the corneal periphery the line gradually adapts a conical shape due to the increasing total corneal thickness (Fig. 1D). The line becomes visible as early as 2 weeks after treatment and was not present prior to treatment (n=16).

Discussion

When treating patients with corneal X-linking, special emphasis has to be taken to ensure protection of the corneal endothelium from potential UVA irradiation damage. The stromal depth of effective X-linking treatment depends on the concentration of riboflavin solution and the intensity of UVA light. The ideal riboflavin concentration and UVA intensity levels were identified through dose/concentration essays in vitro and in various animal models. [57-59, 61, 66-68]

The parameters currently used in humans (international multicenter clinical phase 2 study monitored by us) are 0.1% riboflavin solution and 3 mW/cm^2 of UVA. It has been shown unambiguously that at these settings the effect of X-linking is limited to the anterior 300µm of the cornea. [60] Furthermore, only patients with a central corneal thickness of at least 400 µm are subjected to this treatment.

Besides induction of additional crosslinks between collagen fibers, the X-linking treatment induces various other stromal changes: Wollensak and colleagues have shown induction of keratocyte apoptosis in the rabbit cornea following cross-linking treatment. [60] However, corneal transparency and thickness remained unchanged and keratocyte apoptosis also occurs following PRK, LASIK and even corneal abrasion. [69]

In consequence, following X-linking treatment one should differentiate between the treated anterior corneal stroma and the untreated posterior corneal stroma. The positive effect of corneal X-linking on corneal biomechanics can be monitored indirectly using corneal topography. However, until recently, there was no method available to directly monitor the effect of corneal X-linking on the anterior corneal stroma.

In a recent study, Caporossi's group has performed confocal microscopy analyses in humans following X-linking. [64] Interestingly, they in vivo detected the effective depth of treatment by identifying distinct vertical and lateral transition areas at a depth of 270 to 330µm. Here, the anterior (treated) stroma showed oedema with only few keratocyte nuclei and poor reflectivity whereas the posterior (untreated) stroma showed regular keratocyte population and normal reflectivity. Keratocyte repopulation of the treated stroma started at 1 month after treatment and was completed at 6 months after treatment. Corneal endothelium showed regular morphology up to 6 months after treatment.

In accordance with these findings, we here report identification of a corneal

stromal demarcation line that becomes visible at 2 weeks after X-linking treatment in a depth of approximately 300 µm. To our knowledge, presence of such a demarcation line following X-linking has not been reported to date and ultimately implies either a change in the refractive index and/or reflection properties of treated versus untreated cornea. Based on the findings by Caporossi et al. [64] we suggest that this line actually represents the demarcation line between crosslinked und untreated cornea.

The demarcation line described here represents, besides corneal topography, a direct clinical sign to detect the effect of X-linking in the cornea and, in addition, may help to clinically estimate the thickness of the stromal layer that underwent X-linking.

In conclusion, biomiscroscopic identification of this line represents a simple and effective clinical tool to easily monitor the effective depth of X-linking treatment.

2.6

Corneal Collagen Cross-Linking with Riboflavin/UVA to treat induced Keratectasia after Laser *in situ* Keratomileusis

Abstract

Objective. *Iatrogenic keratectasia after laser in situ keratomileusis (LASIK) represents a major complication in refractive surgery. To date, rigid contact lenses, penetrating keratoplasty or Intacs were the only therapeutic option in many of these cases. In this study, riboflavin/UVA corneal cross-linking (X-linking) was investigated to decide whether it represents an alternative therapeutic means to prevent keratectasia progression.*

Methods. *Corneal X-linking was performed in eight patients with a formerly undiagnosed forme fruste keratoconus or pellucidal marginal corneal degeneration that underwent LASIK for myopic astigmatism and subsequently developed iatrogenic keratectasia. The postoperative follow-up ranged from 7 to 20 months.*

Results. *UV-induced X-linking led to an arrest of keratectasia progression over a postoperative follow-up period of up to 20 months as demonstrated by stable pre- and postoperative corneal topography and reduction of maximal K readings.*

Conclusions. *Riboflavin/UVA corneal cross-linking increases the biomechanical stability of the cornea and may thus be a therapeutic means to slow down, arrest and even partially reverse the progression of LASIK-induced iatrogenic keratectasia.*

Hafezi F, Kanellopoulos J, Wiltfang R, Seiler T.

J Cat Refract Surg. 2007. 33(12):2035-40

Introduction

Since its first description in 1998 iatrogenic keratectasia induced by laser in situ keratomileusis (LASIK) was quickly recognized as one of the major complications in corneal refractive laser surgery. [55, 70] Affected eyes show progressive central or inferior corneal steepening associated with stromal thinning and significant changes of the refractive error. The major risk factors for the induction of keratectasia after LASIK surgery are low residual stromal thickness (RST), re-treatments and pre-existing abnormal corneal topography (for review see [71, 72]). Until lately, treatment options were limited: aside from rigid contact lenses, some reports indicate that insertion of Intacs might help to mechanically stabilize the cornea. [73-75] However, long-term results of this method are not available yet and most cases are nowadays treated by penetrating keratoplasty. [76]

Riboflavin/UVA-induced cross-linking of corneal collagen (X-linking) is a new method to increase the biomechanical stability of the cornea by the induction of additional crosslinks between or within collagen fibers using UVA light and riboflavin as a photomediator. [58] Its therapeutic potential has been demonstrated in a clinical phase I study for the treatment of progressive keratoconus. [62]

Recently, Kohlhaas et al. reported a case of iatrogenic keratectasia after LASIK that was successfully treated by X-linking. [77] Here, we report successful application of this new method in a series of cases with a follow-up period of up to 20 months.

Methods

Surgical technique

The procedure was performed similarly as described previously. [62] After topical anaesthesia with tetracaine 1% and 0.4% oxybuprocaine eye drops, the corneal epithelium was mechanically removed within a diameter of 6 to 8 mm, followed by application of riboflavin (0.1% solution 10 mg riboflavin-5-phosphate in 10 ml dextran-T-500 20% solution) every 3 minutes for approximately 30 minutes until complete penetration of the stroma and yellow staining of the aqueous (riboflavin shielding). UVA irradiation was performed for another 30 minutes with an irradiance of 3mW/cm^2 (total dose density 5.4 mJ/cm^2) Prior to treatment; the irradiance was calibrated using a UVA meter (LaserMate-Q; LASER 2000, Wessling, Germany) at a working distance of 3 cm.

During treatment, riboflavin solution was applied every 5 minutes to saturate

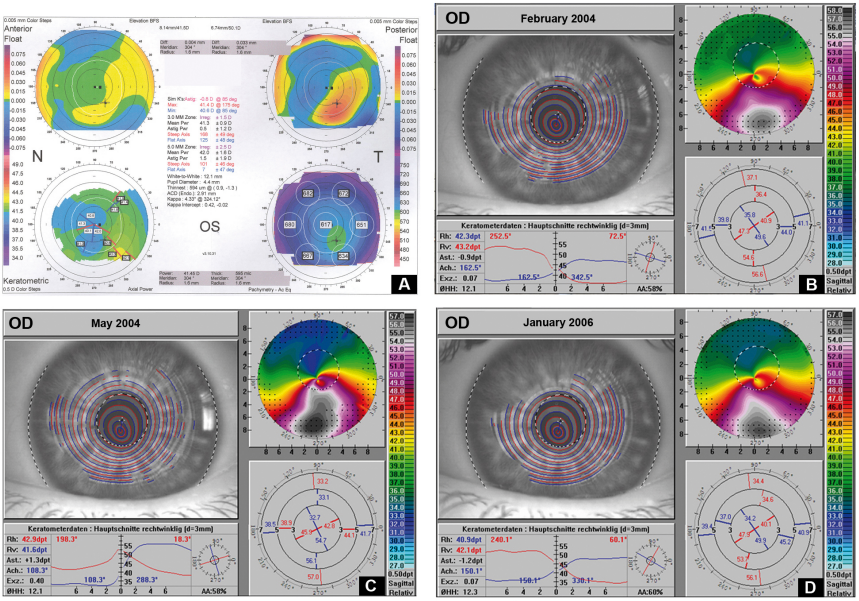

Figure 1. Time course of corneal topographies (axial representation) A: before LASIK surgery. B: At 10 months after LASIK surgery. C: At 13 months after LASIK surgery, one day before UV/riboflavin-induced cross-linking. D: At 20 months after cross-linking, the maximal steepening of the inferior cornea decreased distinctly.

the cornea with riboflavin and drops of balanced salt solution were applied every 2 minutes to moisten the cornea. After the treatment, a bandage contact lens soaked with preservative free antibiotic (Ofloxacin) was applied until complete healing of the corneal epithelium, followed by application of fluorometholon eye drops twice daily for 6 weeks.

Preoperative as well as postoperative examination included slit lamp examination, best spectacle-corrected visual acuity (BSCVA), BSCVA with pinhole, corneal topography as well as Scheimpflug scanning including corneal thickness (Pentacam, Oculus Instruments, Wetzlar, Germany) and applanation tonometry. Inclusion criteria were the verification of progressive keratectasia in corneal topographies using the Schwiegerling Z3 coefficient [65] and increase of maximal K-readings in several consecutive recordings over a period of up to 6 months, a minimal corneal thickness of at least 400 µm and anamnestically reported changes in refraction.

Results

Table 1 summarizes the preoperative and postoperative findings in all patients with iatrogenic keratectasia following LASIK surgery that were treated by X-linking: in 7 of these cases, formerly undiagnosed forme fruste keratoconus (FFKC) was the reason for the biomechanical instability following LASIK, in one case the underlying reason was undiagnosed pellucidal marginal corneal degeneration (PMCD) and in one other case we could not identify a reason. Surgery as well as the postoperative period was uneventful in all cases with one exception where endothelial irregularity and some opacity on the endothelial level were noted. The endothelium cleared up with a normal cell count (2350 cells/mm^2) at 9 months after X-linking. In all cases, progression of keratectasia was arrested and reduction of postoperative cylinder was noted.

Case 1:

LASIK with consecutive iatrogenic keratectasia in preoperatively unrecognized forme fruste or slowly progressive pellucidal marginal corneal degeneration (PMCD)

A 32-year-old male patient presented in 2004 with a history of previous LASIK surgery on the left eye for myopic astigmatism in April 2003. Initially, central corneal pachymetry was 617 µm for the left eye, uncorrected visual acuity (UCVA) was 20/60 and best spectacle-corrected visual acuity (BSCVA) was 20/16 with -2.5cyl-0.75/82°. Corneal topography (axial representation) showed signs of a forme fruste PMCD that was

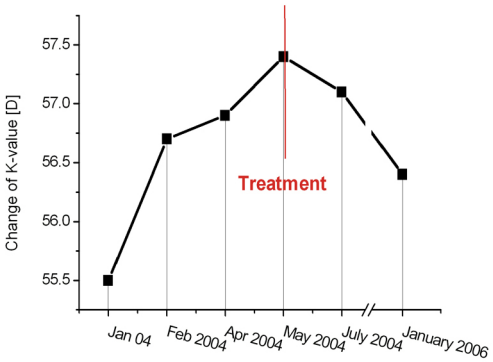

Figure 2. Following initial LASIK surgery, induced keratectasia occurred with progressive increase of maximal K-readings from 55.5 D to 57.4 D until May 2004, the date of X-linking treatment. After X-linking, maximal K-readings decreased to 56.4 D at 20 months after treatment.

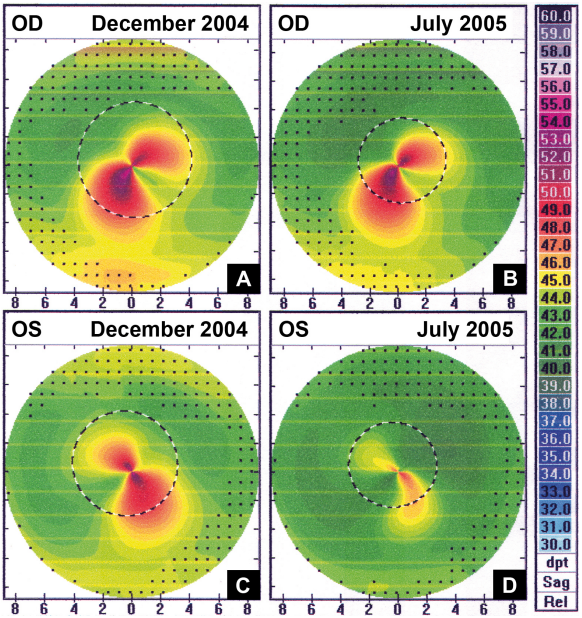

Figure 3. Bilateral iatrogenic keratectasia after LASIK surgery. A: Right cornea with iatrogenic keratectasia at 12 months after LASIK surgery. B: Right cornea topographically unchanged at 19 months after LASIK surgery. C: Left cornea at 12 months after LASIK surgery. D: Left cornea seven months after X-linking with distinct decrease of keratectasia.

not recognized by the surgeon at that time (Fig. 1A). At the first postoperative day, vision was markedly decreased and the patient decided to postpone surgery of the fellow eye.

In our initial examination in February 2004, at 10 months after primary surgery, the left eye showed a UCVA of 20/400, a BSCVA of 20/60 and a corneal thickness of 610 µm. Slit lamp examination revealed a normal state after LASIK. Corneal topography showed decentered ablation with marked inferior steepening (maximal K readings of 55.5D) consistent with the diagnosis of iatrogenic keratectasia after LASIK (Fig. 1B).

In the following 3 months we observed distinct progression of keratectasia in the left eye with a maximal K reading of 57.4D in May 2004 (Fig. 1C). Since penetrating keratoplasty was the only valuable therapeutic alternative, we suggested UV/riboflavin-induced cross-linking as a treatment option to the patient. Informed consent was obtained after the nature of the procedure and its known risks had been explained. During the 20 months following treatment corneal topography of the left eye showed continuous regression of maximal K readings (Fig. 1D and Fig. 2). BSCVA at 20 months after treatment was 20/25 with rigid contact lenses.

Table 1 Underlying reasons and refractive data

		Prior to X-linking						Post X-linking			
Case	Underlying reason	Pachymetry (µm)	BSCVA	Sph	Cyl	Axis	Follow-up / months	BSCVA	Sph	Cyl	Axis
1	forme fruste PMD	610	20/60	1.25	-4.25	101	20	20/25	1.25	-2.25	100
2	no apparent reason	400	20/25	0.00	-3.50	50	7	20/20	0	-1.0	60
3	forme fruste keratoconus	425	20/30	1.00	-3.00	123	12	20/30	0.5	-1.5	115
4	forme fruste keratoconus	400	20/200	-5	-5.5	145	16	20/40	-4	-3.5	155
5	forme fruste keratoconus	420	20/200	-7	-4	115	15	20/50	-5.5	-3.35	110
6	forme fruste keratoconus	480	20/50	-2	-3.5	105	20	20/25	-1.75	-2.25	115
7	forme fruste keratoconus	465	20/200	-3	-5.25	75	18	20/50	-3.75	-3.25	80
8	forme fruste keratoconus	420	20/100	-3.5	-3.75	85	12	20/25	-3.75	-2.25	85

Case 2:

Bilateral keratectasia after LASIK without apparent preoperative ectatic disorder

Another patient showed bilateral keratectasia (Fig. 3A,C) one year after LASIK surgery with slow progression observed in both eyes. X-linking was performed in the left, non-dominant eye. Preoperative central corneal thickness was 400 µm. At 2 weeks after treatment, we noticed localized endothelial damage with concomitant stromal oedema in the central cornea. Stromal oedema slowly resolved within the following 6 weeks. At 7 months after treatment, corneal topography of the left eye showed a significant decrease of central corneal steepening (Fig. 3D) whereas in the right eye, corneal steepening remained unchanged (Fig. 3B). At 9 months, the central irregular endothelium had cleared and the endothelial cell count yielded 2350 cells/mm^2 with mild polymorphism.

Discussion

Although LASIK surgery has become increasingly safe and predictable in the last years, induced keratectasia remains a rare but devastating complication for which the underlying reasons are yet not fully understood. Therefore, it certainly is an advantage to have new therapeutic means to handle a complication of such severity after elective surgery. Clearly, prevention of induced keratectasia was the better strategy and special emphasis should be taken to recognize corneas at risk preoperatively.

Reduction of corneal biomechanical strength seems to be an essential element in the chain of events leading to induced keratectasia after LASIK. The anterior part of the corneal stroma confers more biomechanical strength to the cornea than the posterior stroma [78] and it is the anterior stroma that is weakened by flap generation and tissue ablation in LASIK surgery. It would therefore be of great clinical value to have a tool to de-

termine the individual biomechanical strength of a cornea preoperatively. Such a tool would enable us to detect corneas at risk preoperatively. Unfortunately, such a technique is not yet available but there are promising approaches currently investigated such as determination of corneal hysteresis using an ocular response analyzer or interferometric measurements. [79, 80]

A possible future scenario would then be to either treat these corneas by advanced surface ablation, if applicable or perform a pre-treatment with X-linking, followed by LASIK surgery.

Our results show that riboflavin/UVA corneal cross-linking can at least slow down, arrest progressive, and even partially reverse iatrogenic keratectasia after LASIK. The observed reduction of maximal K-values is due to the increased biomechanical stability of the cornea after cross-linking and is in line with similar findings in primary keratoconus patients treated similarly. [62] These preliminary results demonstrate at least a middle-term efficacy of the technique. However, as with any new surgical technique, safety is a concern. With this technique, special emphasis should be taken preoperatively on minimal corneal thickness because of potential cytotoxic effects of UVA on corneal endothelial cells.

Previous experimental studies in the rabbit cornea as well as in vitro studies in endothelial cell cultures on cytotoxicity to the corneal endothelium have clearly shown that the cytotoxic effect starts at a local irradiance of 0.35 mW/cm^2. [59, 61] Assuming a stroma saturated with riboflavin and a surface irradiance of 3 mW/cm^2, endothelial damage would occur at a depth of 320 µm and less. Therefore, we recommend a preoperative corneal thickness of at least 400 µm to protect the corneal endothelium by the overlying stroma saturated with riboflavin ("riboflavin shielding"). After intraoperative removal of the epithelium, minimal stromal thickness gets close to the 320 µm-limit leading to an increased risk for localized endothelial cell damage. In the previous clinical phase 1 study minimal corneal thickness was more than 400µm in all cases and no endothelial damage was observed. [62]

In the second case presented here where localized endothelial damage after X-linking was observed, central corneal thickness was 400 µm including the epithelium. In such cases, it is recommended to increase corneal thickness to 400 µm and more by swelling using saline solution. A similar scenario may occur if the UVA light source provides an average irradiance of 3 mW/cm^2, however, the irradiation field contains "hot spots". In such a case the dam-

age threshold for endothelial cells may be exceeded locally and therefore, a UV light homogenous within the field of application is mandatory for safety of UVA/riboflavin cross-linking of the cornea (Spoerl et al., submitted)

A major factor predisposing to LASIK-induced keratectasia comprises unrecognized thinning corneal disorders such as keratoconus (KC) or pellucid marginal corneal degeneration (PMCD) including formes frustes of both diseases. In both conditions, altered collagen orientation and structure lead to a decreased biomechanical strength of the tissue. [81, 82] Although all authors agree that corneal thinning disorders represent a contraindication for LASIK and although various indices have been proposed for the recognition of ectatic disorders in corneal topography, [65, 83] the identification of formes frustes of KC or PMCD still remains difficult in some cases.

Other factors include re-treatments, thin corneas and low residual stromal thickness (RST), either due to generation of thick flaps or excessive tissue ablation. [71, 72, 84-87] Here, some authors suggest that an absolute RST of at least 250 µm should be always respected whereas others suggest that the risk for ectasia occurs when the ablation reduces corneal thickness to 55% or more of the preoperative values [55, 70, 86, 87] or even that the minimal corneal thickness might be specific to the individual eye. [71] In some cases of iatrogenic keratectasia, however, even postoperatively, the reason for the keratectasia remains unclear and we have to assume a decreased but asymptomatic biomechanical strength as described in case 2 of this study.

In conclusion, riboflavin/UVA corneal cross-linking increases the biomechanical stability of the cornea and may thus be a therapeutic means to slow down or even arrest the progression of LASIK-induced keratectasia. Further studies must include larger patient numbers and longer follow-ups to verify the permanency of the induced effects and safety and efficacy of X-linking.

Part 3

Prevention of Complications in Refractive Laser Surgery

3.1

Ablation Profiles in Corneal Laser Surgery.

Current and Future Concepts.

Abstract

Objective. *The predictability and quality of results in corneal refractive laser surgery are determined by a number of factors. The calculation and choice of the ablation profile represent central elements. The growing knowledge about the physical and optical properties of the eye in recent years has led to the development of different strategies in the generation of ablation profiles. Here we describe the advantages and disadvantages of current ablation profiles and provides an outlook of future methods for the calculation of ablation profiles. Currently, differentation is taken between cornea-based ablation profiles and the entire human optics. With exception of „Ray tracing", all ablation profiles share the use of theoretical eye models but with different assumptions and data measurement. These type of eye models are subject to continous development and improvement.*

Conclusions. *Whereas all other ablation profiles use standardized eye models to calculate the data, Ray tracing would enable the calculation of an ablation profile based on an individualized eye model. The latter created the use of wavefront analysis, corneal topopgraphy and biometry from the individual patient. This strategy might in the future enable one achieve the perfect ablation profile.*

Mrochen M, Hafezi F, Jankov M, Seiler T.

Ophthalmologe 2006; 103:175-183

Ablation profiles based on the entire optics

„Classic“ ablation profile

The ablation profile based on the Munnerlyn formula represents the oldest profile used in refractive laser surgery (Fig. 1). It was introduced in 1988. Soon thereafter, the ablation profile was used in photorefractive keratectomy (PRK) and in laser in situ keratomileusis (LASIK), [88] which was solely based on the subjective refraction of the patient. Although well-suited for sphero-cylindrical corrections, this ablation profile does not take into consideration the corneal asphericity. Thus, the ablation profile is rather suited for paraxiel space and small optical zones.

Wavefront-optimized ablation profile

Wavefront errors of high order increase after refractive surgery. [14, 89-92] Kohnen et al. investigated the optical ablation after LASIK for myopia and hyperopia. [93] This investigation showed the induction of primary positive spherical aberations in myopic corrections and the induction of primary negative spherical aberations in hyperoic corrections. Conclusively, there is an increase of astigmatism of higher order (4th Zernike order). Each form has a significant influence on visual acuity. [94] Wavefront-optimized ablation profiles have been introduced to compensate for this increase. [95] The aim is to retain the physiological state of the eye and not to change it by a refractive procedure.

Some laser manufacturers have replaced the „classic,“ Munnerlyn formula based ablation profile by this optimized ablation profile. The main difference of action is in the periphery of the ablation zone where spherical aberration is affected (Fig. 1). Wavefront optimized treatments do not require time consuming aberrometry and interpretation of data, which are necessary for wavefront-guided ablation profiles. The authors used the wavefront optimized treated ablation profile routinely on the non-dominate eye.

Conclusively, induced spherical aberations reduces the quality of the optical image. All other aberations that are not taken into consideration by this ablation profile are less relevant that spherical aberation alone. Therefore, the aim of wavefront optimized treatment is to maintain the preoperative state of the eye.

In the correction of myopia, the advantages of this aberation profile have been shown clinically in a FDA controlled trial. The refractive rate of suc-

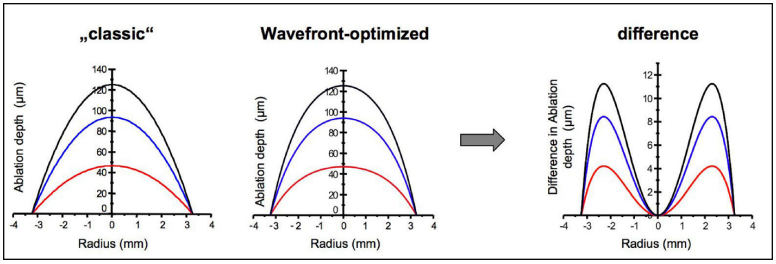

Figure 1. Generation of a topography-guided ablation profile.

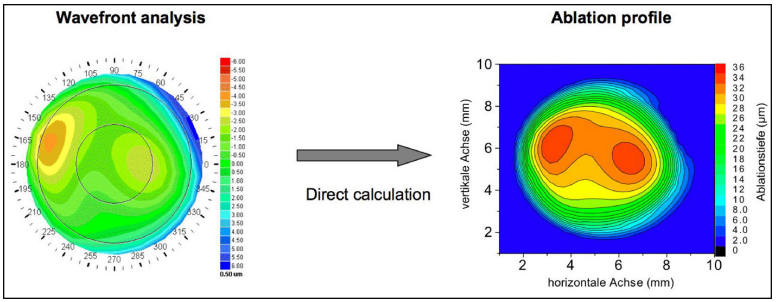

Figure 2. Difference between the „classic“ Munnerlyn and the wavefront-optimized ablation profile.

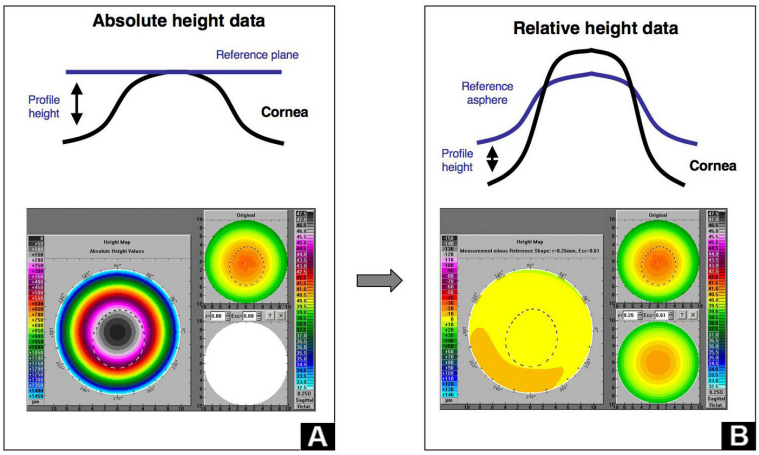

Figure 3. Generation of a wavefront-guided ablation profile.

cess, as defined by the percentage of operated eyes lying within an interval of ±0.5D of target refraction, is over 80%. This rate is considered today's standard. In more than 60% of the eyes operated, there is a post-operative increase in visual acuity of at least one Snellen line. In addition, a patient survey proved significant improvement in mesopic vision.

the eye while the consideration of the errors of the entire optics.

The currently used measurement systems are the Hartmann-Shack-Sensor and the Tscherning aberometer. In both systems, laser beams cross the optics and the resulting beam deviation is measured. In the case of the Hartmann-Shack sensor, the light beam that had been scattered by the retina is transferred to a point matrix using a micro-

Table 1 Overview on ablation profiles

Based on the cornea	Advantages	Disadvantages
Q factor	Uses corneal curvature und corneal asphericity, preserves prolate shape, big optical zones, specific for induced aberrations	No intraocular structures
Topography-guided	Individual corneal shape corneal irrgularities considered, prolate corneal shap possible, predominantly used in high irregularities	No intraocular structures, low precision of current systems
Based on total optics		
Classic ablation profile	Simple calculation, paraxial optics, established method	Only valuable for small optical zones, corneal curvature and corneal asphericity not considered, only sphero-cylindrical corrections, no intraocular structures
Wavefront-optimized	Precompansation of systematic wavefront errors, preservation of corneal physiology	Presumption of a single optical surface, no intraocular structures, inaccurary of measurement, only rotational symmetric aberrations
Wavefront-guided	All optical aberrations	Presumption of a single optical surface, no intraocular structures, corneal shape not considered
Ray tracing	Consideration of all optical aberrations, corneal topography and biometry	Currently higher risk of measurement errors

Wavefront-guided ablation profile

Theo Seiler performed the first wavefront-guided treatment in 1999. Since then, this type of ablation profile has become the best practice model in primary treatments. [31, 96, 97] Similar to topography-guided treatments, wavefront-guided profiles are customized according to the individual errors of lens structure. In contrast, the Tscherning aberrometer projects a point matrix onto the retina. The resulting matrix is recorded using a camera system. Next, the resulting individual wavefront is approximated using Zernike polynomials, and the ablation profile is then directly calculated (Fig. 2). The generation of a wavefront-guided profile therefore also represents an approximation, how-

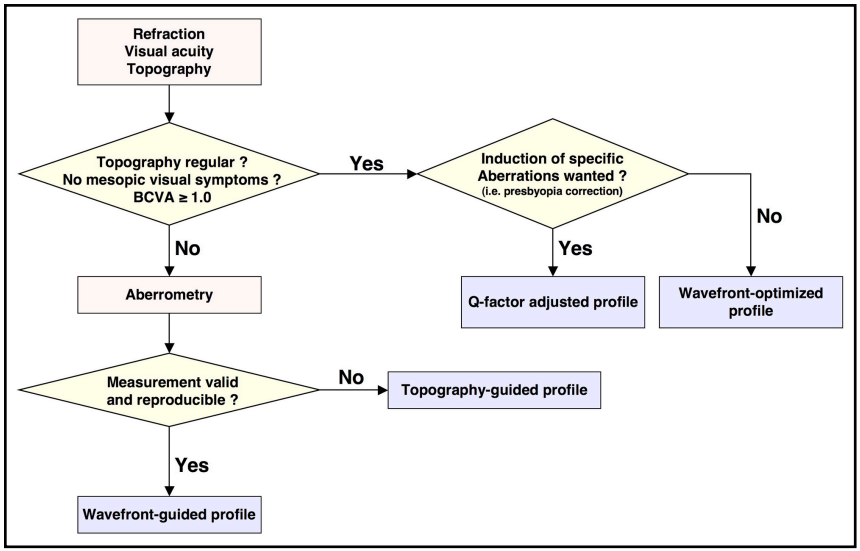

Figure 4. Decision-making process for the selection of ablation profiles.

ever, the high number of polynomials used leads to a high level of precision.

The wavefront-guided treatment has become the most frequently used ablation profile and has been incorporated by all major excimer laser producers. Upon the introduction of this profile in 1999, various authors stated that this profile might be able to increase UCVA („eagle eye") and almost reach the absolute limit given by the interphotoreceptor distance of the retina. However, these high expectations were only reached in 5-20% of patients. Possible reasons include laser-tissue interactions, the individual corneal healing response, induced aberrations during generation of the flap and microdecentrations during spherocylindrical ablation (i.e. zyclorotation).

Nevertheless the wavefront-guided profile shows one significant advantage over the formlery used „classic" profile: the total aberrations of the eye either remained stable or reduced. Thus, the frequent complication of glare and halos under mesopic conditions, as observed in corrections using the „classic" profile, were eliminated. [98]

A remaining critical issue is the preoperative predictability regarding which eyes will benefit from such a treatment. A number of studies show that eyes with

a preoperative wavefront error of higher order of more than 0.3 µm (rmsh = root mean square of higher order aberrations, OSA notations, pupil diameter 7 mm) will profit from a wavefront-guided treatment. The optical aberrations strongly increase with the diameter of the human optics and are neglectable in optical (pupil) diameters of less than 4 mm. Therefore, even the wavefront-guided profiles use a „classic" profile for the ablation of the central optics and only correct for spherocylindrical error., The peripheral zones are then treated using the individual wavefront data. Conclusively, the treatment of the central cornea determines postoperative refraction and treatment of the corneal periphery increases the quality of postoperative vision.

Ablation profiles based on the cornea

Topography-guided ablation profile

Multiple laser manufacturer have had varying success offering topography-guided ablation profiles. [5, 29, 99] A difference height map is calculated on a cornea topography (Fig. 3A), and the relative height data area is determined by using a reference asphere (Fig. 3B). This difference map is then approximated using polynomials that are used with the refractive data. This ablation profile adapts to the individual cornea curvature and takes into account the wavefront error of the anterior corneal surface. This profile is sometimes called „cornea wavefront," which is a misleading term. The topography-guided profile is particularly useful in the reduction of major irregularities of the corneal anterior surface, i.e. in cornea scars, irregular astigmatism following keratoplasties and cataract operations (Hafezi et al., personal communication), in decentered ablation, small optical zones or „central steep islands" following refractive surgery. This profile reduces massive irregularities and aberrations.

A topography-guided ablation profile can only be used in primary treatments since the reduction of cornea aberration might lead to an increase of the total aberrations of the optics. [100]

Q Factor-adjusted ablation profile

The wavefront-guided treatment leads to a significant reduction of aberrations if the pre-operative total aberrations were significant. This constellation is found in approximately 20% of cases. In all other cases, the aim is rather to preserve the physiological state of op-

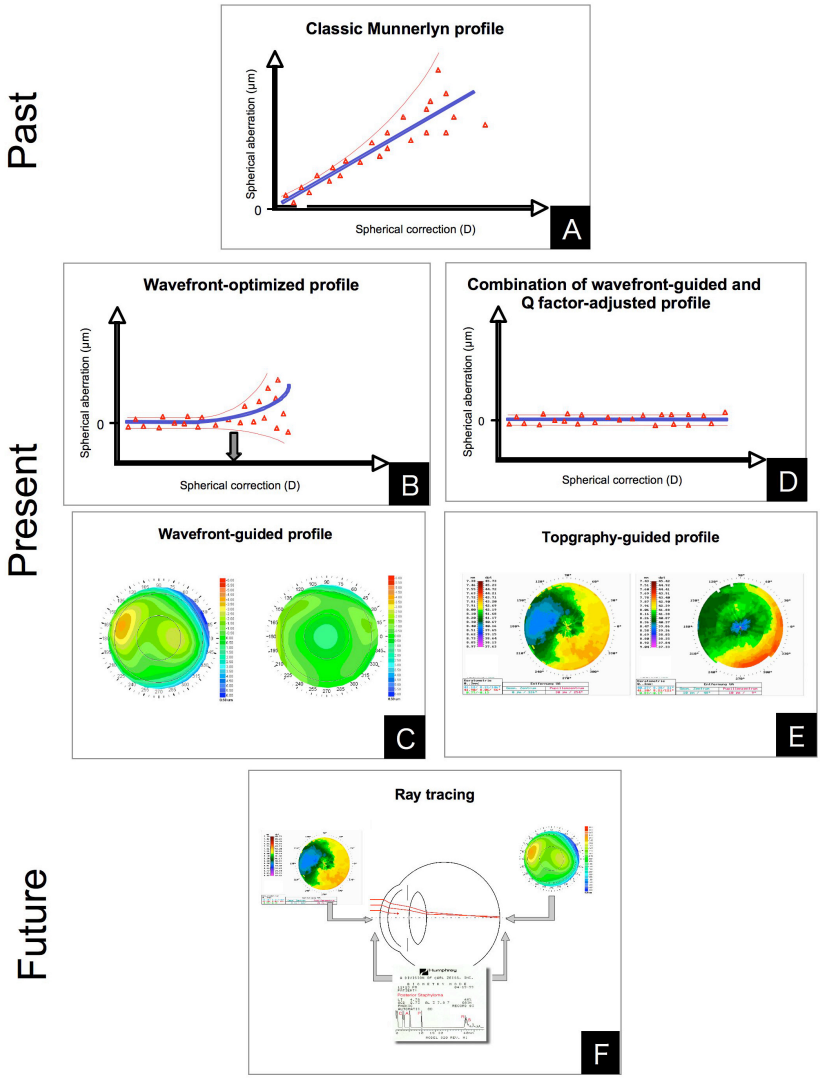

Figure 5. Overview of past, current and future ablation profiles.

tics in the most optimal way. Cornea asphericity determines the quality of the image, whereas the corneal curvature determines refractive changes. This asphercity represents the aim of the Q factor-adjusted ablation profile - preservation of the pre-operated asphericity and the ability of inducing specific aberration for the treatment of astigmatism and presbyopia.

The Q factor is the determinant of corneal asphericity, which lies between -0.8 and 0.4 in the normal population with a peak of -0.2. [101] Therefore, the human cornea physiologically shows a slightly prolate form - it flattens from the center to the preiphery. It has been shown repeatedly that refractive laser surgery for the correction of myopia shifts corneal asphercity to an oblate cornea. Several scientific groups have calculated the ideal postoperative corneal asphercity to be -0.4. [102, 103]

In a recent study, Koller et al. compared Q factor-adjusted and wavefront guided treatements in paired eyes. [10] They found no significant or clinically relevant differences regarding the refractive and the visual results. Only, „coma-like" aberrations were better treated using wavefront guided profiles.

Another aspect of corneal asphercity is correction of astigmatism. Asphericty is not equal in all meridians and can enhance or weaken corneal astigmatism. Therefore, correction of the central astigmatism is not sufficient for achieveing an ideal aspheric corneal form since meridian differences of asphericity need to be taken into consideration.

Future ablation profiles

"Ray tracing"

Ray tracing profile considers not only corneal topographic data but also aberrometry and biometry. Ray tracing is defined as the tracing and calculation of light rays through an optical system. The unique feature of Ray tracing is that in contrast with all aberration profiles used, Ray tracing does not rely on a „general" eye model as the basis of the calculation of the aberration profile. It rather uses an individualized eye model based on the biometric and topographic data of the particular patient. This model should help achieve a precise refractive result to enhance the quality of the retinal image for all pupil diameters (Fig. 5F).

Discussion

Refractive laser surgery of the cornea has seen great advances in the past years. On one hand, technological advances like the continous improvement of the laser systems from the „scanning slit" to modern „flying spot lasers" have been made. On the other hand, ablation profiles have been continously improved. Figure 4 shows a decision tree that should help the refractive surgeon to use the best suited ablation profile. The wavefront-optimized profile, which has been derived from the „classic" profile (Fig. 5A), precompensates for the spherical aberration induced by the refractive procedure itself (Fig. 5B). The variance of refractive results is low for minor corrections but rises with the height of myopia.

In other words; the wavefront optimized profile shows good results for minor myopic corrections but can lead to unprecise results in myopic corrections for more than -7D. With these findings, further ablation profiles were established like the wavefront-guided profile (Fig. 5C) and the Q factor-adjusted profile (Fig. 5D).

Latest results indicate that patients with a rmsh-OSA value of more than 0.3µm (7.0mm pupil) show a lesser postoperative variance when a wavefront guided-profile is used (G. Kezirian, personal communication). In patients with a rmsh-OSA of less than 0.3µm a combination of wavefront optimized or Q factor-adjusted profile is sufficient (T. Seiler, personal communication). In cases where a wavefront analysis is not possible for technical reasons (vitreous opacities, reflections of an intraocular lens, high corneal aberrations) or in cases with a highly irregular cornea, a topographically-guided profile (Fig. 5E) should be used.

The Ray tracing method could be an alternative in the future (Fig. 5F). Whereas all other ablation profiles use standardized eye models to calculate the data, Ray tracing would enable the calculation of an ablation profile based on an individualized eye model. The latter created the use of wavefront analysis, corneal topopgraphy and biometry from the individual patient. This strategy might enable one achieve the perfect ablation profile.

3.2

Transferring Wavefront Measurements into Corneal Ablations: an Overview of Related Topics

Abstract

Objective. *We give an overview of possible side effects that are specific for, or of particular relevance in, customized treatments. Certain processes involved in customized ablations have the potential to alter the quality of the optical correction. Professionals associated with customized treatment should be informed and trained with respect to possible sources of error.*

Conclusions. *The use of wavefront aberrations and corneal topography as a basis for customized ablations is a complex matter. A perfect wavefront measurement does not necessarily guarantee a perfect result after treatment. Other factors related to the technology and the clinical status of the patient must be considered for predicting the outcomes of a customized ablation. Besides this, the chain of processes involved in customized surgery requires not only well-trained surgeons; all professionals involved in the diagnosis and treatment should be informed and trained with respect to possible sources of error of customized ablations.*

Mrochen M, Bueeler M, Iseli HP, Hafezi F, Seiler T.

J Refract Surg 2004; 20:S550-S554

Introduction

The aim of this report is to give an overview of side effects and possible sources of error that might affect predictability, efficacy, or safety when transferring a theoretical ablation profile onto a vital cornea. To demonstrate the complexity of this issue, we are focusing on side effects directly linked to the technology used for pre- and intraoperative diagnostics and treatment (Fig. 1). Our intention with this report is to sensitize clinicians and other professionals to the impact of side effects on optical outcomes.

The eye needs standardization

The influences of a patient's eye condition during corneal topography or wavefront sensing have been studied in detail and reported frequently in the literature. Reasons are manifold and range from tear film conditions to patients' ability to fixate, status of accommodation, or head tilts that are usually difficult to control. A problem of clinical relevance is the influence of the tear film during wavefront sensing. Usually, single spots are not well detected in Shack-Hartmann or Tscherning images and, thus, the wavefront is plagued with a larger error. The question is: Should the investigator apply artificial tears to achieve a more precise detection of spots with the risk of altering the individual wavefront by the introduction of this additional factor? This specific example might show the importance of standard procedures in clinical routine. Further clinical research should focus on such standards for wavefront sensing and corneal topography. One should keep in mind that optical aberrations are not stable and vary over time and age. [104, 105] In addition, fluctuations of optical aberrations with accommodation or the pulse heart rate have been shown. [106] Consequently, standards for wavefront sensing should address such factors.

Fixation during measurement and treatment

The report of optical errors such as wavefront aberrations with respect to the line of sight is accepted in ophthalmology. However, to determine the line of sight, precise measurements of the pupil location are not the only prerequisite. Centration also requires the patient's ability to fixate on a fixation light that is coaxially aligned to the optical axis of the measuring device. Creating a flap or removing the epithelium during

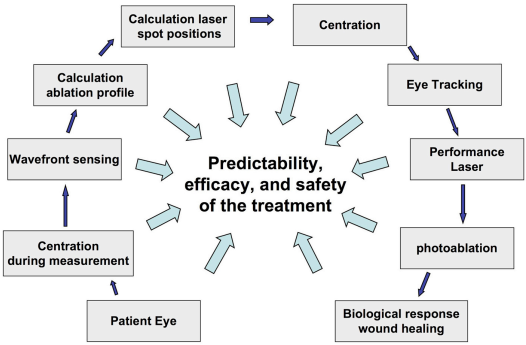

Figure 1. Overview of the processes involved in customized ablation. Each process has specific sources of error that may affect the outcome of a refractive procedure.

treatment reduces the image quality of the fixation light. Thus, the patient may lose the capability of accurate fixation. Similarly, precision of detection of the entrance pupil is reduced due to light scattered by a rough cornea. Generally, centration is a task of 6 degrees of freedom. The eye is able to perform horizontal and vertical shifts; it is able to rotate around its longitudinal, horizontal, and vertical axes; and it can move back and forth. Most commercially available eye-tracking systems measure and compensate lateral eye movements along the horizontal and vertical axis of the eye and some eye-tracking systems are capable of compensating for rotations around the longitudinal axis (cyclotorsion). Nevertheless, all eye-tracking devices (centration and registration) need the cooperation of the patient. Eye-tracking systems are built to compensate for eye movement and to center the measurement and the treatment with respect to the line of sight. Besides the benefits, the use of an eye-tracking system bares the risk of new possible sources of error such as inaccurate calibration between the detection of the eye's position (e.g., video camera) and the optical path of the laser beam (scanning mirrors). Such an error may result in under- or overcorrection, systematic decentrations, or large spherical aberrations.

Wavefront sensing and corneal topography

Calibration errors or misalignment of the optical scheme are a source of error because the user might not be able to determine such errors before each measurement. Wavefront and topography data that are used for a customized treatment should be used only after verification of the system calibration. Whereas in optical diagnosis such errors might not play a significant role, they may have a substantial impact when treatments are based on data measured incorrectly. We should keep in mind that an ablation of only 10 µm can cause a change of several diopters when the treatment is performed within a small zone. Manufacturers provide test eyes and certain verification methods for the calibration of their devices to avoid such calibration errors. Those tests are often time consuming but they should be performed before measurements for customized treatment are initiated.

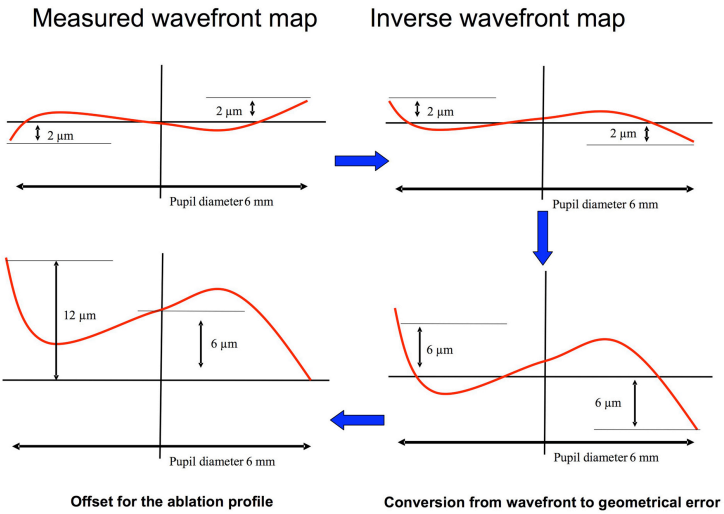

Figure 2. The principle of transferring a wavefront map into an ablation profile. Inversion of the wavefront map, conversion into geometrical shape information and offset for the ablation profile.

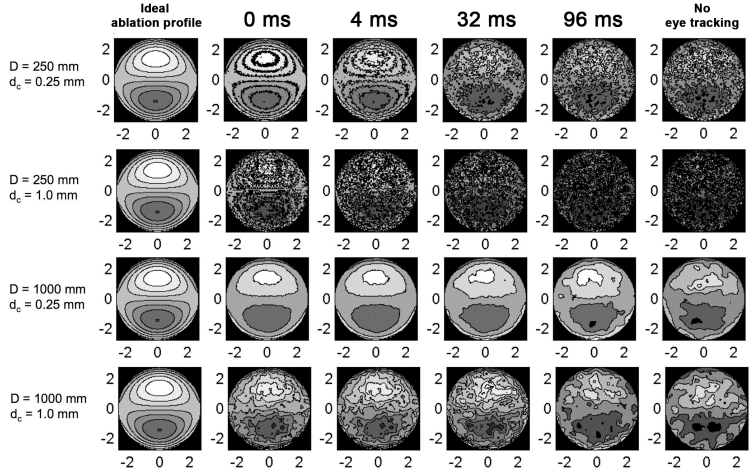

Figure 3. Ablated profiles after simulated scanning spot correction of vertical coma. Each row corresponds to a different combination of spot size D and central ablation depth per pulse dc. The first column shows the ideal ablation profile. The following columns depict the approximations of the same profile resulting from scanning spot laser ablation performed with increasing eye tracker latency.

Wavefront reconstruct algorithms

In principle, wavefront sensors determine the first derivative of the wavefront (slope) at a specific point within the pupil. One gets a set of measured wavefront slopes distributed over the entire pupil. Wavefront reconstruction methods fit the slope data to a set of polynomials with a least square technique. Typically, the polynomial set for wavefront fitting has been either Zernike or Taylor polynomials. The least square techniques minimize the absolute error between the measured slopes and the reconstructed wavefront. From the principles of fitting, there is a residual error between the reconstructed wavefront and the measured slopes. [107] The amount of residual error depends on the number of sample points and the number of polynomials used for fitting. As a rule of thumb, the number of sampling points should be three times more than the number of polynomials. Especially in highly aberrated eyes, the fitting errors can cause a significant under- or overestimation of wavefront aberrations and may lead to poor outcomes when used for ablation profile calculations.

Ablation profile calculation

The design of ablation profiles is usually based on theoretical eye models that should represent the optical behaviour of the human eye. The simplest way is to use the refractive power and shape of the anterior front surface of the cornea as a basis to calculate the required tissue removal for a spherocylindrical correction within a given optical zone. This general assumption, originally made by Munnerlyn [88], was used to determine the amount of tissue that must be removed from a spherical cornea to achieve a postoperative spherical cornea with a different radius of curvature by simple geometrical considerations. This derivation assumed both the thin lens theory and paraxial optics. Later, various authors improved the assumptions for pre- and postoperative corneal shape by the introduction of corneal asphericity or methods for precompensating specific higher-order aberrations.

Three general steps can achieve an ablation profile from a wavefront measurement:

1) Inversion of the wavefront map: As the aim is to correct the wavefront, one must reverse signs/orientation of the wavefront. If two or more wavefront aberrations are calculated in the same reference plane, they can be added or subtracted.

2) Conversion of the wavefront map: The wavefront information must be transferred into corresponding geometrical shape information. In a first approximation, this can be done by simply assuming the wavefront is equal to the optical path difference in the eye, which usually is correct for small aberrations observed in normal eyes. As the optical path difference is the product of geometrical length times the refractive index, one could easily derive the ablation profile in terms of a height map.

3) Offset for the ablation profile: As refractive surgery lasers are only able to remove tissue, one must consider this fact in ablation profile design. The geometrical information derived from the wavefront must be shifted by the amplitude of the height profile.

Figure 2 gives an example for this transfer of the ablation profile. An initial wavefront with peak-to-peak values of only 4 µm results in an ablation profile with a maximal ablation depth of approximately 12 µm. Generally, ablation profile design requires an eye model including optical and geometrical assumptions of the individual eye. Including more measured data into such a model will improve the eye model in predicting the optical situation of an

individual eye. In contrast, including more measured data for the individual ablation profile calculations also bares the risk of introducing more sources of error in the calculation process. We should remember that all measurements are plagued with a certain error and, if measurements are combined, the errors are usually increased-law of error propagation.

Spot size, single spot ablation depth and eye-tracking latency

Only limited data on the theoretical impact of intraoperative eye movements on the optical outcome of refractive treatments with a scanning spot laser are published. [108] In scanning spot laser surgery, the ideal corneal surface is approximated by directing and overlapping a finite number of laser pulses. Displacements of single laser shots from their ideal overlap positions may have the potential to significantly decrease the accuracy of the desired correction and to increase the surface roughness after ablation. When the eye does not move, a small spot is able to correct finer details (higher Zernike modes) than a larger spot. [109]

This situation changes when positioning errors of the single laser spots due to incomplete compensation of eye movements are introduced (Fig. 3). In this more realistic case, a reduction of the spot diameter reduces the stability of the correction toward spot displacements. So far, combinations of a large spot diameter (typically 0.75 to 1.00 mm) and a small ablation depth per pulse (typically 0.2 to 0.3 µm) yield the best parameters in case of typical eye-tracking latencies (1 ms). [108]

Radiant exposure (fluence)

Changes in the ablation depth for each single laser pulse, when moving the laser beam from the corneal apex toward the limbus, changes the angle of light incidence resulting in significant undercorrection in the periphery and consequently generation of spherical aberrations are known. [110] Energy drifts or fluctuations during a treatment may further influence the optical outcome. Even more important is the stability of the laser ablation. If the radiant exposure is reduced and reaches values in the order of the ablation threshold, one receives unpredictable ablation depths.

The ablation process gets more sensitive regarding environmental conditions such as temperature, individual variations in the ablation rates, humidity, alcohol concentration in the air, or airflow. For example, after the epithelium is removed or the flap is opened, the cornea starts to dehydrate. Decreasing the water content results in higher ablation efficiency for the collagen structure and, thus, in a higher amount of effective ablation depth after the cornea has been rehydrated. [36] Furthermore, a thin water film might shield the laser radiation after the corneal wound bed is cleaned with a liquid before ablation. Even water has been assumed to have a small absorption coefficient at 193 nm radiation under physiological conditions; absorption increases by several orders of magnitude during the photoablation process. [111]

An increase in radiant exposure leads to a more stable and reliable ablation per pulse; however, increasing the radiant exposure will also increase the amplitudes of the acoustic waves that are induced during the ablation process. [112] Those high stress waves may harm the corneal endothelium or other fragile structures in the eye.

Consequently, the range of radiant exposures that can be used in clinical routine is limited to a range of approximately 150 to 600 mJ/cm^2 dependent on the type of beam profile used-Gaussian or top hat.

Postoperative variability in wound healing

The influence of the individual variability in wound healing on optical outcomes in terms of wavefront aberrations is thus far unknown. Future clinical trials should provide data on biomechanical effects, epithelium remodelling, and stromal wound healing in terms of predictability of individual results. Based on such data, one may be able to simulate the expected outcome for a specific eye and to include such factors in the ablation profile design.

Conclusion

In summary, the use of wavefront aberrations and corneal topography as a basis for customized ablations is a complex matter. A perfect wavefront measurement does not necessarily guarantee a perfect result after treatment. Other factors related to the technology and the clinical status of the patient must be considered for predicting the outcomes of a customized ablation. Besides this,

the chain of processes involved in customized surgery requires not only well-trained surgeons; all professionals involved in the diagnosis and treatment should be informed and trained with respect to possible sources of error of customized ablations.

3.3

Q-factor Customized Ablation Profile for the Correction of Myopic Astigmatism

Abstract

Objective. *To compare the results of the Q-factor customized aspheric ablation profile with the wavefront-guided customized ablation pattern for the correction of myopic astigmatism.*

Methods. *Thirty-five patients were enrolled in a controlled study in which the nondominant eye was treated with the Q-factor customized profile (custom-Q study group) and the dominant eye was treated with wavefront-guided customized ablation (control group). Preoperative and 1-month postoperative high-contrast visual acuity, low-contrast visual acuity, and glare visual acuity, as well as aberrometry and asphericity of the cornea, were compared between the 2 groups. All eyes received laser in situ keratomileusis surgery, and the laser treatment was accomplished with the Wavelight Eye-Q 400 Hz excimer laser.*

Results. *For corrections up to -9 diopters (D) of myopia, there were no statistically significant differences between the 2 groups regarding any visual or optical parameter except coma-like aberrations (3rd Zernike order), where the wavefront-guided group was significantly better 1 month after surgery (P = 0.002). For corrections up to -5 D (spherical equivalent), the Q-factor optimized treated eyes had a significantly smaller shift toward oblate cornea: $\Delta Q_{15} = 0.25$ in Q-factor customized versus $\Delta Q_{15} = 0.38$ in wavefront-guided treatment (P = 0.04).*

Conclusions. *Regarding safety and refractive efficacy, custom-Q ablation profiles were clinically equivalent to wavefront-guided profiles in corrections of myopia up to -9 D and astigmatism up to 2.5 D. Corneal asphericity was less impaired by the custom-Q treatment up to -5 D of myopia.*

Koller T, Iseli HP, Hafezi F, Mrochen M, Seiler T.

J Cataract Refract Surg 2006; 32(4):584-589

Introduction

Corneal refractive surgery is based on the change in corneal curvature to compensate for refractive errors of the eye. After many mechanical approaches, such as radial keratotomy, keratomileusis, and astigmatic keratotomies, ablative procedures using the excimer laser have become the most successful technique. It was mainly the submicron precision and the high repeatability of the ablation of the cornea accompanied by minimal side effects that guaranteed this success.

Standard ablation profiles for the correction of myopic astigmatism were based on the removal of convex–concave tissue lenticules with spherocylindrical surfaces. [88] Although these algorithms proved to be effective to compensate for refractive error, the quality of vision deteriorated significantly, especially under mesopic and low-contrast conditions. [89, 113-115] As a logical consequence, research was directed toward aspheric ablation profiles, wavefront analysis of the eyes operated on, and the optical aberrations induced by the operations. [14, 116, 117]

The results of a preoperative wavefront analysis were used to create individualized ablation patterns to also compensate for pre-existing aberrations [102, 118]; however, this analysis is time consuming and appears not to be necessary in the majority of the cases. Therefore, new aspheric non-individualized algorithms were designed to compensate for the spherical aberration induced, [95] which led to an improved visual outcome. [119] On the other hand, it has been known for many years that any refractive treatment of the cornea must respect the preoperative and postoperative asphericity of the cornea.

Table 1 Demographic and refractive data of the study group
(n=35; side: nondominant 15 right eyes (42.9%) and 20 left eyes (57.1%))

	Mean ± SD	Range
Age (y)	35.37 ± 8.64	23 to 53
Sphere, dominant eyes (D)	-4.65 ± 2.0	-1.75 to -9.0
Sphere, nondominant eyes (D)	-4.96 ± 2.21	-1.0 to -9.0
Cylinder, dominant eyes (D)	-0.68 ± 0.75	0 to -2.5
Cylinder, nondominant eyes (D)	-0.62 ± 0.61	0 to -2.25
Q-factor 15 degrees, dominant eyes (D)	-0.21 ± 0.12	-0.04 to -0.53
Q-factor 15 degrees, nondominant eyes (D)	-0.20 ± 0.14	-0-03 to -0.58
Rsmh, dominant eyes (D)	0.242 ± 0.086	0.106 to 0.472
Rsmh, nondominant eyes (D)	0.237 ± 0.070	0.11 to 0.346

Rsmh = wavefront error of higher orders (including 3rd to 6th Zernike order)

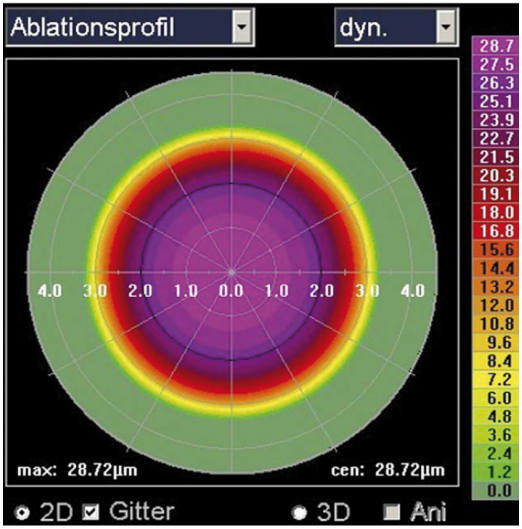

Figure 1. Ablation pattern for an attempted change in asphericity of ΔQ = -0.6. In the central part, the ablation depth is virtually constant and resembles a phototherapeutic keratectomy. Toward the periphery, a flattening produces the prolate cornea. The central ablation depth is 28.5 µm.

[120-122] The outer surface of the human cornea is physiologically not spherical but rather like a conoid. [123] On average, the central part of the cornea has a stronger curvature than the periphery or, in other words, the refractive power of the outer corneal surface decreases from central toward peripheral. For this form, the term prolate cornea has been coined, and the opposite form is called oblate cornea.

The physiologic asphericity of the cornea shows a significant individual variation ranging from mild oblate to moderate prolate. [123] Therefore, it was necessary to introduce a shape factor to characterize the amount of asphericity of the cornea numerically, the so-called Q-factor. Gatinel et al. [124] and Manns et al. [125] emphasized that the preoperative and postoperative Q-factors have significant influence on the ablation depth and profile to be used, and Manns et al. [125] concluded that a minimum of spherical aberration would be obtained at a target Q-factor of approximately -0.4. These calculations were based on an

Table 2 Refractive and visual outcomes at 1 month after surgery

	Mean ± SD		
	Wavefront-guided grou	Custom-Q group	
Parameter	**Dominant Eyes**	**Nondominant Eyes**	***P* Value**
Spherical equivalent (D)			
Preoperative (D)	-4.99 ± 2.05	-5.28 ± 2.25	0.289
Postoperative (D)	0.05 ± 0.44	-0-09 ± 0.58	0.072
Efficiency (%)	99.4 ± 4.6	97.7 ± 10.5	0.249
Cylinder			
Preoperative (D)	-0.68 ± 0.75	-0.61 ± 0.61	0.369
Postoperative (D)	-0.11 ± 0.26	-0.11 ± 0.21	0.457
Efficiency (%)	92.6 ± 18	92.2 ± 19	0.690
BSCVA			
Preoperative (D)	1.127 ± 0.183	1.040 ± 0.247	0.049
Postoperative (D)	1.160 ± 0.201	1.054 ± 0.257	0.031
Low-contrast VA			
Preoperative (D)	0.724 ± 0.099	0.725 ± 0.134	0.480
Postoperative (D)	0.704 ± 0.132	0.690 ± 0.182	0.377
Glare VA			
Preoperative (D)	0.565 ± 0.088	0.533 ± 0.140	0.343
Postoperative (D)	0.555 ± 0.133	0.528 ± 0.163	0.246
Q-Factor Q15			
Preoperative (D)	-0.21 ± 0.12	-0.20 ± 0.14	0.335
Postoperative (D)	0.47 ± 0.46	0.50 ± 0.49	0.395

BSCVA = best spectacle-corrected visual acuity; VA = visual acuity

aspheric eye model, and the approximate target value of -0.4 to -0.5 holds for the whole range of myopic corrections up to -10 diopters (D).

In this study, we present refractive, optical, and visual results of an aspheric ablation algorithm that takes the preoperative and attempted postoperative Q-factor of the cornea to be operated on into account. The nondominant eye of patients with myopic astigmatism was corrected using this algorithm, and the outcome at 1 month was compared with that in the dominant fellow eye that was treated by wavefront-guided ablation. Our interest was focused on the quality of vision and the induced wavefront aberrations.

Patients and methods

Study Group

Thirty-five patients seeking laser correction at the Institute for Refractive and Ophthalmic Surgery (IROC) were enrolled in this study. The age of the patients ranged from 23 to 53 years (mean 35.37 years ± 8.64 [SD]). The refractive

3.3 Q-factor profile

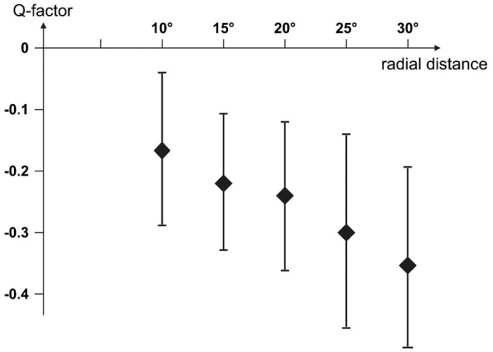

Figure 2. Preoperative asphericity Q as a function of the radial distance from the apex of the cornea. A radial distance of 30 degrees is equivalent to an optical zone diameter of approximately 7.5 mm.

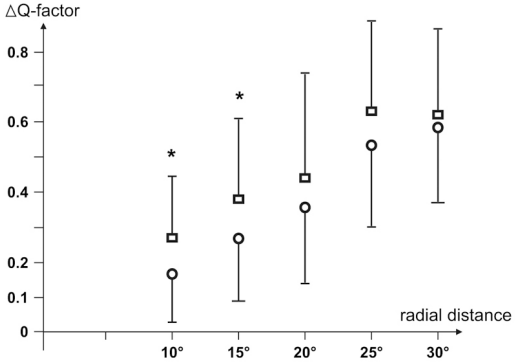

Figure 3. Increase in asphericity ΔQ = Qpost – Qpre in the wavefront-guided (rectangles) and the Q factor-customized (circles) treated eyes in myopic corrections of -5 D and less. A positive value of ΔQ indicates a shift toward an oblate cornea. The bars depict the standard deviation. The difference between the groups is statistically significant for radial distances 10 degrees and 15 degrees from the apex (*).

and demographic data are listed in Table 1. All patients had LASIK in both eyes, the nondominant eye (study group) being operated on first and the dominant eye (control group) 1 day later. On average, best spectacle-corrected visual

acuity (BSCVA) was significantly better in the dominant eye (1.127 ± 0.182 versus 1.040 ± 0.247, P = 0.049). The target refraction was emmetropia in 59 eyes and slight myopia between -0.50 D and -1.25 D in 11 eyes because of intended monovision. After a complete ophthalmic examination and a thorough discussion of the risks and benefits of the surgery, the patients gave written informed consent. Exclusion criteria were any pathology of the eyes, age under 20 years, asymmetric astigmatism detected in corneal topography, central corneal thickness less than 500 µm and residual stromal thickness of less than 270 µm, and high-order wavefront error (rmsh) of more than 0.35 µm in the nondominant eye (pupil size 7 mm). The study protocol was approved by the review board of the IROC.

Examinations

The complete preoperative ophthalmic examination consisted of autorefractometry and autokeratometry (Humphrey Model 599, Zeiss), corneal topography (Keratograph C, Oculus, equipped with Topolyzer software, Wavelight), manifest refraction using the fogging technique, uncorrected visual acuity (UCVA) and BSCVA, glare visual acuity and low-contrast visual acuity (Humphrey Model 599), wavefront analysis with pupils dilated to at least 7 mm in diameter (Wavefront Analyzer, Wavelight), applanation tonometry, central ultrasound pachymetry (SP-2000, Tomey), and slitlamp inspection of the anterior and posterior segments of the eyes. All root-mean-square (RMS) values are reported at a pupil size of 7 mm. The

Table 3 Safety of wavefront-guided versus custom-Q treatment

	Lines lost			Lines lost	
VA Type / Group	**2 or more**	**1**	***Unchanged***	**1**	**2 or more**
BCVA					
WG	1	5	18	8	3
Custom-Q	1	5	18	8	3
Low-contrast VA					
WG	1	4	27	3	0
Custom-Q	2	4	25	4	0
Glare VA					
WG	3	5	19	6	2
Custom-Q	5	4	17	4	5

BCVA = best corrected visual acuity; Custom-Q = Q-factor customized treated eyes
VA = visual acuity; WG = wavefront-guided treated eyes

determinable glare visual acuity and low-contrast acuity values range on a decimal scale from 0 to 0.8 (equivalent to 20/25), whereas for UCVA and BSCVA, the maximum was 2.0 (equivalent to 20/10).

The patients were seen on postoperative days 1 and 3 (if necessary) and 1 month after surgery. On postoperative days 1 and 3, UCVA was measured and a slitlamp inspection was performed. At the 1-month follow-up, the examination was identical to preoperatively.

Q-Factor Analysis and Asphericity Treatment

Preoperative and postoperative Q-factor analysis was performed by means of the corneal topographer. Only automatically taken topographies were accepted. The Q-factor was calculated by the topography software in all 4 main hemimeridians at radial distances 10, 15, 20, 25, and 30 degrees from the apex of the cornea, and for treatment, the average of 2 opposite hemimeridians was used as the Q-factor in the main axes. The preoperative and postoperative Q-factors for numeric evaluation are the averages of all 4 hemimeridians. Since the aim was a postoperative prolate cornea, the target Q-factor was -0.4 within a diameter of 6.5 mm in all cases. A typical ablation pattern attempting an asphericity change of $\Delta Q = -0.6$ within an optical zone of 6.5 mm in diameter is shown in Figure 1.

Surgical Technique

All operations were performed as LASIK procedures. The microkeratome used was the M2 (Moria), with appropriate suction rings selected according to the specifications of the manufacturer. The laser treatment was performed by means of the Eye-Q excimer laser with the custom-Q software (Wavelight). This device works at a repetition rate of 400 Hz and produces a spot size of 0.68 mm (Full Width at Half Maximum, FWHM) with a truncated Gaussian energy profile. Eye tracking is accomplished with a latency of 6 ms. The optical zone of full treatment had a diameter of 6.5 mm with a transition zone of 1.25 mm in both groups. After the flap was repositioned, the patient was given a bandage lens that was soaked with preservative-free ofloxacin 0.3% (Floxal SDU) eye drops for 20 minutes. The bandage lens was removed the next morning. The surgery in the fellow eye was done on 2 consecutive days. The postoperative medication consisted of fluorometholon 0.1% (FML) twice a day for 1 week and artificial tears (Hylo-Comod) at the patient's discretion.

Statistical Analysis

Preoperative and postoperative parameters in the 2 groups as well as the preoperative versus postoperative changes (paired differences in each group were compared using the paired 2-sided t test. A P value less than 0.05 was considered statistically significant.

The vector analysis of astigmatism correction consisted of the calculation of the change in refractive cylinder in the preoperative axis, [126] and its percentage of the preoperative refractive astigmatism served as a measure for the efficiency of astigmatism correction. Similarly, to take the attempted undercorrection in some eyes of the custom Q-group into account, the spherical correction efficiency was calculated as the percentage of the preoperative versus postoperative change in spherical equivalent compared to the target change in spherical equivalent.

Results

The surgery was uneventful in all cases. At postoperative day 1, 2 eyes showed a minor diffuse lamellar keratitis that resolved within 3 days using FML drops 4 times a day. At the 1-month examination, all eyes showed a regular state after LASIK.

The refractive and visual data at the 1-month follow-up are listed in Table 2. Twenty-eight eyes in the custom-group (80%) and 30 eyes in the wavefront-guided group (86%) were within ±0.5 D of the target refraction. The preoperative statistically significant difference in BSCVA, better in the dominant eye, remained significant 1 month after surgery (P = 0.031). Regarding safety, both groups showed an identical distribution of lost versus gained lines of BSCVA (Table 3). The eyes that lost 2 lines (1 in each group) belonged to 1 patient suffering from severely dry eyes.

Low-contrast visual acuity and glare visual acuity were preoperatively and postoperatively not statistically different in the 2 groups (Table 2). Also, the preoperative versus postoperative changes did not demonstrate statistical significance in glare acuity (P = 0.724) or low-contrast acuity (P = 0.418).

Regarding the asphericity of the cornea, all eyes demonstrated a tendency toward an oblate cornea after surgery (Table 2). The preoperative Q-factor as a function of the radial distance from the apex is shown in Figure 2. The increase in asphericity $\Delta Q = Q_{post} - Q_{pre}$ was approximately 4% higher for the custom-Q group. For all radial distances, the difference in ΔQ between the groups was not statistically significant. For corrections of

-5 D (spherical equivalent) and less, however, the results were different (Fig. 3), showing a significantly smaller shift toward oblate in the Q-factor customized group.

The total rmsh was preoperatively nearly identical in the 2 groups (0.242 ± 0.086 µm and 0.237 ± 0.070 µm, Table 1) and remained postoperatively similar in both groups (0.442 ± 0.142 µm in the custom-Q and 0.381 ± 0.146 µm in the wavefront-guided group [P = 0.113]). The only statistically significant difference regarding wavefront errors was obtained in the postoperative coma-like aberrations S3 (RMS sum of 3rd-order aberrations) with 0.296 ± 0.115 µm in the custom-Q group versus 0.192 ± 0.088 µm in the wavefront-guided group (P = 0.002). Another important detail is the similar induced spherical aberration (postoperative minus preoperative) in the 2 groups: 0.287 ± 0.219 µm versus 0.295 ± 0.264 µm (P = 0.457).

Discussion

Wavefront-guided customized ablation appears to be the gold standard for ablative treatment of myopic astigmatism regarding the optical performance of the postoperative eye. [127, 128] Therefore, it was logical to compare a new algorithm such as the custom-Q profile with this standard. To exclude individual abnormal healing responses, we compared fellow eyes with the dominant eye treated with wavefront-guided ablation and the nondominant eye treated with Q-factor customized. The choice to treat the dominant eyes with wavefront-guided ablation was mainly based on ethical considerations because of the superiority of wavefront-guided algorithms presumed before the study. Regarding refractive and visual outcomes in the study, however, we could not find any relevant differences (Tables 2 and 3) and conclude that the 2 treatment strategies appear to be clinically equivalent.

An important result is the only minor decrease in low-contrast visual acuity in both groups, which is remarkable because after conventional photorefractive keratectomy and LASIK, low-contrast visual acuity shows a significant reduction. [114, 129] Although not statistically significant, the better spherical success index (Table 2) in the wavefront-guided group means that the nomogram for spherical custom-Q treatments has to be improved, whereas the efficiency regarding astigmatic treatments was nearly equal in both groups. The small differences reported in this study might have become statistically significant if the group size would have been increased; however, a group of 35

matched pairs is sufficient to detect a clinically meaningful result.

Although the preoperative and postoperative overall optical performance of the eyes treated by the 2 different profiles was very similar in the 2 groups, we found a statistically significant difference regarding the outcome of coma-like 3rd-order aberrations S3. Whereas preoperative versus postoperative S3 increased in the Q-factor customized group from 0.181 ± 0.072 µm preoperatively to 0.296 ± 0.115 µm postoperatively, S3 remained virtually constant in the wavefront-guided group, with 0.182 ± 0.094 µm preoperatively versus 0.192 ± 0.088 µm postoperatively.

This result is not surprising because the Q-factor customized approach does not correct coma-like aberrations. On the other hand, the increase in the total wavefront error due to the operation by a factor of 1.83 in the custom-Q group and 1.67 in the wavefront-guided group compares favourably with the increased factors with standard ablation profiles reported in the literature, which range from 1.92 [130] to 17. [14] Such an increase in wavefront error during myopia correction is usually due to the inevitably induced spherical aberration, which was identically small in the 2 groups. Chaalita et al. measured higher order aberrations and correlated them with subjective complaints of patients after LASIK surgery. [13] Whereas the total rmsh and spherical aberration were good quantitative descriptors for starburst and glare, coma was significantly related to double vision. In this study, the postoperative glare visual acuity was on average better compared with the preoperative in both groups, which is consistent with the relatively small increase in spherical aberration and total wavefront error.

So, if the optical performance of the eyes treated by the 2 alternative approaches is similar but coma-like aberrations do better using wavefront-guided ablation, why should the wavefront-guided approach not be preferred in any case? Wavefront-guided ablation requires a time-consuming preoperative wavefront analysis including dilation of the pupil. In a high-volume refractive surgery practice, there is often little time to do such an intensive examination in any case. Not to speak of refractive surgery in third world-countries where for economic reasons such time-consuming analysis is not well accepted. These and other aspects decrease the market penetration of wavefront-guided ablation and create the demand for alternative customized ablation profiles.

We would have expected to find a significant difference in postoperative

Q-factors between the groups since we aimed on a postoperative Q-factor of -0.4 in the custom- Q group. Both goals were clearly missed, at least in higher corrections, because there was an underlying strong shift toward an oblate cornea due to the myopic correction that is linearly related with the amount of myopia correction. [130] Thus, on average, a 4% greater shift toward oblate in the custom-Q group is well explained by the 3% higher myopia correction in this group compared with the wavefront-guided group (Table 2). A combination of 2 reasons have recently been considered to be responsible for this shift toward oblate corneal shape [131]: a peripheral undercorrection due to a reduced laser efficacy [110] and the structural response of the cornea that is biomechanically weakened by the LASIK operation itself. [132] Both ablation profiles used in this study include a so-called correction matrix that compensates for the reduced laser ablation in the peripheral cornea. [95] Therefore, we believe that in our cases, the shift was mainly due to a biological response of the cornea.

A totally different picture is drawn when considering myopic corrections of -5 D and less. The corneas of the Q-factor optimized treated eyes were less oblate for all radial distances from the apex (Fig. 3); the difference was statistically significant only within the inner 3.5 mm of the cornea (Q_{10} and Q_{15}).

As shown in Figure 1, the Q-factor adjustment consists of a kind of additional correction in the midperiphery of the cornea, resembling a hyperopic correction. To avoid such consecutive hyperopic correction, the central part must be treated by means of a phototherapeutic keratectomy, which enhances the central ablation depth as previously described. [124] An intended change in Q-factor ΔQ of -0.6 within an optical zone of 6.5 mm requires 28.5 µm more central tissue removal (Fig. 1). This increased central keratectomy depth may limit the application of Q-factor optimized ablation to corrections of only mild to moderate myopia. A stronger attempted asphericity correction, for example, a target Q of -1.0, might have yielded more prolate postoperative corneas, but, on the other hand, such a strong Q-factor correction would increase the central keratectomy depth by another 30 µm, which we judged not to be appropriate with respect to the already well-preserved low-contrast visual acuity data in this study.

This study is limited regarding the short follow-up of only 1 month. We intended to present early postoperative data because the corneal optics may be affected by stromal and epithelial heal-

ing. Nevertheless, it would be interesting to observe whether corneal optics have some regression. Also, eyes with high preoperative wavefront errors of higher order (at least of the nondominant eye) were excluded from the study. Those eyes, however, should be treated by wavefront-guided customized ablation anyway.

In summary, this study demonstrated that a Q-factor optimized ablation profile yielded visual, optical, and refractive results comparable to those of the wavefront-guided customized technique for corrections of myopia up to -9 D. A significantly better result in corneal optics, however, was obtained only with corrections up to -5 D. The Q-factor optimized ablation represents a customized approach that is much less time consuming than the wavefront-guided technique since it is based on preoperative corneal topography, which is mandatory in any case to detect keratectatic disorders.

The Q-factor optimized profile has, therefore, the potential to replace currently used standard profiles for corrections of myopic astigmatism.

3.4

Clinical Photoablation With a 500-Hz Scanning Spot Excimer Laser

Abstract

Objective. *The aim of this study was to use a 500-Hz scanning spot laser (Concept500, Wavelight Laser Technologie AG, Erlangen, Germany) to investigate potential side effects that might be associated with the use of a high repetition rate laser platform.*

Methods. *Seven eyes were treated using a 500-Hz scanning spot laser for laser in situ keratomileusis (LASIK). The local frequency of the ablation was kept below 40 Hz to avoid local heating of corneal tissue. With the exception of the high repetition rate (500 Hz), all other laser parameters such as fluence, algorithm, ablation profile, and spot diameter were identical to a standard Wavelight Allegretto laser system. Patients were examined at 1 month and 1 year after initial treatment. Preoperative and postoperative examination included manifest sphere and cylinder, uncorrected and best spectacle-corrected visual acuity (BSCVA).*

Results. *All eyes were treated for myopia or myopic astigmatism. Five eyes received spherocylindrical and two eyes spherical ablation only. No adverse events correlated with the use of a high repetition rate laser system were observed during surgery or at any point during follow-up. All eyes maintained or had improved BSCVA at 12 months after treatment when compared to preoperative values.*

Conclusions. *The use of an excimer laser wit a maximal repetition rate of 500 Hz and a local repetition rate of less than 40 Hz was free of any specific side effect that might be associated with the use of such a high repetition rate.*

Iseli HP, Mrochen M, Hafezi F, Seiler T.

J Refract Surg 2004; 20(6):831-834

Introduction

Customized laser surgery with scanning spot lasers allows adjustment of spherical or cylindrical aberrations, but also aberrations of higher order and in detail, irregular astigmatism. Data obtained from wavefront analysis or corneal topography may be used to establish more complex ablation profiles compared to the simple ablation profiles used in sphero-cylindrical corrections. [29, 31, 118, 133-137]

Besides precise measurement of the wavefront, the success of such a procedure depends on the way in which the ablation profile is transferred onto the cornea. Here, two additional parameters play a vital role-beam diameter and speed of treatment.

The beam diameter [109, 138, 139] is a key parameter to provide correction of higher order aberrations. A small diameter enables the surgeon to reshape the cornea by applying a complex ablation profile. However, the use of such a small laser spot demands fast eye tracking, accurate scanning mirrors, and highly stable excimer lasers. In addition, laser treatment should be performed within 30 to 60 seconds because the cornea might dry and the fixation ability of the patient might decrease when treatment time is too long. Therefore, smaller laser spots need higher repetition rates to avoid these effects. On the other hand, a high repetition rate might induce an increased temperature load to the tissue.

The aim of this pilot study was to investigate potential clinical side effects related to the use of a high repetition rate. Such thermal side effects could manifest as increased inflammation in the early postoperative period, opacities in the interface, and irregularities as detected in corneal topography.

Patients and methods

Patients

A prospective study of LASIK with a high repetition rate laser system for myopia and astigmatism was initiated. There were seven males (three right eyes, four left eyes) who ranged in age from 30 to 40 years (mean age 35 years).

Inclusion criteria were patient age 21 years, manifest refraction less than -12.00 diopters (D) in sphere and less than 4.00D in cylinder, stable manifest refraction over the previous 2 years, the pupil of the eye treated was not deformed, the patient agreed to participate in the study, and to attend follow-up examinations for up to 1 year after surgery. Informed consent was obtained

from all patients after a thorough explanation of the procedure and its potential risks. The institutional review board of the University eye clinic approved this pilot study.

Patients were excluded from the study if they had a systemic or ocular disease likely to influence corneal healing, a history of glaucoma, retinal disorders that might limit visual acuity (e.g., myopic maculopathy) or complicate the LASIK procedure (e.g., equatorial degenerations), previous ocular surgery, or suffered from dry eyes substantiated by a pathologic Schirmer test. One eye with amblyopia (the first eye in this pilot study) and a best spectacle-corrected visual acuity (BSCVA) of 20/30 was included in the series. Contact lens use was ceased 2 weeks before preoperative examination.

Table 1 Safety after LASIK with a 500-Hz scanning spot laser

	Time after LASIK	
Variable	**1 mo (n=7)**	**12 mo (n=7)**
Loss of lines of BSCVA	0	0
BSCVA worse than 20/40	1	0
BSCVA worse than 20/40 if 20/20 or better at baselin	0	0
Irregular corneal topography	0	0

Clinical Examinations

The following examinations were performed: uncorrected (UCVA) and best spectacle-corrected (BSCVA) visual acuity (Snellen visual acuity chart), corneal topography (Topolyzer, Wavelight Laser Technologie AG, Erlangen, Germany), applanation tonometry, pachymetry, slit-lamp microscopy of the anterior segment, and contact lens ophthalmoscopy of the posterior segments. Patients were examined at 1 day, 1 month, and 12 months after surgery. At the day 1 postoperative examination only, UCVA, BSCVA, and slit-lamp microscopy were performed (data not shown). Preoperative spherical equivalent refraction ranged from -0.35 to -9.75 D, and astigmatism ranged from 0 to 3.50 D: between 0 and -0.99 D in two eyes, -3.00 to -3.99 D in two eyes, -4.00 to -4.99 D in two eyes, and -5.00 to -5.99 D in one eye; cylinder was between 0 and 1.00 D in three eyes, 1.00 to 2.00 D in three eyes, and 3.00 to 4.00 D in one eye.

Surgery

All LASIK procedures were performed between September and December 2001 under topical anaesthesia (pro-

paracaine 0.5%). First, a flap with a diameter of 9.0 mm and a thickness of approximately 130 µm was created with a superior hinge, using a Supratome microkeratome (Schwind Eye-Tech-Solution, Kleinostheim, Germany).

Ablation

Laser treatments were performed using a 500-Hz scanning spot laser system (Concept500, Wavelight Laser Technologie AG, Erlangen, Germany). A Gaussian beam profile with truncated wings was used to reduce thermal load of the surrounding tissue by sub-threshold laser energy. The ablation diameter of a single spot at the cornea was 0.9 mm. The mean radiant exposure was 0.2 J/cm^2. The scanning program was adjusted to provide a local repetition rate of 40 Hz or less. The sampling rate of the video-based eye tracker was 500 Hz, thus reducing the latency between registration of the eye position and mirror alignment to approximately 4 ms. (The eye tracking frequency and the repetition rate of the laser were both 500 Hz; each treatment point on the cornea was treated at a maximum 40 times per second.) Automatic pupil detection allowed accurate centering of the treatment zone. During treatment, the patient was advised to concentrate on a fixation target mounted coaxially to the optical axis of the laser system. In all treatments, the ablation zone was 6.5 mm and the overall treatment zone was 7.2 mm in diameter. Treatment time was less than 5 seconds per diopter of myopia. After photoablation, the flap was repositioned and the interface was rinsed with balanced salt solution. A bandage lens soaked in ofloxacine 0.5% solution was applied for the first night after surgery. Fluorometholon drops 0.1% were used twice daily for 1 week.

Table 2 Efficacy after LASIK with a 500-Hz scanning spot laser

	Time after LASIK	
Variable	1 mo (n=7)	12 mo (n=7)
UCVA 20/20 or better	5	4
UCVA 20/40 or better	6	7
Manifest spherical equivalent refraction ±0.5D	6	5
Manifest spherical equivalent refraction ±1.0D	7	7

All treatments were based on manifest refraction with target refraction in all eyes of plano, except one eye for which the target refraction was -0.75 D. Nomogram adjustments were not applied in this study. Preoperative calibration tests of the laser system included energy measurements, laser beam pro-

filing, ablation of test target, scanning mirror alignment check (checkerboard pattern ablation on test target), and testing of the optical alignment of the fixation light and the video eye tracker. Clinical results were analyzed regarding safety, efficacy, and predictability after follow-up at 1 and 12 months.

Results

All operations were uneventful. All corneas remained clear during and after photoablation. Slit-lamp microscopy revealed no signs of corneal opacities and/or thermal damage in the interface immediately after surgery or at any postoperative examination. On the first postoperative day, UCVA was 20/40 or better in all eyes. Follow-up examinations were performed at 1 and 12 months after surgery.

Safety was evaluated by maintenance of BSCVA. All eyes had stable or better BSCVA 12 months after surgery when compared to preoperative values (Table 1). The first eye of the cohort was amblyopic with a BSCVA of 20/40 before surgery; at 1 month after surgery, BSCVA was 20/50, and at 12 months after surgery, 20/30. No irregularities were detected in corneal topography at any examination beyond the first postoperative day.

At 12 months, all eyes achieved UCVA of 20/40 or better. Four of seven eyes had 20/20 or better, with one eye intentionally undercorrected to -0.75 D and one eye amblyopic.

At 12 months after surgery, mean spherical equivalent refraction in all eyes did not exceed ±1.00 D (Table 2); five of seven eyes (71.4%) were within ±0.50 D. Cylinder was reduced to less than -1.00 D in all eyes.

Discussion

The purpose of this study was to investigate possible clinical side effects that might be associated with use of a high repetition rate excimer laser for laser vision correction. Our results demonstrate that the use of repetition rates as high as 500 Hz did not affect the clinical outcomes of LASIK procedures. None of the operated eyes showed an adverse reaction that could be related to the higher repetition rate of the laser.

Although ultraviolet photoablation with the ArF excimer laser is a "cold ablation," the temperature rises above 200°C within several nanoseconds. [140] Bende and co-workers found a mean in situ temperature increase in tissue surrounding the ablation area of approximately 8°C. [141] Similar results have been pub-

lished by Maldonado-Codina and colleagues [142] and by Betney and colleagues. [143] Excimer laser platforms usually work with a repetition rate of 10 to 50 Hz and a radiant exposure (fluence) of approximately 0.2 J/cm^2; this results in an average power on the corneal surface of approximately 0.8 to 3.8 W, assuming a typical treatment zone of 6.0 to 7.0 mm in diameter. In principle, the total energy (sum of all laser spots applied) needed to remove the same amount of tissue with smaller scanning spots should be the same as when using larger spots. The energy of a single laser pulse used in our study was approximately 2 mJ at a mean radiant exposure of 0.2 mJ/cm^2. The scanning algorithm of the Concept500 laser takes into consideration that the local frequency should be below 40 Hz. Thus, the laser spots (0.9-mm diameter) are distributed systematically within the 6.0- to 7.0-mm-diameter treatment zone. The resulting average power distributed within the treatment zone is almost identical to the power distribution in standard laser systems. Consequently, one might not expect a significantly higher thermal load during corneal laser surgery with a high repetition rate laser system. [144]

Laser in situ keratomileusis is widely accepted as a safe procedure for correction of refractive errors. Remarkable improvements have been made by the introduction of customized laser ablation-superior to conventional photoablation-by including correction of higher order optical aberrations.

A recent study by Huang and Arif [109] showed that, based on fundamental considerations with currently used beam diameters of 1.0 mm and less, it should be possible to eliminate most higher order optical aberrations in a normal eye. Thus, current laser technology should be adequate for corneal reshaping in the majority of cases. However, the quality of the correction declines steadily as beam size increases. [138] Therefore, customized photoablation may require additional reduction in laser spot size to enable finer and more complex ablation profiles in highly aberrated eyes or in eyes with local irregularities such as steep central islands. [109]

In contrast, reducing the spot size for customized ablation has a distinct effect on other technical parameters, such as the eye tracking system. Bueeler and colleagues [138] studied the effect of various laser parameters on the optical outcome of photorefractive procedures. Numerical simulations of the entire ablation process were performed on a schematic model eye by varying ablation depth per pulse, laser spot size, eye tracker latency, and magnitude of refrac-

tive correction. They showed unambiguously that contrast transfer decreased significantly with increased latency of the eye tracker. For constant laser and tracking parameters, this decrease was more significant for higher myopic corrections. Treatments performed with smaller spot sizes and smaller ablation depths per pulse were more sensitive to tracking latency. Assuming defined eye tracker latency, the most stable results were obtained for large beam diameters and high central ablation depths per pulse. However, a tracking latency below 10 ms would allow for a reduction of the beam diameter to 0.50 mm. In our study, treatments were performed with a 500-Hz scanning spot laser with a spot size of 0.9 mm. Latency was on the order of 4 ms, ensuring an optimized balance between spot size and eye tracker performance.

In addition to its influence on the aforementioned technical parameters, reducing the spot diameter systematically increases the number of laser pulses. In brief, the number of laser pulses that must be applied for a myopic correction increases with the decrease of the square of the spot diameter. Ablation time should not exceed 60 seconds because of possible corneal drying or decrease in the patient's concentration during the treatment. A minimal ablation zone of 6.0 mm, small spot size <0.5 mm, and a limited treatment time might require a much faster scanning spot laser, superior to current commercially available systems.

In our pilot series of seven eyes, the use of the 500-Hz excimer laser did not reveal any specific clinical side effects potentially associated with the use of a high repetition rate. New laser systems equipped with high repetition rates may facilitate customized treatments with smaller laser spots (diameter <0.9 mm) for highly aberrated eyes that cannot be treated with currently available systems.

References

1. Horackova M, Vlkova E, Hejcmanova M. [New incision versus corneal flap uncover: comparison of two techniques of repeated surgery after primary LASIK in myopia]. Cesk Slov Oftalmol 2005; 61(2):96-105

2. Hersh PS, Fry KL, Bishop DS. Incidence and associations of retreatment after LASIK. Ophthalmology 2003; 110(4):748-754

3. Alessio G, Boscia F, La Tegola MG, Sborgia C. Topography-driven excimer laser for the retreatment of decentralized myopic photorefractive keratectomy. Ophthalmology 2001; 108(9):1695-1703

4. Hjortdal JO, Ehlers N. Treatment of post-keratoplasty astigmatism by topography supported customized laser ablation. Acta Ophthalmol Scand 2001; 79(4):376-380

5. Kymionis GD, Panagopoulou SI, Aslanides IM, Plainis S, Astyrakakis N, Pallikaris IG. Topographically supported customized ablation for the management of decentered laser in situ keratomileusis. Am J Ophthalmol 2004; 137(5):806-811

6. Lin DY, Manche EE. Custom-contoured ablation pattern method for the treatment of decentered laser ablations. J Cataract Refract Surg 2004; 30(8):1675-1684

7. Stojanovic A, Suput D. Strategic planning in topography-guided ablation of irregular astigmatism after laser refractive surgery. J Refract Surg 2005; 21(4):369-376

8. Wiesinger-Jendritza B, Knorz MC, Hugger P, Liermann A. Laser in situ keratomileusis assisted by corneal topography. J Cataract Refract Surg 1998; 24(2):166-174

9. Wu HK. Astigmatism and LASIK. Curr Opin Ophthalmol 2002; 13(4):250-255

10. Koller T, Iseli HP, Hafezi F, Mrochen M, Seiler T. Q-factor customized ablation profile for the correction of myopic astigmatism. J Cataract Refract Surg 2006; 32(4):584-589

11. Carones F, Vigo L, Scandola E. Wavefront-guided treatment of abnormal eyes using the LADARVision platform. J Refract Surg 2003; 19(6):S703-708

12. Hafezi F, Mrochen M, Fankhauser F, 2nd, Seiler T. Anterior lamellar keratoplasty with a microkeratome: a method for managing complications after refractive surgery. J Refract Surg 2003; 19(1):52-57

13. Chalita MR, Chavala S, Xu M, Krueger RR. Wavefront analysis in post-LASIK eyes and its correlation with visual symptoms, refraction, and topography. Ophthalmology 2004; 111(3):447-453

14. Seiler T, Kaemmerer M, Mierdel P, Krinke HE. Ocular optical aberrations after photorefractive keratectomy for myopia and myopic astigmatism. Arch Ophthalmol 2000; 118(1):17-21

15. Alkara N, Genth U, Seiler T. [A prospective clinical study of correction of myopic astigmatism by combined treatment with PRK and T-incision and photoastigmatic refractive keratectomy. The results after one year]. Ophthalmologe 1998; 95(10):677-683

16. Bharti S, Bharti R, Samantaray D. Comparison of cross cylinder ablation using the optimized ablation transition zone and the torsion error detector for correction of astigmatism. J Refract Surg 2004; 20(5 Suppl):S663-665

17. Holladay JT, Moran JR, Kezirian GM. Analysis of aggregate surgically induced refractive change, prediction error, and intraocular astigmatism. J Cataract Refract Surg 2001; 27(1):61-79

18. Seiler T, Koller T. [Asphericity of the cornea and astigmatism]. Klin Monatsbl Augenheilkd 2005; 222(12):977-982

19. Becker R, Krzizok TH, Wassill H. Use of preoperative assessment of positionally induced cyclotorsion: a video-oculographic study. Br J Ophthalmol 2004; 88(3):417-421

20. Alio JL, Javaloy J, Osman AA, Galvis V, Tello A, Haroun HE. Laser in situ keratomileusis to correct post-keratoplasty astigmatism; 1-step versus 2-step procedure. J Cataract Refract Surg 2004; 30(11):2303-2310

21. Melki SA, Azar DT. LASIK complications: etiology, management, and prevention. Surv Ophthalmol 2001; 46(2):95-116

22. Colin J, Cochener B, Gallinaro C. Central steep islands immediately following excimer photorefractive keratectomy for myopia. Refract Corneal Surg 1993; 9(5):395-396

23. Krueger RR, Saedy NF, McDonnell PJ. Clinical analysis of steep central islands after excimer laser photorefractive keratectomy. Arch Ophthalmol 1996; 114(4):377-381

24. Lin DT. Corneal topographic analysis after excimer photorefractive keratectomy. Ophthalmology 1994; 101(8):1432-1439

25. McGhee CN, Bryce IG. Natural history of central topographic islands following excimer laser photorefractive keratectomy. J Cataract Refract Surg 1996; 22(9):1151-1158

26. Schmidt-Petersen H, Seiler T. ["Central islands"--an early postoperative complication after photorefractive keratectomy]. Klin Monatsbl Augenheilkd 1996; 208(6):423-427

27. Slowik C, Somodi S, Richter A, Guthoff R. Assessment of corneal alterations following laser in situ keratomileusis by confocal slit scanning microscopy. Ger J Ophthalmol 1996; 5(6):526-531

28. Hafezi F, Mrochen M, Iseli HP, Seiler T. A 2-step procedure to enlarge small optical zones after photorefractive keratectomy for high myopia. J Cataract Refract Surg 2005; (in press)

29. Knorz MC, Jendritza B. Topographically-guided laser in situ keratomileusis to treat corneal irregularities. Ophthalmology 2000; 107(6):1138-1143

30. Lafond G, Solomon L, Bonnet S. Retreatment to enlarge small excimer laser optical zones using combined myopic and hyperopic ablations. J Refract Surg 2004; 20(1):46-52

31. Mrochen M, Krueger RR, Bueeler M, Seiler T. Aberration-sensing and wavefront-guided laser in situ keratomileusis: management of decentered ablation. J Refract Surg 2002; 18(4):418-429

32. Kang SW, Chung ES, Kim WJ. Clinical analysis of central islands after laser in situ keratomileusis. J Cataract Refract Surg 2000; 26(4):536-542

33. Maguen E, Salz JJ, Nesburn AB, Warren C, Macy JI, Papaioannou T, Hofbauer J, Berlin MS. Results of excimer laser photorefractive keratectomy for the correction of myopia. Ophthalmology 1994; 101(9):1548-1556; discussion 1556-1547

34. Muller B, Boeck T, Hartmann C. Effect of excimer laser beam delivery and beam shaping on corneal sphericity in photorefractive keratectomy. J Cataract Refract Surg 2004; 30(2):464-470

35. Seiler T, Holschbach A, Derse M, Jean B, Genth U. Complications of myopic photorefractive keratectomy with the excimer laser. Ophthalmology 1994; 101(1):153-160

36. Dougherty PJ, Wellish KL, Maloney RK. Excimer laser ablation rate and corneal hydration. Am J Ophthalmol 1994; 118(2):169-176

37. Oshika T, Klyce SD, Smolek MK, McDonald MB. Corneal hydration and central islands after excimer laser photorefractive keratectomy. J Cataract Refract Surg 1998; 24(12):1575-1580

38. Noack J, Tonnies R, Hohla K, Birngruber R, Vogel A. Influence of ablation plume dynamics on the formation of central islands in excimer laser photorefractive keratectomy. Ophthalmology 1997; 104(5):823-830

39. Cua IY, Pepose JS. Proper positioning of the plume evacuator in the VISX Star3 excimer laser minimizes central island formation in patients undergoing laser in situ keratomileusis. J Refract Surg 2003; 19(3):309-315

40. Forster W, Clemens S, Bruning, Magnago T, Elsner C, Krueger R. Steep central islands after myopic photorefractive keratectomy. J Cataract Refract Surg 1998; 24(7):899-904

41. Knorz MC, Liermann A, Seiberth V, Steiner H, Wiesinger B. Laser in situ keratomileusis to correct myopia of -6.00 to -29.00 diopters. J Refract Surg 1996; 12(5):575-584

42. Knorz MC, Wiesinger B, Liermann A, Seiberth V, Liesenhoff H. Laser in situ keratomileusis for moderate and high myopia and myopic astigmatism. Ophthalmology 1998; 105(5):932-940

43. Manche EE, Maloney RK, Smith RJ. Treatment of topographic central islands following refractive surgery. J Cataract Refract Surg 1998; 24(4):464-470

44. Nagy ZZ, Krueger RR, Suveges I. Central bump-like opacity as a complication of high hyperopic photorefractive keratectomy. Am J Ophthalmol 1999; 128(5):636-638

45. Quurke A, Schmidt-Petersen H, Seiler T. [Complications in photorefractive keratectomy for myopia correction]. Ophthalmologe 1998; 95(10):734-740

46. Jimenez-Alfaro I, Perez-Santonja JJ, Gomez Telleria G, Bueno Palacin JL, Puy P. Therapeutic lamellar keratoplasty with an automated microkeratome. J Cataract Refract Surg 2001; 27(8):1161-1165.

47. Arentsen JJ, Lamellar grafting, in Corneal surgery, Brighthill FS, Editor. 1993, Mosby: St. Louis. p. 360-368.

48. Shimazaki J. The evolution of lamellar keratoplasty. Curr Opin Ophthalmol 2000; 11(4):217-223

49. Melles GR, Lander F, Rietveld FJ, Remeijer L, Beekhuis WH, Binder PS. A new surgical technique for deep stromal, anterior lamellar keratoplasty. Br J Ophthalmol 1999; 83(3):327-333.

50. Seiler T. Refractive corneal surgery with lasers. Curr Opin Ophthalmol 1996; 7(4):47-51

51. Miyata K, Takahashi T, Tomidokoro A, Ono K, Oshika T. Iatrogenic keratectasia after phototherapeutic keratectomy. Br J Ophthalmol 2001; 85(2):247-248

52. Parmar D, Claoue C. Keratectasia following excimer laser photorefractive keratectomy. Acta Ophthalmol Scand 2004; 82(1):102-105

53. Brunette I, Gresset J, Boivin JF, Pop M, Thompson P, Lafond GP, Makni H. Functional outcome and satisfaction after photorefractive keratectomy. Part 2: survey of 690 patients. Ophthalmology 2000; 107(9):1790-1796

54. Shimizu K, Amano S, Tanaka S. Photorefractive keratectomy for myopia: one-year follow-up in 97 eyes. J Refract Corneal Surg 1994; 10(2 Suppl):S178-187

55. Seiler T, Koufala K, Richter G. Iatrogenic keratectasia after laser in situ keratomileusis. J Refract Surg 1998; 14(3):312-317

56. Cannon DJ, Foster CS. Collagen crosslinking in keratoconus. Invest Ophthalmol Vis Sci 1978; 17(1):63-65

57. Spoerl E, Huhle M, Seiler T. Induction of cross-links in corneal tissue. Exp Eye Res 1998; 66(1):97-103

58. Spoerl E, Seiler T. Techniques for stiffening the cornea. J Refract Surg 1999; 15(6):711-713

59. Wollensak G, Spoerl E, Wilsch M, Seiler T. Endothelial cell damage after riboflavin-ultraviolet-A treatment in the rabbit. J Cataract Refract Surg 2003; 29(9):1786-1790

60. Wollensak G, Spoerl E, Wilsch M, Seiler T. Keratocyte apoptosis after corneal collagen cross-linking using riboflavin/UVA treatment. Cornea 2004; 23(1):43-49

61. Wollensak G, Sporl E, Reber F, Pillunat L, Funk R. Corneal endothelial cytotoxicity of riboflavin/UVA treatment in vitro. Ophthalmic Res 2003; 35(6):324-328

62. Wollensak G, Spoerl E, Seiler T. Riboflavin/ultraviolet-a-induced collagen crosslinking for the treatment of keratoconus. Am J Ophthalmol 2003; 135(5):620-627

63. Wollensak G, Spoerl E, Seiler T. Stress-strain measurements of human and porcine corneas after riboflavin-ultraviolet-A-induced cross-linking. J Cataract Refract Surg 2003; 29(9):1780-1785

64. Caporossi A, Baiocchi S, Mazzotta C, Traversi C, Caporossi T. Parasurgical therapy for keratoconus by riboflavin-ultraviolet type A rays induced cross-linking of corneal collagen: preliminary refractive results in an Italian study. J Cataract Refract Surg 2006; 32(5):837-845

65. Schwiegerling J, Greivenkamp JE. Keratoconus detection based on videokeratoscopic height data. Optom Vis Sci 1996; 73(12):721-728

66. Sporl E, Huhle M, Kasper M, Seiler T. [Increased rigidity of the cornea caused by intrastromal cross-linking]. Ophthalmologe 1997; 94(12):902-906

67. Sporl E, Schreiber J, Hellmund K, Seiler T, Knuschke P. [Studies on the stabilization of the cornea in rabbits]. Ophthalmologe 2000; 97(3):203-206

68. Wollensak G, Sporl E, Seiler T. [Treatment of keratoconus by collagen cross linking]. Ophthalmologe 2003; 100(1):44-49

69. Wilson SE. Role of apoptosis in wound healing in the cornea. Cornea 2000; 19(3 Suppl):S7-12

70. Seiler T, Quurke AW. Iatrogenic keratectasia after LASIK in a case of forme fruste keratoconus. J Cataract Refract Surg 1998; 24(7):1007-1009

71. Binder PS. Ectasia after laser in situ keratomileusis. J Cataract Refract Surg 2003; 29(12):2419-2429

72. Randleman JB, Russell B, Ward MA, Thompson KP, Stulting RD. Risk factors and prognosis for corneal ectasia after LASIK. Ophthalmology 2003; 110(2):267-275

73. Kymionis GD, Siganos CS, Kounis G, Astyrakakis N, Kalyvianaki MI, Pallikaris IG. Management of post-LASIK corneal ectasia with Intacs inserts: one-year results. Arch Ophthalmol 2003; 121(3):322-326

74. Lovisolo CF, Fleming JF. Intracorneal ring segments for iatrogenic keratectasia after laser in situ keratomileusis or photorefractive keratectomy. J Refract Surg 2002; 18(5):535-541

75. Siganos CS, Kymionis GD, Astyrakakis N, Pallikaris IG. Management of corneal ectasia after laser in situ keratomileusis with INTACS. J Refract Surg 2002; 18(1):43-46

76. Seitz B, Rozsival P, Feuermannova A, Langenbucher A, Naumann GO. Penetrating keratoplasty for iatrogenic keratoconus after repeat myopic laser in situ keratomileusis: histologic findings and literature review. J Cataract Refract Surg 2003; 29(11):2217-2224

77. Kohlhaas M, Spoerl E, Speck A, Schilde T, Sandner D, Pillunat LE. [A new treatment of keratectasia after LASIK with riboflavin/UVA light cross-linking]. Klin Monatsbl Augenheilkd 2005; 222(5):430-436

78. Park D, Perez E, Miller D. Corneal lamellar strength as determined by thickness, position and fibril orientation. Inest Ophthalmol Vis Sci 1995; 36(4):S39

79. Jaycock PD, Lobo L, Ibrahim J, Tyrer J, Marshall J. Interferometric technique to measure biomechanical changes in the cornea induced by refractive surgery. J Cataract Refract Surg 2005; 31(1):175-184

80. Luce DA. Determining in vivo biomechanical properties of the cornea with an ocular response analyzer. J Cataract Refract Surg 2005; 31(1):156-162

81. Meek KM, Tuft SJ, Huang Y, Gill PS, Hayes S, Newton RH, Bron AJ. Changes in collagen orientation and distribution in keratoconus corneas. Invest Ophthalmol Vis Sci 2005; 46(6):1948-1956

82. Rodrigues MM, Newsome DA, Krachmer JH, Eiferman RA. Pellucid marginal corneal degeneration: a clinicopathologic study of two cases. Exp Eye Res 1981; 33(3):277-288

83. Rabinowitz YS. Videokeratographic indices to aid in screening for keratoconus. J Refract Surg 1995; 11(5):371-379

84. Comaish IF, Lawless MA. Progressive post-LASIK keratectasia: biomechanical instability or chronic disease process? J Cataract Refract Surg 2002; 28(12):2206-2213

85. Koch DD. The riddle of iatrogenic keratectasia. J Cataract Refract Surg 1999; 25(4):453-454

86. Kohnen T. Iatrogenic keratectasia: current knowledge, current measurements. J Cataract Refract Surg 2002; 28(12):2065-2066

87. Seiler T. Iatrogenic keratectasia: academic anxiety or serious risk? J Cataract Refract Surg 1999; 25(10):1307-1308

88. Munnerlyn CR, Koons SJ, Marshall J. Photorefractive keratectomy: a technique for laser refractive surgery. J Cataract Refract Surg 1988; 14(1):46-52

89. Holladay JT, Dudeja DR, Chang J. Functional vision and corneal changes after laser in situ keratomileusis determined by contrast sensitivity, glare testing, and corneal topography. J Cataract Refract Surg 1999; 25(5):663-669

90. Moreno-Barriuso E, Lloves JM, Marcos S, Navarro R, Llorente L, Barbero S. Ocular aberrations before and after myopic corneal refractive surgery: LASIK-induced changes measured with laser ray tracing. Invest Ophthalmol Vis Sci 2001; 42(6):1396-1403

91. Oliver KM, Hemenger RP, Corbett MC, O'Brart DP, Verma S, Marshall J, Tomlinson A. Corneal optical aberrations induced by photorefractive keratectomy. J Refract Surg 1997; 13(3):246-254

92. Oshika T, Miyata K, Tokunaga T, Samejima T, Amano S, Tanaka S, Hirohara Y, Mihashi T, Maeda N, Fujikado T. Higher order wavefront aberrations of cornea and magnitude of refractive correction in laser in situ keratomileusis. Ophthalmology 2002; 109(6):1154-1158

93. Kohnen T, Mahmoud K, Buhren J. Comparison of corneal higher-order aberrations induced by myopic and hyperopic LASIK. Ophthalmology 2005; 112(10):1692

94. Applegate RA, Marsack JD, Ramos R, Sarver EJ. Interaction between aberrations to improve or reduce visual performance. J Cataract Refract Surg 2003; 29(8):1487-1495

95. Mrochen M, Donitzky C, Wullner C, Loffler J. Wavefront-optimized ablation profiles: theoretical background. J Cataract Refract Surg 2004; 30(4):775-785

96. Kohnen T, Buhren J. [Current state of wavefront guided corneal surgery to correct refraction disorders]. Ophthalmologe 2004; 101(6):631-645; quiz 646-637

97. Mrochen M, Seiler T. [Fundamentals of wavefront-guided refractive corneal surgery]. Ophthalmologe 2001; 98(8):703-714

98. Alio JL, Montes-Mico R. Wavefront-Guided versus Standard LASIK Enhancement for Residual Refractive Errors. Ophthalmology 2005;

99. Kanellopoulos AJ. Topography-guided custom retreatments in 27 symptomatic eyes. J Refract Surg 2005; 21(5):S513-518

100. Seiler T, Dastjerdi MH. Customized corneal ablation. Curr Opin Ophthalmol 2002; 13(4):256-260

101. Atchison DA, Scott DH, Cox MJ, Mathematical treatment of ocular aberrations: a users guide, in Optics and Photonics. Vision Science and its apllications, Lakshiminarayanan V, Editor. 2000, Optical Society of America: Washington, D.C. p. 110-130.

102. MacRae S, Schwiegerling J, Snyder RW. Customized and low spherical aberration corneal ablation design. J Refract Surg 1999; 15(2 Suppl):S246-248

103. Schwiegerling J, Snyder RW. Corneal ablation patterns to correct for spherical aberration in photorefractive keratectomy. J Cataract Refract Surg 2000; 26(2):214-221

104. Brunette I, Bueno JM, Parent M, Hamam H, Simonet P. Monochromatic aberrations as a function of age, from childhood to advanced age. Invest Ophthalmol Vis Sci 2003; 44(12):5438-5446

105. Thibos LN, Bradley A, Variation in ocular aberrations over seconds, minutes, hours, days, months and years., in Wavefront customized visual correction: the quest for super vision II., Krueger RR, Applegate RA, MacRae S, Editors. 2004, Slack Inc.: Thorfare,NJ.

106. Larichev A, Ivanov P, Nemeth SC, Edwards A, Soliz P. High speed measurements of human eye aberrations with a Hartmann-Shack sensor. in Invest Ophthalmol Vis Sci. 2001. Ft. Lauderdale.

107. Smolek MK, Klyce SD. Zernike polynomial fitting fails to represent all visually significant corneal aberrations. Invest Ophthalmol Vis Sci 2003; 44(11):4676-4681

108. Bueeler M, Mrochen M. Simulation of eye-tracker latency, spot size, and ablation pulse depth on the correction of higher order wavefront aberrations with scanning spot laser systems. J Refract Surg 2005; 21(1):28-36

109. Huang D, Arif M. Spot size and quality of scanning laser correction of higher-order wavefront aberrations. J Cataract Refract Surg 2002; 28(3):407-416

110. Mrochen M, Seiler T. Influence of corneal curvature on calculation of ablation patterns used in photorefractive laser surgery. J Refract Surg 2001; 17(5):S584-587

111. Vogel A, Venugopalan V. Mechanisms of pulsed laser ablation of biological tissues. Chem Rev 2003; 103(2):577-644

112. Krueger RR, Seiler T, Gruchman T, Mrochen M, Berlin MS. Stress wave amplitudes during laser surgery of the cornea. Ophthalmology 2001; 108(6):1070-1074

113. O'Brart DP, Lohmann CP, Fitzke FW, Klonos G, Corbett MC, Kerr-Muir MG, Marshall J. Disturbances in night vision after excimer laser photorefractive keratectomy. Eye 1994; 8 (Pt 1):46-51

114. Seiler T, Kahle G, Kriegerowski M. Excimer laser (193 nm) myopic keratomileusis in sighted and blind human eyes. Refract Corneal Surg 1990; 6(3):165-173

115. Verdon W, Bullimore M, Maloney RK. Visual performance after photorefractive keratectomy. A prospective study. Arch Ophthalmol 1996; 114(12):1465-1472

116. Applegate RA, Howland HC. Refractive surgery, optical aberrations, and visual performance. J Refract Surg 1997; 13(3):295-299

117. Seiler T, Genth U, Holschbach A, Derse M. Aspheric photorefractive keratectomy with excimer laser. Refract Corneal Surg 1993; 9(3):166-172

118. Mrochen M, Kaemmerer M, Seiler T. Wavefront-guided laser in situ keratomileusis: early results in three eyes. J Refract Surg 2000; 16(2):116-121

119. Kezirian GM, Stonecipher KG. Subjective assessment of mesopic visual function after laser in situ keratomileusis. Ophthalmol Clin North Am 2004; 17(2):211-224, vii

120. Anera RG, Jimenez JR, Jimenez del Barco L, Bermudez J, Hita E. Changes in corneal asphericity after laser in situ keratomileusis. J Cataract Refract Surg 2003; 29(4):762-768

121. Henslee SL, Rowsey JJ. New corneal shapes in keratorefractive surgery. Ophthalmology 1983; 90(3):245-250

122. Patel S, Marshall J, Fitzke FW, 3rd. Model for predicting the optical performance of the eye in refractive surgery. Refract Corneal Surg 1993; 9(5):366-375

123. Kiely P, Smith G, Carney L. The mean shape of the human cornea. Opt Acta 1982; 29:1027-1040

124. Gatinel D, Malet J, Hoang-Xuan T, Azar DT. Analysis of customized corneal ablations: theoretical limitations of increasing negative asphericity. Invest Ophthalmol Vis Sci 2002; 43(4):941-948

125. Manns F, Ho A, Parel JM, Culbertson W. Ablation profiles for wavefront-guided correction of myopia and primary spherical aberration. J Cataract Refract Surg 2002; 28(5):766-774

126. Seiler T, Wollensak J. [Mathematical presentation of postoperative regular corneal astigmatism]. Klin Monatsbl Augenheilkd 1993; 203(1):70-76

127. Kohnen T, Buhren J, Kuhne C, Mirshahi A. Wavefront-guided LASIK with the Zyoptix 3.1 system for the correction of myopia and compound myopic astigmatism with 1-year follow-up: clinical outcome and change in higher order aberrations. Ophthalmology 2004; 111(12):2175-2185

128. Sandoval HP, de Castro LE, Vroman DT, Solomon KD. Refractive Surgery Survey 2004. J Cataract Refract Surg 2005; 31(1):221-233

129. Yamane N, Miyata K, Samejima T, Hiraoka T, Kiuchi T, Okamoto F, Hirohara Y, Mihashi T, Oshika T. Ocular higher-order aberrations and contrast sensitivity after conventional laser in situ keratomileusis. Invest Ophthalmol Vis Sci 2004; 45(11):3986-3990

130. Marcos S, Barbero S, Llorente L, Merayo-Lloves J. Optical response to LASIK surgery for myopia from total and corneal aberration measurements. Invest Ophthalmol Vis Sci 2001; 42(13):3349-3356

131. Yoon G, Macrae S, Williams DR, Cox IG. Causes of spherical aberration induced by laser refractive surgery. J Cataract Refract Surg 2005; 31(1):127-135

132. Roberts C. Biomechanics of the cornea and wavefront-guided laser refractive surgery. J Refract Surg 2002; 18(5):S589-592

133. Gibralter R, Trokel SL. Correction of irregular astigmatism with the excimer laser. Ophthalmology 1994; 101(7):1310-1314; discussion 1314-1315

134. Nagy ZZ. Laser in situ keratomileusis combined with topography-supported customized ablation after repeated penetrating keratoplasty. J Cataract Refract Surg 2003; 29(4):792-794

135. Nuijts RM, Nabar VA, Hament WJ, Eggink FA. Wavefront-guided versus standard laser in situ keratomileusis to correct low to moderate myopia. J Cataract Refract Surg 2002; 28(11):1907-1913

136. Schwiegerling J, Snyder RW, Lee JH. Wavefront and topography: keratome-induced corneal changes demonstrate that both are needed for custom ablation. J Refract Surg 2002; 18(5):S584-588

137. Seitz B, Langenbucher A, Kus MM, Harrer M. Experimental correction of irregular corneal astigmatism using topography-based flying-spot-mode excimer laser photoablation. Am J Ophthalmol 1998; 125(2):252-256

138. Bueeler M, Mrochen M, Seiler T. Effect of eye movements during refractive surgery with a scanning spot laser. Ophthalmic Tech 2003; 20:S4931-S4942

139. Guirao A, Williams DR, MacRae SM. Effect of beam size on the expected benefit of customized laser refractive surgery. J Refract Surg 2003; 19(1):15-23

140. Ishihara M, Arai T, Sato S, Morimoto Y, Obara M, Kikuchi M. Measurement of the surface temperature of the cornea during ArF excimer laser ablation by thermal radiometry with a 15-nanosecond time response. Lasers Surg Med 2002; 30(1):54-59141. Bende T, Seiler T, Wollensak J. Side effects in excimer corneal surgery. Corneal thermal gradients. Graefes Arch Clin Exp Ophthalmol 1988; 226(3):277-280

142. Maldonado-Codina C, Morgan PB, Efron N. Thermal consequences of photorefractive keratectomy. Cornea 2001; 20(5):509-515

143. Betney S, Morgan PB, Doyle SJ, Efron N. Corneal temperature changes during photorefractive keratectomy. Cornea 1997; 16(2):158-161

144. Vetrugno M, Maino A, Valenzano E, Cardia L. Corneal temperature changes during photorefractive keratectomy using the Laserscan 2000 flying spot laser. J Refract Surg 2001; 17(4):454-459

Summary

Management of complications in refractive laser surgery

The first part of this thesis focuses on the management of complications in refractive laser surgery:

Reoperations after LASIK surgery

The frequency of refractive surgery has increased drastically in the past years. In analogy, the incidence of reoperations after LASIK surgery has followed this trend. In **Chapter 2.1**, we have analyzed all reoperations performed at our institute over the period of one year. The majority of reoperations is performed as LASIK surgery with re-lift of the primary flap, which is now seen as an easy-to-perform and safe procedure. The main indications for reoperations are residual astigmatism and increased patient's expectations in slight under- or overcorrection.

Customized ablation algorithm for the treatment of steep central islands after refractive laser surgery

Most of the technical advances in refractive laser surgery were only achieved in the past few years and many patients who were treated earlier show previous optical complications such as small optical zones, decentered ablations and formation of steep central islands. The latter often remains as an unresolved therapeutical problem with current laser ablation profiles. In **Chapter 2.2**, we present a new ablation strategy to correct for steep central islands after previous photorefractive keratectomy (PRK) and laser in situ keratomileusis (LASIK).

Anterior lamellar keratoplasty with a microceratome: a method for managing complications after refractive surgery

In 1999, the frequency of refractive laser surgery had exceeded that of cataract surgery in the USA by a factor of 2 and had become the most frequently performed procedure in ophthalmology. In the years thereafter, a significant increase in the total number of postoperative complications was noted. Many of these complications affect the anterior corneal stroma such as severe scarring after PRK, cutting errors and recurrent epithelial ingrowth after LASIK. In cases where the posterior corneal stroma is intact, lamellar keratoplasty is the procedure of choice. Up to now, the prepa-

ration of the donor lamella and the recipient wound bed were performed manually leading to some degree of irregular corneal surface even with experienced surgeons. In **Chapter 2.3,** we present the first results of **automated anterior lamellar keratoplasty**. This new technique combines the known technique of superficial lamellar keratoplasty with the automated preparation of the donor lamella. The recipient wound bed uses microceratomes originally developed for LASIK. The advantages of this technique are a more uniform donor and recipient match, the possibility of postoperative correction of irregular astigmatism performing a re-lift of the flap, and customized ablation.

Small optical zones after PRK for high myopia are also often observed complications of procedures performed in the "early days" of refractive laser surgery. Many of the former refractive patients who were treated in the late 1980s and early 1990s are seeking help from recently developed techniques such as customized ablations. However, many patients presenting with small optical zones have residual myopia combined with critically low central corneal thickness and beginning presbyopia. In **Chapter 2.4** we present a **2-step technique** that we have developed for the treatment of such cases. In a first step, a clear lens exchange shifts the patient to hyper-opia. After this procedure, the calculation of a topography-based ablation profile shows that ablation in the central cornea will be minimal, enabling the surgeon to perform a customized topography-guided treatment.

Corneal collagen cross-linking by UVA/riboflavin (X-linking) represents a recently developed method for the treatment of progressive keratoconus. In **Chapter 2.5** we demonstrate that the effect of crosslinking on the cornea can be identified as soon as several weeks after treatment by identifcation of a stromal demarcation line. In **Chapter 2.6** we investigated whether this technique would also arrest **iatrogenic keratectasia after LASIK**. With a postoperative follow-up time of up to 20 months we demonstrated that X-linking slows down, arrests and even partially reverses the progression of LASIK-induced iatrogenic keratectasia.

Prevention of complications in refractive laser surgery

The second part of this thesis discusses strategies for the prevention of complications in refractive laser surgery:

Ablation profiles in corneal laser surgery: current and future concepts

The preoperative calculation and choice of the appropriate ablation profile represent a central element for the quality and predictability of results in corneal refractive laser surgery.

In **Chapter 3.1** we describe past, current and potential future ablation profiles. Ablation profiles may either be based on the entire optics such as the classic Munnerlyn profile used for almost 20 years and the recently introduced wavefront-optimized and **wavefront-guided profiles**. Ablation profiles may also be based on the cornea solely such as topography-guided or Q factor-adjusted profiles. Future ablation profiles ("ray tracing") might incorporate topographic, aberrometric and biometric data to establish an even more accurate ablation profile. Each eye should be carefully examined prior to surgery and the best-suited profile should be evaluated for the individual eye.

Wavefront-guided customized ablation profiles are currently the most frequently used profiles in corneal refractive laser surgery. A number of factors influence the safety, efficacy and predictability of such treatments. These factors include correct centration during measurement of the wavefront, proper wavefront sensing and **transfer of the wavefront measurement into an ablation profile**. This step consists of three phases: inversion of the wavefront map, conversion of the wavefront map and offset for the ablation profile. The different phases and potential sources of error are discussed in **Chapter 3.2**.

A yet unresolved issue in refractive laser surgery is management of laser correction in presbyopia. Many presbyopic patients do not only seek to be independent of glasses or contact lenses for distant but also for near vision. Monovision has been offered by many surgeons as an alternative to reading glasses. However, this method of aiming at emmetropia on the dominant eye and leaving minor myopia on the non-dominant eye is not always tolerated well and shows some major disadvantages such as reduced stereo vision as well as glare and halos on the non-dominant eye.
Q factor-adjusted ablation profiles were developed only recently and represent a promising alternative to wavefront-guided profiles. The Q factor is a

shape factor that characterizes the asphericity of the human cornea. Changing the peripheral corneal asphericity to a more prolate form (Q factor) might be a means to induce better near visual acuity while at the same time keeping good far visual acuity. In **Chapter 3.3** we compare patients that have been treated using Q factor-adjusted ablation profiles with patients treated by wavefront-guided profiles and analyze the outcomes.

The speed by which a laser treatment can be performed is an essential step in the predictability of a refractive laser surgery procedure. The tissue ablation performed by a single laser spot is calculated based on a certain degree of corneal dehydration.

Once the flap is lifted in LASIK surgery, corneal hydration might shift and change within seconds to minutes. Thus, the faster tissue ablation occurs, the more accurate the result will be. Whereas first-generation scanning spot excimer lasers performed photoablation at rates of 50 to 200 Hz, the newest prototypes show repetition rates of up to **500 Hz**. In **Chapter 3.4** we investigated potential side effects that might be associated with the use of such a high repetition rate laser platform.

Samenvatting

Behandeling van complicaties van refractiechirurgie met de laser

Het eerste gedeelte van dit proefschrift gaat over de behandeling van complicaties van refractiechirurgie met de laser:

Re-operaties na LASIK chirurgie

De frequentie waarmee refractiechirurgie wordt toegepast is de laatste jaren enorm toegenomen. Analoog hieraan heeft de incidentie van re-operaties na LASIK-chirurgie deze trend gevolgd. In **hoofdstuk 2.1** hebben we alle re-operaties geanalyseerd, die in de periode van één jaar in ons instituut zijn verricht. Het merendeel van de re-operaties wordt verricht door LASIK-chirurgie via een re-lift van de primaire flap, wat nu wordt beschouwd als een gemakkelijk uit te voeren en veilige ingreep. De belangrijkste indicaties voor re-operaties zijn resterend astigmatisme en het toegenomen verwachtingspatroon van de patiënt ten aanzien van geringe onder- en overcorrectie.

Maatwerk ablatie-algoritme voor de behandeling van *steep central islands* na refractiechirurgie met de laser

De grootste technische vooruitgang bij refractiechirurgie met de laser is pas in de laatste jaren bereikt en veel patiënten die in de periode hiervoor zijn behandeld hebben optische complicaties zoals kleine optische zones, gedecentreerde ablaties en vorming van *steep central islands*. Deze laatste complicatie blijft ook met de huidige schema's voor laser-ablatie moeilijk behandelbaar. In **hoofdstuk 2.2** wordt een nieuwe laser ablatie strategie voor de behandeling van *steep central islands* na eerdere fotorefractieve keratectomie (PRK) en laser in situ keratomileusis (LASIK) besproken.

Anterieure lamellaire keratoplastiek met een microtoom: een methode voor behandeling van complicaties na refractiechirurgie

In 1999 was de frequentie van refractiechirurgie met de laser in de Verenigde Staten twee keer zo hoog als die van cataractchirurgie; daarmee is het de meest uitgevoerde oogheelkundige ingreep geworden. In de jaren hierna ontstond een sterke toename van het aantal postoperatieve complicaties. Veel van deze complicaties betrof het voorste

stroma, zoals ernstige littekenvorming na PRK, snijfouten, en terugkerende epitheel-ingroei na LASIK. In gevallen waarbij het achterste deel van het stroma intact is, geniet een lamellaire keratoplastiek de voorkeur. Tot voor kort werd de donorlamel en het wondbed van de recipiënt manueel geprepareerd, hetgeen zelfs bij ervaren chirurgen leidde tot een wisselende mate van irregulair cornea-oppervlak. In **hoofdstuk 2.3** worden de eerste resultaten behandeld van **geautomatiseerde anterieure lamellaire keratoplastiek**.

Deze nieuwe techniek combineert de bestaande techniek van superficiële lamellaire keratoplastiek met automatische preparatie van de donorlamel en het recipiënt wondbed door middel van microtomen, die ontwikkeld waren voor LASIK. De voordelen van deze techniek zijn een betere match tussen donor en recipiënt en de mogelijkheid van postoperatieve correctie van irregulier astigmatisme via een re-lift van de flap en maatwerk ablatie. Vorming van kleine optische zones na PRK voor hoge myopie is een andere, veel voorkomende complicatie van ingrepen uit de 'vroege periode' van de refractiechirurgie, eind jaren 1980 en begin jaren 1990. Veel patiënten, behandeld in deze periode, zoeken hun toevlucht tot recent ontwikkelde technieken zoals maatwerk ablaties. Vele patiënten met kleine optische zones hebben resterende myopie gecombineerd met een kritisch geringe centrale cornea-dikte en beginnende presbyopie.

In **hoofdstuk 2.4** presenteren we een **twee-staps techniek**, die speciaal voor de behandeling van zulke patiënten ontwikkeld werd. In de eerste stap leidt een *clear lens exchange* tot hyperopie van het behandelde oog. Nadien laat een calculatie van een op topografie gebaseerd ablatie-profiel zien dat ablatie van de centrale cornea minimaal zal zijn, zodat de chirurg een behandeling kan uitvoeren, aan de hand van topografische bevindingen.

Corneale collageen cross-linking door UVA/riboflavine (X-linking) is een recent ontwikkelde methode voor de behandeling van progressieve keratoconus. In **hoofdstuk 2.5** laten we zien dat het effect van cross-linking op het hoornvlies al binnen enkele weken na behandeling kan worden vastgesteld door de identificatie van een stromale demarcatie-lijn. In **hoofdstuk 2.6** onderzochten we of deze techniek ook de **iatrogene progressieve keratectasie na LASIK** zou kunnen laten stoppen. Met een postoperatieve follow-up tot 20 maanden na behandeling laten we zien dat X-linking de progressie van

LASIK-geïnduceerde iatrogene keratectasie vertraagt, stopzet, of zelfs ongedaan maakt.

Preventie van complicaties van refractiechirurgie met de laser

Het tweede gedeelte van dit proefschrift behandelt strategieën voor de preventie van complicaties van refractiechirurgie met de laser:

Ablatie-profielen in de chirurgie van de cornea met de laser: huidige en toekomstige concepten

De preoperatieve calculatie en keuze van optimaal ablatieprofiel zijn essentieel voor de kwaliteit en voorspelbaarheid van resultaten van corneale refractieve laser chirurgie.

In **hoofdstuk 3.1** beschrijven we oude, huidige en potentieel toekomstige ablatie-profielen. Ablatie-profielen kunnen ofwel gebaseerd zijn op de totale optiek zoals bij het klassieke Munnerlyn-profiel, dat gedurende bijna 20 jaar gebruikt werd, ofwel op recent geïntroduceerde *wave-front-optimized* en *wave-front-guided* profielen. Ablatie-profielen kunnen ook gebaseerd worden op alleen het hoornvlies, zoals bij de topografie-gestuurde of Q-factor-aangepaste profielen. Toekomstige ablatie-profielen (*ray-tracing*) zouden topographische, aberrometrische en biometrische data kunnen incorporeren voor een grotere accuratesse. Elk oog zou preoperatief nauwkeurig onderzocht moeten worden, waarbij het meest geschikte ablatieprofiel wordt bepaald.

Wavefront-guided maatwerk ablatie-profie-len zijn de meest toegepaste profielen in de refractiechirurgie met de laser van het hoornvlies. Een aantal factoren beïnvloedt de veilig-heid, doeltreffendheid en voorspelbaarheid van zulke behandelingen. Deze factoren bestaan uit correcte centratie tijdens meting van de wavefront, adequate wavefront sensing en **omzetting van een wavefront meting in een ablatieprofiel**. Deze stap bestaat uit 3 fasen: inversie van een wavefront-kaart, conversie van een *wavefront*-kaart en offset voor een ablatieprofiel. De verschillende fasen en potentiële oorzaken van fouten worden behandeld in **hoofdstuk 3.2**.

Een nog niet opgeloste kwestie bij de refractiechirurgie met de laser is de behandeling van refractie-problemen bij patiënten met presbyopie. Veel presbyope patiënten willen zowel voor ver als

dichtbij zien niet langer afhankelijk zijn van bril of contactlenzen. Monovision wordt door vele chirurgen aangeboden als alternatief voor de leesbril. Hierbij is het dominante oog emmetroop (gemaakt) en het niet-dominante oog gering myoop (gemaakt). Monovision wordt echter niet door een ieder goed verdragen en heeft als belangrijke bijwerking een gereduceerd stereozien, evenals glare- en halo-klachten van het niet-domi-nante oog.

Q-factor-adjusted ablatie-profielen werden recent ontwikkeld en zijn een veelbelovend alternatief voor wave-front-guided profielen. De Q-factor is een factor die de asfericiteit van de cornea aangeeft. Verandering van de de perifere corneale asfericiteit naar een plattere vorm (Q-factor) zou een een middel kunnen zijn om beter nabij zien te verkrijgen met behoud van goed veraf zien. In **hoofdstuk 3.3** vergelijken we patiënten die behandeld zijn met *Q-factor-adjusted* ablatieprofielen met anderen die behandeld werden met wave-front-guided profielen. Ook evalueren we de resultaten.

De snelheid waarmee een laserbehandeling kan worden verricht is belangrijk voor de voorspelbaarheid van de resultaten van refractiechirurgie met de laser. De weefsel-ablatie ten gevolge van een enkele laser spot is afhankelijk van de mate van corneale hydratie. Als de flap wordt opgetild in LASIK-chirurgie kan de hydratiegraad van de cornea binnen enkele seconden tot enkele minuten veranderen. Daarom zal met een snellere behandeling een betrouwbaarder resultaat verkregen kunnen worden. Terwijl de eerste-generatie scanning spot excimer lasers foto-ablatie verrichten met frequenties van 50 tot 200 Hz, is de frequentie bij de laatste prototypen wel **500 Hz**. In **hoofdstuk 3.4** onderzochten we de potentiële bijwerkingen die kunnen ontstaan bij gebruik van deze hoge-frequentie lasersystemen.

Acknowledgements

It is impossible to perform a work such as the one presented here without the help and the support of many others. It was the french philosopher Bernard of Chartres who first described this fact and the ongoing quest for knowledge in the 12th century:

"Pigmaei gigantum humeris impositi plusquam ipsi gigantes vident"
"We are like dwarfs sitting upon the shoulders of giants,
and so able to see more and see farther than the ancients."

Gabriel van Rij
Dear Gabriel, it was a pleasure and an honor for me to be accepted by you as your PhD candidate and I thank you from my heart for this great opportunity.

Theo Seiler
Dear Theo, you were the driving force behind this thesis. In the last years you were an ongoing source of inspiration for me and I admire your perpetual energy to pursue the open questions in the field.

Michael Mrochen and Hans Peter Iseli
Dear Michael, dear Hans Peter. Thank you for your ongoing scientific support, I look forward to the years ahead of us.

Charlotte Remé
Dear Charlotte. Although you were not directly involved in this thesis, you taught me scientific thinking, modesty and lab work, tools that were indispensable for me over the years.

Dion Paridaens
Dear Dion, Thank you for your constructive criticisms. I enjoy our friendship. Don't forget to join us on June 2, 2007.

Gerald Chader
Dear Dr. Chader, thank you so much for advising Mrs. Kristoffersen to join your team in the "Little-Inn-by-the-Sea" for ARVO 2006.

Papa, Mama, Zarrin, Micha, Farah and Fariba
Thank you for all the love you gave me throughout my life. Life would not make sense without you.

...and to my Nikkilove
Hail to the next 60 years...

Biography

Farhad Hafezi was born in Remscheid, Germany, on November 1, 1967 as the son of a Polish mother, Alina, and a Persian father, Abolfazl. He spent the first 13 years of his life in Germany to then move to Fribourg in the French speaking part in Switzerland where his sister, Zarrin, had just started her university studies of English literature.

From 1986 to 1992 he studied medicine at the Universities of Fribourg and Berne where he received his diploma in November 1992. In 1993 he obtained his medical degree from the medical faculty of the University of Berne.

He then moved to Zurich to join the 29th "PG course" , a 2-year postgraduate study in cell and molecular biology now called MSc. From 1994 to 1996 he worked as a scientific post-doc in the laboratory of retinal cell biology of the University Eye Clinic Zurich (Prof. Charlotte E. Remé) where he was engrossed in the field of retinal research.

From 1997 to 2000 he was a clinical resident at the University Eye Clinic of Zurich (Prof. B. Gloor and Prof. T. Seiler). In parallel to his clinical education he continued his work in the laboratory for retinal cell biology.

In 2000 he was nominated staff member of the University Eye Clinic of Zurich (Prof. T. Seiler) where he worked until 2002.

In 2002 he was an oculoplastic fellow at the "Ogziekenhuis Rotterdam" (Dr. A.D.A. Paridaens and Dr. W. van den Bosch).

He then returned to Zurich, Switzerland where he co-founded IROC (Institute for refractive and ophthalmic surgery), a private institution consisting of ophthalmologists and physicists joining forces to perform both patient care and research and development in ophthalmology. His main focus of the past years is refractive laser and corneal surgery.

Own publications

Peer reviewed original articles

1. Bohlen LM, de Courten M, Hafezi F, Shaw S, Riesen W, Weidmann P
Insulin sensitivity and atrial natriuretic factor during beta-receptor modula tion with celiprolol in normal subjects
J Cardiovasc Pharmacol. 1994. 23(6): 877-83

2. Hafezi F, Marti A, Munz K, Reme CE
Light-induced apoptosis: differential timing in the retina and pigment epithelium
Exp Eye Res. 1997. 64(6): 963-70

3. Hafezi F, Steinbach JP, Marti A, Munz K, Wang ZQ, Wagner EF, Aguzzi A, Reme CE
The absence of c-fos prevents light-induced apoptotic cell death of photo receptors in retinal degeneration in vivo
Nat Med. 1997. 3(3): 346-9

4. Hafezi F, Abegg M, Grimm C, Wenzel A, Munz K, Sturmer J, Farber DB, Reme CE
Retinal degeneration in the rd mouse in the absence of c-fos
Invest Ophthalmol Vis Sci. 1998. 39(12): 2239-44

5. Hafezi F, Reinboth JJ, Wenzel A, Munz K, Reme CE
HPETE, an arachidonic acid metabolite, induces apoptosis in the rat retina in vitro
Klinische Monatsblatter Fur Augenheilkunde. 1998. 212(6): 469-72

6. Marti A, Hafezi F, Lansel N, Hegi ME, Wenzel A, Grimm C, Niemeyer G, Reme CE
Light-induced cell death of retinal photoreceptors in the absence of p53
Invest Ophthalmol Vis Sci. 1998. 39(5): 846-9

7. Hafezi F, Grimm C, Wenzel A, Abegg M, Yaniv M, Reme CE
Retinal photoreceptors are apoptosis-competent in the absence of JunD/AP-1
Cell Death Differ. 1999. 6(10): 934-6

8. Hafezi F, Marti A, Grimm C, Wenzel A, Reme CE
Differential DNA binding activities of the transcription factors AP-1 and Oct-1 during light-induced apoptosis of photoreceptors
Vision Res. 1999. 39(15): 2511-8

9. Lansel N, Hafezi F, Marti A, Hegi M, Reme C, Niemeyer G
The mouse ERG before and after light damage is independent of p53
Documenta Ophthalmologica. 1999. 96(4): 311-20

10. Reme CE, Wolfrum U, Imsand C, Hafezi F, Williams TP
Photoreceptor autophagy: effects of light history on number and opsin content of degradative vacuoles
Invest Ophthalmol Vis Sci. 1999. 40(10): 2398-404

11. Fleischmann A, Hafezi F, Elliott C, Reme CE, Ruther U, Wagner EF
Fra-1 replaces c-Fos-dependent functions in mice
Genes Dev. 2000. 14(21): 2695-700

12. Grimm C, Wenzel A, Hafezi F, Reme CE
Gene expression in the mouse retina: the effect of damaging light
Mol Vis. 2000. 6: 252-60

13. Grimm C, Wenzel A, Hafezi F, Yu S, Redmond TM, Reme CE
Protection of Rpe65-deficient mice identifies rhodopsin as a mediator of light-induced retinal degeneration
Nat Genet. 2000. 25(1): 63-6

14. Kueng-Hitz N, Grimm C, Lansel N, Hafezi F, He L, Fox DA, Reme CE, Niemeyer G, Wenzel A
The retina of c-fos-/- mice: electrophysiologic, morphologic and biochemical aspects
Invest Ophthalmol Vis Sci. 2000. 41(3): 909-16

15. Wenzel A, Grimm C, Marti A, Kueng-Hitz N, Hafezi F, Niemeyer G, Reme CE
c-Fos controls the "private pathway" of light-induced apoptosis of retinal photoreceptors
J Neurosci. 2000. 20(1): 81-8

16. Grimm C, Wenzel A, Behrens A, Hafezi F, Wagner EF, Reme CE
AP-1 mediated retinal photoreceptor apoptosis is independent of N-terminal phosphorylation of c-Jun
Cell Death Differ. 2001. 8(8): 859-67

17. Grimm C, Wenzel A, Williams T, Rol P, Hafezi F, Reme C
Rhodopsin-mediated blue-light damage to the rat retina: effect of photoreversal of bleaching
Invest Ophthalmol Vis Sci. 2001. 42(2): 497-505

18. Keller C, Grimm C, Wenzel A, Hafezi F, Reme C
Protective effect of halothane anesthesia on retinal light damage: inhibition of metabolic rhodopsin regeneration
Invest Ophthalmol Vis Sci. 2001. 42(2): 476-80

19. Wenzel A, Grimm C, Seeliger MW, Jaissle G, Hafezi F, Kretschmer R, Zrenner E, Reme CE
Prevention of photoreceptor apoptosis by activation of the glucocorticoid receptor
Invest Ophthalmol Vis Sci. 2001. 42(7): 1653-9

20. Wenzel A, Reme CE, Williams TP, Hafezi F, Grimm C
The Rpe65 Leu450Met variation increases retinal resistance against light-induced degeneration by slowing rhodopsin regeneration
J Neurosci. 2001. 21(1): 53-8

21. Iseli HP, Wenzel A, Hafezi F, CE RE, Grimm dagger C
Light damage susceptibility and RPE65 in rats
Exp Eye Res. 2002. 75(4): 407-13

22. Wenzel A, Iseli HP, Fleischmann A, Hafezi F, Grimm C, Wagner EF, Reme CE
Fra-1 substitutes for c-Fos in AP-1-mediated signal transduction in retinal apoptosis
J Neurochem. 2002. 80(6): 1089-94

23. Hafezi F, Mrochen M, Fankhauser F, 2nd, Seiler T
Anterior lamellar keratoplasty with a microkeratome: a method for managing complications after refractive surgery
J Refract Surg. 2003. 19(1): 52-7

24. Iseli HP, Mrochen M, Hafezi F, Seller T
Clinical photoablation with a 500-Hz scanning spot excimer laser
J Refract Surg. 2004. 20(6): 831-4

25. Hafezi F, Mrochen M, Seiler T
Two-step procedure to enlarge small optical zones after photorefractive keratectomy for high myopia
J Cataract Refract Surg. 2005. 31(12): 2254-6

26. Iseli HP, Bueeler M, Hafezi F, Seiler T, Mrochen M
Dependence of wave front refraction on pupil size due to the presence of higher order aberrations
Eur J Ophthalmol. 2005. 15(6): 680-7

27. Ittner LM, Wurdak H, Schwerdtfeger K, Kunz T, Ille F, Leveen P, Hjalt TA, Suter U, Karlsson S, Hafezi F, Born W, Sommer L
Compound developmental eye disorders following inactivation of TGFbeta signaling in neural-crest stem cells
J Biol. 2005. 4(3): 11

28. Stanescu D, Iseli HP, Schwerdtfeger K, Ittner LM, Reme CE, Hafezi F
Continuous expression of the homeobox gene Pax6 in the ageing human retina
Eye. 2005:

29. Hafezi F, Jankov M, Mrochen M, Wullner C, Seiler T
Customized ablation algorithm for the treatment of steep central islands after refractive laser surgery
J Cataract Refract Surg. 2006. 32(5): 717-21

30. Koller T, Iseli HP, Hafezi F, Mrochen M, Seiler T
Q-factor customized ablation profile for the correction of myopic astigmatism
J Cataract Refract Surg. 2006. 32(4): 584-9

31. Seiler T, Hafezi F
Corneal cross-linking-induced stromal demarcation line
Cornea. 2006. 25(9): 1057-9

32. Seiler T, Hafezi F, Iseli HP, Koller T, Alkara N
Reoperations after LASIK
Klin Monatsbl Augenheilkd. 2006. 223(6): 509-12

33. Hafezi F, Kanellopulos J, Wiltfang, R, Seiler T
Corneal collagen crosslinking with riboflavin and ultraviolet A to treat induced keratectasia after laser in situ keratomileusis
J Cat Refract Surg. 2007. 33(12):2035-40

34. Ittner LM, Schwerdtfeger K, Kunz TH, Muff R, Husmann K, Grimm C, Hafezi F, Lang KS, Kurrer MO, Götz J, Born W, Fischer JA
Transgenic mice with ocular overexpression of an adrenomedullin receptor reflect human acute angle-closure glaucoma
Clin Sci. 2008. 114(1):49-58

Case reports

1. Hafezi F, Boltshauser E, Landau K
Pronounced physiological pupillary hippus
Klinische Monatsblatter Fur Augenheilkunde. 2000. 216(2): 118-19

2. Hafezi F, Welzl-Hinterkorner E, Tholen AM
Idiopathic sclerochoroidal calcification - a case report
Klinische Monatsblatter Fur Augenheilkunde. 2001. 218(3): 197-200

3. Kniestedt C, Hafezi F, Seiler T
Ultrasound biomicroscopical diagnosis of traumatic choroidal effusion without cyclodialysis
Ophthalmologe. 2001. 98(7): 656-59

4. Iseli HP, Hafezi F, Mojon DS
Conservative treatment of vertical diplopia in a patient with silent sinus syndrome
Ophthalmologica. 2003. 217(4): 308-9

5. Neeracher B, Iseli HP, Ganter C, Saupe N, Hafezi F
Hypopigmentation of the fundus oculi and pulmonary fibrosis
Ophthalmologe. 2003. 100(6): 480-81

6. Hafezi F, Bockholts D, van den Bosch WA, Paridaens AD
Giant mucocele of all paranasal sinuses with massive bilateral globe displacement
Ophthalmologe. 2006. 103(4): 340-1

7. Hafezi F, Paridaens D
Unusual orbital trauma with diplopia
Ophthalmologe. 2007. 104(2): 163-4

8. Moesen I, Hafezi F, Paridaens D
Corneal dellen secondary to conjunctival chemosis following transconjunctival orbital decompression
Klin Monatsbl Augenheilkd. 2007. 224(11):856-7

9. Paarlberg JC, den Hollander JC, Hafezi F, Paridaens D
Adenoid cystic carcinoma of the upper eyelid
Ophthalmologe. 2007. 104(12):1066-7

Reviews

1. Reme C, Reinboth J, Clausen M, Hafezi F
Light damage revisited: converging evidence, diverging views?
Graefes Arch Clin Exp Ophthalmol. 1996. 234(1): 2-11

2. Hafezi F, Wenzel A, Grimm C, Reme CE
Retinal degeneration, apoptosis and the c-fos gene
Neuro-Ophthalmology. 1998. 20(3): 143-48

3. Remé CE, Rol P, Hafezi F
Im Fokus des Auges: Lichttherapie und ihre vermeidbaren Gefahren
Therapiewoche. 1998. 14: 119-23

4. Abegg M, Hafezi F, Wenzel A, Grimm C, Reme CE
Therapeutic strategies in RP (retinitis pigmentosa): light at the end of the tunnel?
Klin Monatsbl Augenheilkd. 2000. 216(2): 83-9

5. Hafezi F, Grimm C, Simmen BC, Wenzel A, Reme CE
Molecular ophthalmology: an update on animal models for retinal degenerations and dystrophies
Br J Ophthalmol. 2000. 84(8): 922-7

6. Reme CE, Grimm C, Hafezi F, Wenzel A, Williams TP
Apoptosis in the Retina: The Silent Death of Vision
News Physiol Sci. 2000. 15: 120-24

7. Hafezi F, Grimm C, Wenzel A, Iseli HP, Reme C
Die Netzhautdegeneration: mit molekularen Mitteln auf dem Weg zur Therapie
Ars Medici. 2002. 20: 948-52

8. Reme CE, Grimm C, Hafezi F, Iseli HP, Wenzel A
Why study rod cell death in retinal degenerations and how?
Doc Ophthalmol. 2003. 106(1): 25-9

9. Seiler T, Iseli HP, Hafezi F, Mrochen M.
Supernormales Sehvermögen
Dtsch Ärzteblatt. 2003. 100(11): 700-04

10. Hafezi F
Häufige Fehlstellungen der Augenlider in der medizinischen Praxis
Ars Medici. 2004. 17: 1-5

11. Mrochen M, Bueeler M, Iseli HP, Hafezi F, Seiler T
Transferring Wavefront Measurements Into Corneal Ablations: An Overview of Related Topics
J Refract Surg. 2004. 20: S580-84

12. Mrochen M, Hafezi F, Iseli HP, Loffler J, Seiler T
Nomograms for the improvement of refractive outcomes
Ophthalmologe. 2006. 103(4): 331-8

13. Mrochen M, Hafezi F, Jankov M, Seiler T
Ablation profiles in corneal laser surgery. Current and future concepts
Ophthalmologe. 2006. 103(3): 175-83

Book chapters

1. Reme CE, Weller M, Szczesny P, Munz K, Hafezi F, Reinboth JJ, Clausen M
Light-induced apoptosis in the rat retina in vivo: morphological features, threshold and time course, in Degenerative diseases of the retina, Anderson RE, LaVail MM, Hollyfield JG, Editors. 1995, Plenum Press: New York. 19-25.

2. Hafezi F, Marti A, Munz K, Remé CE
Early events in light-induced apoptosis of photoreceptors and pigment epithelium of rats in vivo, in Les Seminaires ophthalmologiques Ipsen. 1997, Editions Irvinn: Paris. 13-17.

3. Remé CE, Hafezi F, Grimm C, Wenzel A
UV- und Lichtschäden des Auges - wie kann man sich schützen? in Physikalische Therapiemassnahmen in der Dermatologie, Dummer R, Panizzon R, Burg G, Editors. 1997, Blackwell Wissenschaftsverlag: Berlin. 200-09.

4. Hafezi F, Marti A, Steinbach JP, Munz K, Aguzzi A, Remé CE
Light-induced retinal degeneration is prevented in mice lacking c-fos, in Degenerative retinal diseases, LaVail MM, Hollyfield JG, Anderson RE, Editors. 1998, Plenum Press: New York. 193-98.

5. Reme CE, Grimm C, Hafezi F, Marti A, Wenzel A
Apoptotic cell death in retinal degenerations, in Prog Retin Eye Res, Osborne NN, Chader GJ, Editors. 1998, Pergamon Press: New York, Tokyo. 443-64.

6. Remé CE, Bush R, Hafezi F, Wenzel A, Grimm C
Photostasis and beyond: where adaptation ends, in Photostasis and related phenomena, Williams TP, Thistle AB, Editors. 1998, Plenum Press: New York. 199-206.

7. Remé CE, Hafezi F, Marti A, Munz K, Reinboth JJ
Light damage to retina and pigment epithelium, in The Retinal Pigment Epithelium, current aspects of function and disease, Marmor MF, Wolfensberger T, Editors. 1998, Oxford University Press: Oxford. 563-86.

8. Hafezi F, Abegg M, Wenzel A, Grimm C, Remé CE
Lichtschäden des Auges: ein Überblick, in Risikofaktoren für Augenerkrankun gen, Erb C, Flammer J, Editors. 1999, Hans Huber: Bern, Göttingen, Toronto, Seattle. 277-83.

9. Mrochen M, Jankov M, Iseli HP, Hafezi F, Seiler T
Retinal imaging aberrometry - the WaveLight Wavefront analyzer, in Customized corneal ablation, MacRae S, Krueger RR, Applegate RA, Editors. 2003, Slack Incorporated: New York. 113-18.

10. Hafezi F, Iseli HP, Seiler T
Automated anterior lamellar keratoplasty for the management of complications in refractive surgery, in Surgical techniques in anterior and posterior lamellar corneal surgery, John T, Editor. 2006, Slack Inc.: New York. (in press).